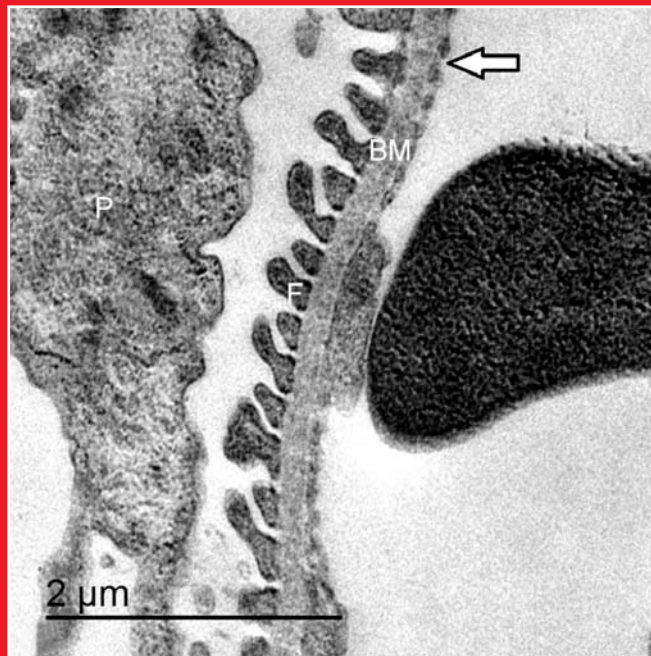


anatomy

An International Journal of Experimental and Clinical Anatomy

Volume 13 / Issue 3 / December 2019

Published three times a year



Official Publication of the Turkish Society of Anatomy and Clinical Anatomy

Aim and Scope

Anatomy, an international journal of experimental and clinical anatomy, is a peer-reviewed journal published three times a year with an objective to publish manuscripts with high scientific quality from all areas of anatomy. The journal offers a forum for anatomical investigations involving gross, histologic, developmental, neurological, radiological and clinical anatomy, and anatomy teaching methods and techniques. The journal is open to original papers covering a link between gross anatomy and areas related with clinical anatomy such as experimental and functional anatomy, neuroanatomy, comparative anatomy, modern imaging techniques, molecular biology, cell biology, embryology, morphological studies of veterinary discipline, and teaching anatomy. The journal is currently indexing and abstracting in TUBITAK ULAKBIM Turkish Medical Index, Proquest, EBSCO Host, Index Copernicus and Google Scholar.

Publication Ethics

Anatomy is committed to upholding the highest standards of publication ethics and observes the principles of Journal's Publication Ethics and Malpractice Statement which is based on the recommendations and guidelines for journal editors developed by the Committee on Publication Ethics (COPE), Council of Science Editors (CSE), World Association of Medical Editors (WAME) and International Committee of Medical Journal Editors (ICMJE). For detailed information please visit the online version of the journal which is available at www.anatomy.org.tr

Authorship

All persons designated as authors should have participated sufficiently in the work to take public responsibility for the content of the manuscript. Authorship credit should be based on substantial contributions to (1) conception and design or analysis and interpretation of data, (2) drafting of the manuscript or revising it for important intellectual content and, (3) final approval of the version to be published. The Editor may require the authors to justify assignment of authorship. In the case of collective authorship, the key persons responsible for the article should be identified and others contributing to the work should be recognized with proper acknowledgment.

Copyright

Copyright © 2019, by the Turkish Society of Anatomy and Clinical Anatomy, TSACA. All rights reserved. No part of this publication may be reproduced, stored or transmitted in any form without permission in writing from the copyright holder beforehand, exceptionally for research purpose, criticism or review. The publisher and the Turkish Society of Anatomy and Clinical Anatomy assume no liability for any material published in the journal. All statements are the responsibility of the authors. Although all advertising material is expected to conform ethical standards, inclusion in this publication does not constitute a guarantee or endorsement of the quality or value of such product or of the claims made of it by its manufacturer. Permission requests should be addressed to the publisher.

Publication Information

Anatomy (p-ISSN 1307-8798; e-ISSN 1308-8459) is published by Deomed Publishing, Istanbul, for the Turkish Society of Anatomy and Clinical Anatomy, TSACA. Due the Press Law of Turkish Republic dated as June 26, 2004 and numbered as 5187, this publication is classified as a periodical in English language.

Ownership

On behalf of the Turkish Society of Anatomy and Clinical Anatomy, Ahmet Kağan Karabulut, MD, PhD; Konya

Responsible Managing Editor

Nihal Apaydın, MD, PhD; Ankara

Administrative Office

Güven Mah. Güvenlik Cad. Onlar Ap. 129/2 Aşağı Ayrancı, Ankara
Phone: +90 312 447 55 52-53

Publisher

Deomed Publishing
Gür Sok. No:7/B Kadıköy, İstanbul, Turkey
Phone: +90 216 414 83 43 (Pbx) / Fax: +90 216 414 83 42
www.deomed.com / e-mail: medya@deomed.com

Submission of Manuscripts

Contributions should be submitted for publication under the following categories to:

Gülgün Şengül, MD
Editor-in-Chief, *Anatomy*

Department of Anatomy,
Faculty of Medicine, Ege University,
35100, Bornova, Izmir, Turkey
Phone: 0090 232 390 39 84
Fax: 0090 232 342 21 42
e-mail: gulgun.sengul@gmail.com; gulgun.sengul@ege.edu.tr

Categories of Articles

• **Original Articles** describe substantial original research that falls within the scope of the Journal.

• **Teaching Anatomy** section contains regular or all formats of papers which are relevant to comparing teaching models or to introducing novel techniques, including especially the own experiences of the authors.

• **Reviews** section highlights current development in relevant areas of anatomy. The reviews are generally invited; other prospective authors should consult with the Editor-in-Chief.

• **Case Reports** include new, noteworthy or unusual cases which could be of help for basic notions and clinical practice.

• **Technical Note** articles cover technical innovations and developments with a specific technique or procedure or a modification of an existing technique. They should be sectioned like an original research article but not exceed 2000 words.

• **Viewpoint** articles give opinions on controversial topics or future projections, some of these are invited.

• **Historical View** category presents overview articles about historical sections from all areas of anatomy.

• **Terminology Zone** category is a platform for the articles which discuss some terminological controversies or opinions.

The categories above are peer-reviewed. They should include abstract and keywords. There are also categories including Letters to the Editor, Book Reviews, Abstracts, Obituary, News and Announcements which do not require a peer review process.

For detailed instructions concerning the submission of manuscripts, please refer to the Instructions to Authors.

Subscription

Please send your order to Deomed Publishing, Gür Sok. No: 7/B Kadıköy, İstanbul, Turkey. e-mail: aliko@deomed.com

• **Annual rates:** Institutional 100 EUR, Individual 50 EUR (include postage and local VAT). Supplements are not included in the subscription rates.

Membership of the Turkish Society of Anatomy and Clinical Anatomy, TSACA includes a reduced subscription rate to this journal.

• **Change of address:** Please send to the publisher at least six weeks in advance, including both old and new addresses.

• **Cancellations:** Subscription cancellations will not be accepted after the first issue has been mailed.

The online version of this journal is available at www.anatomy.org.tr

Advertising and Reprint Requests

Please direct to publisher. e-mail: medya@deomed.com

Printing and Binding

Yek Press, İstanbul, Turkey, Phone: +90 212 430 50 00
Printed in Turkey on acid-free paper (March 2020).

Honorary Editor

Doğan Akşit, Ankara, Turkey

Founding Editors

Salih Murat Akkın, Gaziantep, Turkey

Hakan Hamdi Çelik, Ankara, Turkey

Former Editor-in-Chief &

Advising Editor

Salih Murat Akkın, Gaziantep, Turkey

Editor-in-Chief

Gülgün Şengül, Izmir, Turkey

Editors

Nihal Apaydın, Ankara, Turkey

Kyung Ah Park, Seoul, Korea

George Paxinos, Sydney, Australia

Luis Puelles, Murcia, Spain

Mustafa F. Sargon, Ankara, Turkey

Ümit S. Şehirli, Istanbul, Turkey

Shane Tubbs, Birmingham, AL, USA

Emel Ulupınar, Eskişehir, Turkey

Associate Editors

Vaclav Baca, Prague, Czech Republic

Çağatay Barut, Istanbul, Turkey

Jon Cornwall, Dunedin, New Zealand

Ayhan Cömert, Ankara, Turkey

Georg Feigl, Graz, Austria

Zeliha Kurtoğlu Olgunus, Mersin, Turkey

Scott Lozanoff, Honolulu, HI, USA

Levent Sarıkçıoğlu, Antalya, Turkey

Cristian Stefan, Boston, MA, USA

Executive Board of Turkish Society of Anatomy and Clinical Anatomy

Esat Adıgüzel (President)

Zeliha Kurtoğlu Olgunus (Vice President)

Çağatay Barut (Vice President)

Piraye Kervancıoğlu (Secretary General)

Ayhan Cömert (Treasurer)

İlke Ali Gürses (Vice Treasurer)

Nadire Ünver Doğan (Member)

Scientific Advisory Board

Peter H. Abrahams
Cambridge, UK

Halil İbrahim Açar
Ankara, Turkey

Esat Adıgüzel
Denizli, Turkey

Marian Adamkov
Martin, Slovakia

Mustafa Aktekin
Istanbul, Turkey

Mahindra Kumar Anand
Gujarat, India

Doychin Angelov
Cologne, Germany

Serap Arbak
Istanbul, Turkey

Alp Bayramoğlu
Istanbul, Turkey

Brion Benninger
Lebanon, OR, USA

Susana Biasutto
Cordoba, Argentina

Dragica Bobinac
Rijeka, Croatia

David Bolender
Milwaukee, WI, USA

Eric Brenner
Innsbruck, Austria

Mustafa Büyükmumcu
Konya, Turkey

Richard Halti Cabral
Sao Paulo, Brazil

Safiye Çavdar
Istanbul, Turkey

Katharina D'Herde
Ghent, Belgium

Fabrice Duparc
Rouen, France

Behice Durgun
Adana, Turkey

İzzet Duyar
Istanbul, Turkey

Mirela Eric
Novi Sad, Serbia

Cumhur Ertekin
Izmir, Turkey

Mete Ertürk
Izmir, Turkey

Reha Erzurumlu
Baltimore, MD, USA

Ali Firat Esmer
Ankara, Turkey

António José Gonçalves Ferreira
Lisboa, Portugal

Quentin Fogg
Melbourne, Australia

Christian Fontaine
Lille, France

Rod Green
Bendigo, Australia

Bruno Grignon
Nancy Cedex, France

Nadir Gülekon
Ankara, Turkey

Mürvet Hayran
Izmir, Turkey

David Heylings
Norwich, UK

Lazar Jeleu
Sofia, Bulgaria

David Kachlík
Prague, Czech Republic

Samet Kapakin
Erzurum, Turkey

Ahmet Kağan Karabulut
Konya, Turkey

Piraye Kervancıoğlu
Gaziantep, Turkey

Hee-Jin Kim
Seoul, Korea

Necdet Kocabiyik
Ankara, Turkey

Cem Kopuz
Samsun, Turkey

Mustafa Ayberk Kurt
Bursa, Turkey

Marios Loukas
Grenada, West Indies

Veronica Macchi
Padua, Italy

Mehmet Ali Malas
Izmir, Turkey

Petru Matusz
Timisoara, Romania

Bernard Moxham
Cardiff, Wales, UK

Konstantinos Natsis
Thessaloniki, Greece

Helen Nicholson
Dunedin, New Zealand

Davut Özbağ
Malatya, Turkey

P. Hande Özdinler
Chicago, IL, USA

Adnan Öztürk
Istanbul, Turkey

Mehmet Hakan Öztürk
Mersin, Turkey

Diogo Pais
Lisboa, Portugal

Friedrich Paulsen
Erlangen, Germany

Wojciech Pawlina
Rochester, MN, USA

Tuncay Veysel Peker
Ankara, Turkey

Vid Persaud
Winnipeg, MB, Canada

David Porta
Louisville, KY, USA

Jose Ramon Sanudo
Madrid, Spain

Tatsuo Sato
Tokyo, Japan

Mohammadali M. Shoja
Birmingham, AL, USA

Ahmet Sinav
Sakarya, Turkey

Takis Skandalakis
Athens, Greece

Vildan Sümbüloğlu
Gaziantep, Turkey (*Biostatistics*)

Muzaffer Şeker
Konya, Turkey

Erdoğan Şendemir
Bursa, Turkey

İbrahim Tekdemir
Ankara, Turkey

Hironubu Tokuno
Tokyo, Japan

Trifon Totlis
Thessaloniki, Greece

Mehmet İbrahim Tuğlu
Manisa, Turkey

Selçuk Tunalı
Ankara, Turkey

Uğur Türe
Istanbul, Turkey

Mehmet Üzel
Istanbul, Turkey

Ivan Varga
Bratislava, Slovakia

Tuncay Varol
Manisa, Turkey

Charles Watson
Sydney, Australia

Andreas H. Weiglein
Graz, Austria

Bülent Yalçın
Ankara, Turkey

M. Gazi Yaşargil
Istanbul, Turkey

Özlem Yılmaz
Izmir, Turkey

Hiroshi Yorifuji
Gunma, Japan

Anatomy, an international journal of experimental and clinical anatomy, is the official publication of the Turkish Society of Anatomy and Clinical Anatomy, TSACA. It is a peer-reviewed journal that publishes scientific articles in English. For a manuscript to be published in the journal, it should not be published previously in another journal or as full text in congress books and should be found relevant by the editorial board. Also, manuscripts submitted to *Anatomy* must not be under consideration by any other journal. Relevant manuscripts undergo conventional peer review procedure (at least three reviewers). For the publication of accepted manuscripts, author(s) should reveal to the Editor-in-Chief any conflict of interest and transfer the copyright to the Turkish Society of Anatomy and Clinical Anatomy, TSACA.

In the Materials and Methods section of the manuscripts where experimental studies on humans are presented, a statement that informed consent was obtained from each volunteer or patient after explanation of the procedures should be included. This section also should contain a statement that the investigation conforms with the principles outlined in the appropriate version of 1964 Declaration of Helsinki. For studies involving animals, all work must have been conducted according to applicable national and international guidelines. Prior approval must have been obtained for all protocols from the relevant author's institutional or other appropriate ethics committee, and the institution name and permit numbers must be provided at submission.

Anatomical terms used should comply with Terminologia Anatomica by FCAT (1998).

No publication cost is charged for the manuscripts but reprints and color printings are at authors' cost.

Preparation of manuscripts

During the preparation of the manuscripts, uniform requirements of the International Committee of Medical Journal Editors, a part of which is stated below, are valid (see ICMJE. Uniform requirements for manuscripts submitted to biomedical journals. Updated content is available at www.icmje.org). The manuscript should be typed double-spaced on one side of a 21x 29.7 cm (A4) blank sheet of paper. At the top, bottom and right and left sides of the pages a space of 2.5 cm should be left and all the pages should be numbered except for the title page.

Manuscripts should not exceed 15 pages (except for the title page). They must be accompanied by a cover letter signed by corresponding author and the Conflicts of Interest Disclosure Statement and Copyright Transfer Form signed by all authors. The contents of the manuscript (original articles and articles for Teaching Anatomy category) should include: 1- Title Page, 2- Abstract and Keywords, 3- Introduction, 4- Materials and Methods, 5- Results, 6- Discussion (Conclusion and/or Acknowledgement if necessary), 7- References

Title page

In all manuscripts the title of the manuscript should be written at the top and the full names and surnames and titles of the authors beneath. These should be followed with the affiliation of the author. Manuscripts with long titles are better accompanied underneath by a short version (maximum 80 characters) to be published as running head. In the title page the correspondence address and telephone, fax and e-mail should be written. At the bottom of this page, if present, funding sources supporting the work should be written with full names of all funding organizations and grant numbers. It should also be indicated in a separate line if the study has already been presented in a congress or likewise scientific meeting. Other information such as name and affiliation are not to be indicated in pages other than the title page.

Abstract

Abstract should be written after the title in 100–250 words. In original articles and articles prepared in IMRAD format for Teaching Anatomy category the abstract should be structured under sections Objectives, Methods, Results and Conclusion. Following the abstract at least 3 keywords should be added in alphabetical order separated by semicolons.

References

Authors should provide direct references to original research sources. References should be numbered consecutively in square brackets, according to the order in which they are first mentioned in the manuscript. They should follow the standards detailed in the NLM's Citing Medicine, 2nd edition (Citing medicine: the NLM style

guide for authors, editors, and publishers [Internet]. 2nd edition. Updated content is available at www.ncbi.nlm.nih.gov/books/NBK7256). The names of all contributing authors should be listed, and should be in the order they appear in the original reference. The author is responsible for the accuracy and completeness of references. When necessary, a copy of a referred article can be requested from the author. Journal names should be abbreviated as in *Index Medicus*. Examples of main reference types are shown below:

- **Journal articles:** Author's name(s), article title, journal title (abbreviated), year of publication, volume number, inclusive pages

- *Standard journal article:* Sargon MF, Celik HH, Aksit MD, Karaagaoglu E. Quantitative analysis of myelinated axons of corpus callosum in the human brain. *Int J Neurosci* 2007;117:749–55.

- *Journal article with indication article published electronically before print:* Sengul G, Fu Y, Yu Y, Paxinos G. Spinal cord projections to the cerebellum in the mouse. *Brain Struct Funct Epub* 2014 Jul 10. DOI 10.1007/s00429-014-0840-7.

- **Books:** Author's name(s), book title, place of publication, publisher, year of publication, total pages (entire book) or inclusive pages (contribution to a book or chapter in a book)

- *Entire book:*

- *Standard entire book:* Sengul G, Watson C, Tanaka I, Paxinos G. Atlas of the spinal cord of the rat, mouse, marmoset, rhesus and human. San Diego (CA): Academic Press Elsevier; 2013. 360 p.

- *Book with organization as author:* Federative Committee of Anatomical Terminology (FCAT). Terminologia anatomica. Stuttgart: Thieme; 1998. 292 p.

- *Citation to a book on the Internet:* Bergman RA, Afifi AK, Miyauchi R. Illustrated encyclopedia of human anatomic variation. Opus I: muscular system [Internet]. [Revised on March 24, 2015] Available from: <http://www.anatomyatlases.org/AnatomicVariants/AnatomyHP.shtml>

- *Contribution to a book:*

- *Standard reference to a contributed chapter:* Potten CS, Wilson JW. Development of epithelial stem cell concepts. In: Lanza R, Gearhart J, Blau H, Melton D, Moore M, Pedersen R, Thomson J, West M, editors. Handbook of stem cell. Vol. 2, Adult and fetal. Amsterdam: Elsevier; 2004. p. 1–11.

- *Contributed section with editors:* Johnson D, Ellis H, Collins P, editors. Pectoral girdle and upper limb. In: Standring S, editor. Gray's anatomy: the anatomical basis of clinical practice. 29th ed. Edinburgh (Scotland): Elsevier Churchill Livingstone; 2005. p. 799–942.

- *Chapter in a book:*

- *Standard chapter in a book:* Doyle JR, Botte MJ. Surgical anatomy of the hand and upper extremity. Philadelphia (PA): Lippincott Williams and Wilkins; 2003. Chapter 10, Hand, Part 1, Palmar hand; p. 532–641.

Illustrations and tables

Illustrations and tables should be numbered in different categories in the manuscript and Roman numbers should not be used in numbering. Legends of the illustrations and tables should be added to the end of the manuscript as a separate page. Attention should be paid to the dimensions of the photographs to be proportional with 10x15 cm. Some abbreviations out of standards can be used in related illustrations and tables. In this case, abbreviation used should be explained in the legend. Figures and tables published previously can only be used when necessary for a comparison and only by giving reference after obtaining permission from the author(s) or the publisher (copyright holder).

Control list

- Length of the manuscript (max. 15 pages)
- Manuscript format (double space; one space before punctuation marks except for apostrophes)
- Title page (author names and affiliations; running head; correspondence)
- Abstract (100–250 words)
- Keywords (at least three)
- References (relevant to *Index Medicus*)
- Illustrations and tables (numbering; legends)
- Conflicts of Interest Disclosure Statement and Copyright Transfer Form
- Cover letter

Potential role of empagliflozin in prevention of nephropathy in streptozotocin-nicotinamide-induced type 2 diabetes: an ultrastructural study

Marwa Abd El-Kader , Hagar A. Hashish 

Department of Anatomy and Embryology, School of Medicine, Mansoura University, Mansoura, Egypt

Abstract

Objectives: Diabetic nephropathy is a serious factor in end-stage renal disease worldwide. Sodium-glucose cotransporter 2 inhibitors, the most novel glucose-lowering drug, may have a nephroprotective effect by modulating blood glucose, blood pressure and autophagy. The present work aimed to study the possible protective effect of empagliflozin in Type 2 diabetic nephropathy with special considerations to oxidative stress, fibrosis and ultrastructural modulation including autophagy.

Methods: Thirty-six adult male Sprague-Dawley rats were divided into 3 groups; control, diabetic, and treatment. Type 2 diabetes was induced by pretreatment with nicotinamide followed by single low-dose of streptozotocin (40 mg/kg, i.p). The treatment group received empagliflozin (10 mg/kg/day, intragastric) for 4 weeks. At the end of 4 weeks, parameters of renal function and oxidative stress were analyzed. Kidney samples were collected for histological and ultrastructural studies.

Results: Empagliflozin significantly reduced hyperglycemia, blood urea nitrogen, serum creatinine and oxidative stress which were elevated in the diabetic group. It also decreased renal tissue injury and fibrosis; however, did not lower the increased kidney index and glomerular size. Beside the amelioration of ultrastructure changes, empagliflozin enhanced the autophagy in renal tubular cells, indicated by increased number of autophagic vacuoles.

Conclusion: Empagliflozin provided an efficient, but not complete protection against diabetic nephropathy in streptozotocin-nicotinamide-induced type 2 diabetic rat model. This effect could be related to reduction of hyperglycemia and improvement of cellular defense mechanisms, and reduction of glucose-induced oxidative stress and autophagy.

Keywords: autophagy; diabetes; nephropathy; empagliflozin

Anatomy 2019;13(3):137–148 ©2019 Turkish Society of Anatomy and Clinical Anatomy (TSACA)

Introduction

Diabetic nephropathy (DN) is a major complication of diabetes mellitus, and a serious factor in end stage renal disease (ESRD) worldwide.^[1] Novel management of DN includes control of high blood pressure and blood glucose levels and suppression of the renin angiotensin system to eliminate proteinuria.^[2] However, some patients suffer from deterioration in renal function causing ESRD. So, new effective line of therapy is a must for the control of ESRD.^[3]

The pathogenesis of DN includes different stages; reversible glomerular hyperfiltration, normal glomerular filtration with normo-albuminuria, decreased glomerular filtration with microalbuminuria, decreased glomerular fil-

tration with macroalbuminuria, and finally proteinuria with ESRD.^[4] The mechanism of DN includes hemodynamic factors like oxidative stress and inflammation and metabolic factors. The inflammatory and fibrotic mediators result in loss of podocytes, hypertrophy of GBM, atrophy of tubules, interstitial and tubular inflammation, and fibrosis.^[5]

Autophagy plays an essential role in the stress-response mechanism, the disturbance of which is included in the pathogenesis of diabetes-related complications.^[6,7] Autophagy is responsible for the degradation of damaged proteins and organelles in the cell to preserve homeostasis and cell integrity in both normal and diseased conditions.^[3] Autophagy was suggested to play a major role in

nephroprotection in some animal models, including aging and acute renal injury models.^[8,9]

One of the most novel oral glucose lowering drugs in type 2 DM is sodium-glucose cotransporter 2 (SGLT2) inhibitors.^[10] There are three available drugs of this family; empagliflozin, dapagliflozin and canagliflozin.^[11] SGLT2 inhibitors were reported to disturb diabetic complications and their progression.^[12] SGLT2 inhibitors might have nephroprotective effect by not only controlling the blood glucose level, but also glucose-independent actions such as lowering of the blood pressure.^[13]

Normally, the filtered glucose by healthy kidneys is reabsorbed to circulation and the renal reabsorption of glucose occurs through SGLT2. In type 2 DM, enhanced activity of SGLT2 results in more glucose reabsorption and persistent high blood glucose levels. On the other hand, inhibition of SGLT2 reduced renal reabsorption of glucose up to 50 %.^[14]

SGLT2 inhibitors also causes diuresis with reduction of blood pressure. These drugs cause an initial reduction in the glomerular filtration rate (GFR), followed by stabilization of the GFR.^[15]

The present work aimed to study the possible protective effect of empagliflozin in type 2 DN with special considerations to oxidative stress, fibrosis and ultrastructural changes including autophagy modulation.

Materials and Methods

Thirty-six adult male Sprague Dawley rats, aging 10–12 weeks and weighting 200–250 g were used in this study, purchased from AL-Nile Experimental Animal Center, Mansoura, Egypt. The rats were housed in separate cages at a constant temperature of 20°C and 45% humidity. Rats had a free access to normal rodent chow and drinking water. All experiments were carried out after approval of the Institutional Research Board in Faculty of Medicine, Mansoura University. Streptozotocin (STZ, CAS no: 18883-66-4, Sigma-Aldrich, St Louis, MO, USA) was dissolved in 0.1mM citrate buffer (pH 4.4). Nicotinamide (NA, CAS no: 98-92-0, Sigma-Aldrich, St Louis, MO, USA) was dissolved in normal saline. Empagliflozin (Boehringer Ingelheim Charmaceutical Company, Biberach, Germany) was purchased from local pharmacy.

After acclimatization for one week, the rats were separated randomly into three groups 12 rats each: control group of non-diabetic rats (were given vehicle only); diabetic group of diabetic untreated rats; and empagliflozin treated diabetic rats that received a single daily dose of empagliflozin (10 mg/kg, intragastric) for four weeks.^[16]

Induction of type 2 diabetes was performed by intraperitoneal (i.p.) injection of freshly prepared NA solution (120 mg/kg), after 15 min, the rats were given single STZ injection (40 mg/kg, i.p).^[17] The fasting blood glucose levels were measured seven days after the diabetic induction. The rats with fasting blood glucose more than 126 mg/dL were selected as diabetic.^[18]

The rats were weighed and sacrificed at the end of 4th week under general anesthesia. Blood and kidney samples were collected immediately. The blood samples were centrifuged at 3000 rpm for 15 min. The serum was stored at -20°C till assessment for biochemical parameters. The kidney weights were measured and the kidney index [kidney weight ×100 / body weight] was calculated.^[19] The right kidneys were fixed in 10% formaldehyde for histopathological examination. The left kidneys were used for electron microscopic examination.

Blood glucose monitoring in experimental rats was performed by obtaining a drop of blood from the tail vein before STZ injection, one week after STZ injection to confirm diabetic glucose level and then on the 4th week after STZ injection. Glucose level was evaluated with the ACCU-CHEK glucose meter (Roche Diagnostic Co., Mannheim, Germany). The serum levels of creatinine and blood urea nitrogen (BUN) were evaluated using a spectrophotometric enzymatic kit (Thermo Trace-BECCMAN, Germany). Oxidative marker superoxide dismutase (SOD) and lipid peroxidation marker malondialdehyde (MDA) were measured (absorbance 450 nm and 532 nm, respectively) using a kit (Biovision, cat. No. K335-100 and K739-100, San Francisco, CA, USA).

The formalin-fixed right kidneys were processed for paraffin block preparation. Serial sections were cut at 5 µm and stained with haematoxylin and eosin (H&E) to detect histopathological changes.^[20] Masson's trichrome staining^[21] was used to demonstrate the accumulation of connective tissue in the nephrons. Also, 1 µm semi-thin sections were prepared from left kidneys and stained with toluidine blue to examine under the light microscope. Small pieces (1×2 mm) from cortexes of the left kidneys were cut and fixed in a solution containing glutaraldehyde (3%) and paraformaldehyde (2%) dissolved in 0.1 mol/L phosphate buffer. Specimens were washed in phosphate buffer, post-fixed in osmium tetroxide (1%), and embedded in epon. 1 µm semithin toluidine blue sections were prepared. Ultrathin sections of 50–70 nm were prepared and stained with uranyl acetate and lead citrate.^[22] Those sections were examined with JEOL-100SX transmission electron microscope (TEM; Jeol Inc., Peabody, MA, USA) in Mansoura University.

Morphometric studies were done using NIH Image J program (National Institutes of Health, Bethesda, MD, USA), according to the instructions. The average glomerular diameter [(maximum perpendicular diameter+maximum transverse diameter)/2] was measured in H&E stained sections in randomly chosen 10 glomeruli per animal.^[23] The mean width of glomerular (Bowman's capsule) space in H&E stained sections were measured in 10 non-overlapping fields for each group.^[24] The percentage of blue stained area was measured in Masson's trichrome-stained sections in 10 non-overlapping random fields.^[25] The thickness of GBM was measured and the mean value was calculated in 20 randomly selected ultra-thin fields of cortex from each rat. The number of autophagic vacuoles in podocytes was calculated ($\times 40,000$) in 15 randomly selected fields.^[26]

The data were expressed as mean \pm standard deviation (SD). Analysis of variance (ANOVA) followed by post-hoc Tukey test were used to compare the significance between different groups; $p < 0.05$ was considered statistically significant. All statistics were carried out using IBM SPSS Statistics for Windows (Version 22, Chicago, IL, USA).

Results

The body weight was assessed at the beginning and by the end of the study, the kidney weights were measured and kidney indexes were calculated (**Table 1**). The diabetic group showed significant body weight loss compared to the control group. Treatment with empagliflozin significantly prevented diabetic induced weight loss ($p = 0.07$). The kidney index was increased in both diabetic and treated groups compared to the control group ($p = 0.771$).

Before the induction of DM, the fasting blood glucose level was nearly equal between the experimental groups. One week after diabetes induction, there was a significant increase in blood glucose of both diabetic and treated groups as compared to the control group. At the end of the study, the blood glucose of both diabetic and treated groups was significantly higher than the control group ($p = 0.009$); however, the blood glucose in the treated group was significantly lower than the diabetic group ($p = 0.001$) (**Table 2**).

To assess the effect of empagliflozin on the kidney function, the serum creatinine and BUN were measured in each group (**Table 3**). The diabetic group demonstrated a significant increase in serum creatinine and BUN compared to the control group, indicating a reasonable kidney tissue injury. Administration of empagliflozin achieved a renal protective effect evidenced by a significant decline in the serum creatinine and BUN in the treated group compared to the diabetic group ($p = 0.0771$).

To investigate the protective effect of empagliflozin on diabetes-induced oxidative stress, the levels of antioxidant enzyme SOD and MDA (lipid peroxidation biomarker) were assessed in the renal tissues of each group (**Table 4**). The diabetic group showed a significant decrease in SOD and an increase in MDA levels compared to the control group. The level of SOD was decreased in the treated group compared to the control and diabetic groups. Interestingly, the treated group

Table 1

Comparison of the body weight and kidney index measurements (mean \pm SD; n=12).

	Control	Diabetic	Treated
Body weight (g) (beginning of experiment)	310 \pm 8	290 \pm 65	296 \pm 37
Body weight (g) (end of experiment)	320 \pm 7	200 \pm 25*	287 \pm 50 [†]
Kidney index (kidney wt \times 100/body weight)	.279 \pm .9	.422 \pm .15*	.962 \pm .30* [†]

* $p < 0.05$ compared to the control group; [†] $p < 0.05$ compared to the diabetic group.

Table 2

Comparison of fasting blood glucose levels (mean \pm SD; n=12).

	Control	Diabetic	Treated
Before induction of DM	105.3 \pm 31	108.1 \pm 39	107.4 \pm 42
1 w after induction of DM	109.2 \pm 26	500.1 \pm 134.7*	495.3 \pm 126.9*
Day of sacrifice	106.6 \pm 39.5	441.9 \pm 128.4*	216.2 \pm 91.2 [†]

* $p < 0.05$ compared with the control group; [†] $p < 0.05$ compared with the diabetic group.

Table 3

Comparison of the results of renal function tests (mean \pm SD; n=12).

	Control	Diabetic	Treated
Serum creatinine	1.8 \pm .32	3.7 \pm .46*	1.3 \pm .21*
BUN	18.4 \pm .9	65.2 \pm 1.15*	40.3 \pm 1.46 [†]

* $p < 0.05$ compared to the control group; [†] $p < 0.05$ compared to the diabetic group.

Table 4

Comparison of the levels of oxidative stress markers (mean \pm SD; n=12).

	Control	Diabetic	Treated
SOD %	85.7% \pm 23.8	74.3% \pm 31.7*	65.7% \pm 28.3* [†]
SOD concentration (μ g)	918.2 \pm 167.4	796.1 \pm 148.3*	703.9 \pm 192.6* [†]
MDA (nmol/g)	36.7 \pm 18.4	85.8 \pm 31.8*	48.5 \pm 20.1 [†]

* $p < 0.05$ compared to the control group; [†] $p < 0.05$ compared to the diabetic group.

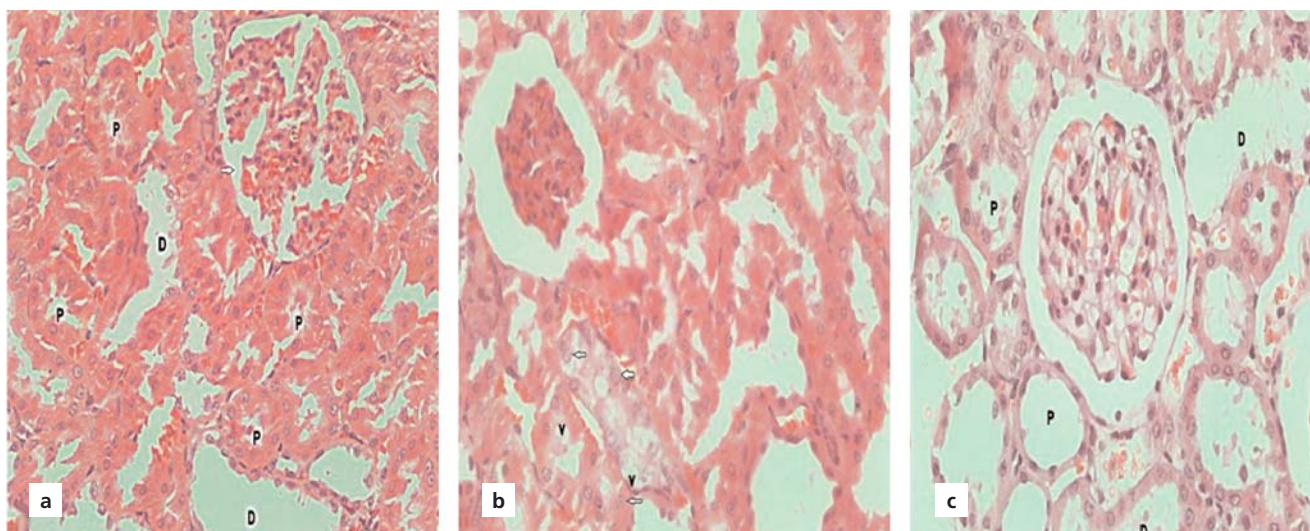


Figure 1. Photomicrographs of the renal cortex. (a) The control group shows renal corpuscle, glomerulus and Bowman’s space (arrow), proximal convoluted tubules with cuboidal cells, vesicular nuclei and deeply stained eosinophilic cytoplasm. The distal convoluted tubules have a wide lumen, with cubical cells and pale eosinophilic cytoplasm; (b) The diabetic groups shows degenerated cells in the tubules (arrows) with cytoplasmic vacuoles; (c) The kidney tissues of treated rats shows renal tubules with normal cells and vesicular nuclei; proximal and distal convoluted tubules. D: distal convoluted tubules; G: glomerulus; P: proximal convoluted tubules; v: cytoplasmic vacuoles (H&E stain; ×100). [Color figure can be viewed in the online issue, which is available at www.anatomy.org.tr]

showed significant decrease in the level of MDA compared to the diabetic group.

H&E stained sections of the renal cortex in the control group showed the normal renal corpuscles with glomeruli and glomerular spaces. While the proximal convoluted tubules were lined by tall cuboidal cells with deeply stained eosinophilic cytoplasm, the distal convoluted tubules had a wide lumen and lined by flat cubical cells with pale eosinophilic cytoplasm (Figure 1a). Degenerated tubular cells with cytoplasmic vacuoles and deeply stained nuclei were also detected in the diabetic group (Figure 1b). The diabetic groups showed a significant increase in the glomerular diameter ($72.6 \pm 8 \mu\text{m}$, $p < 0.05$; Figure 2) and glomerular space ($18.2 \pm 3.9 \mu\text{m}$, $p < 0.05$; Figure 3) compared to the control group (glomerular diameter: $54.7 \pm 10.1 \mu\text{m}$, glomerular space: $7.6 \pm 2.7 \mu\text{m}$). Kidneys of the treated rats showed normal renal corpuscles with a significant decrease in the glomerular diameter ($83 \pm 16.2 \mu\text{m}$, $p < 0.05$; Figure 2) and glomerular space ($10.4 \pm 2.1 \mu\text{m}$, $p < 0.05$; Figure 3) compared to the diabetic group, a large amount of apparent normal renal tubules and vesicular nuclei (Figure 1c).

Masson-trichrome stained sections of the control kidney showed minimal fibrosis with normal collagen distribution within the renal corpuscle and between the tubules (Figure 4a). In the diabetic kidneys, there were massive collagen depositions between the tubules and within the

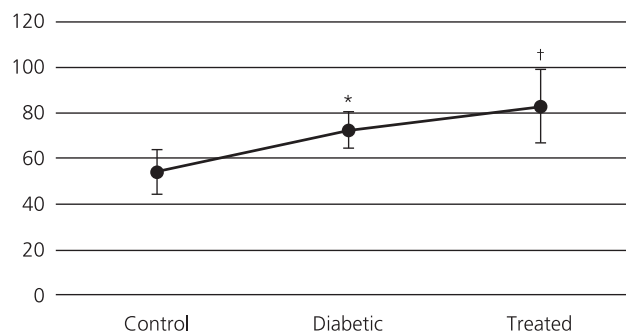


Figure 2. The mean glomerular diameter in control, diabetic and treated groups (mean±SD; n=12). * $p < 0.05$ compared to the control group; † $p < 0.05$ compared to the diabetic group.

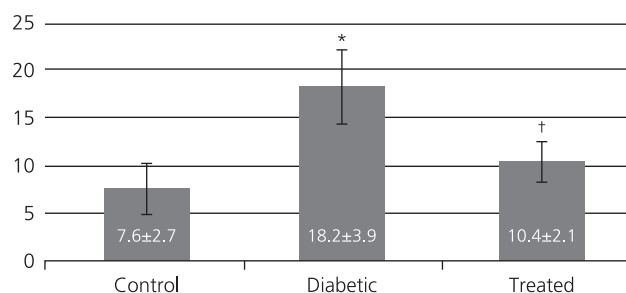


Figure 3. The mean glomerular space in control, diabetic and treated groups (mean±SD; n=12). * $p < 0.05$ compared to the control group; † $p < 0.05$ compared to the diabetic group.

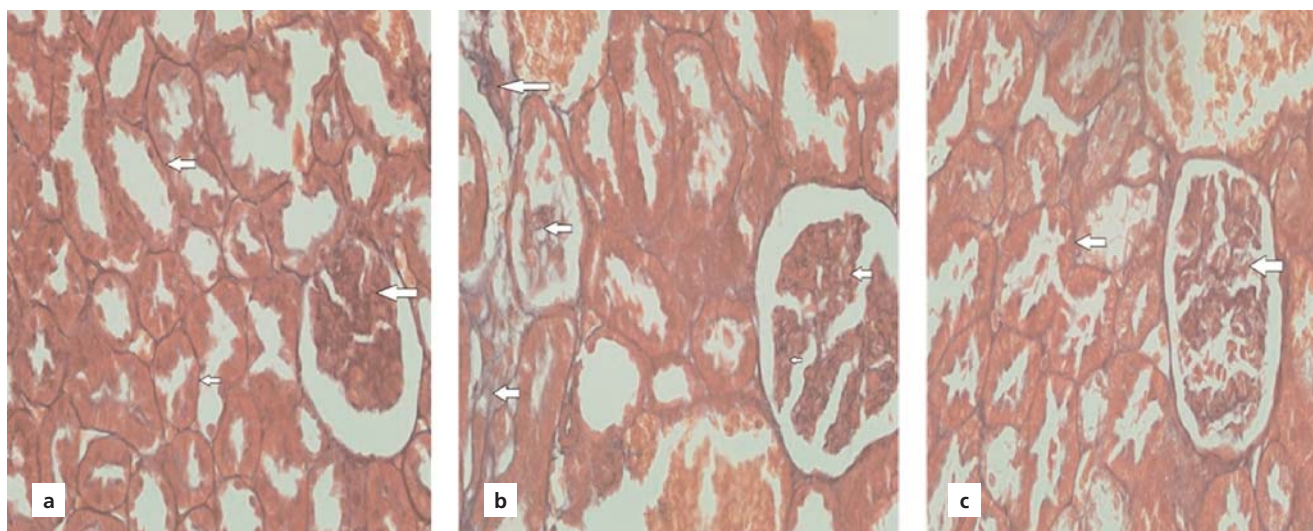


Figure 4. Photomicrographs of the renal cortex. (a) The control group shows minimal fibrosis within the normal area of collagen distribution within the renal corpuscle and among the tubules (arrows); (b) The diabetic kidney shows massive collagen deposition between the tubules and within the glomerulus (arrows); (c) The treatment kidney shows minimal fibrosis within the renal corpuscle and surrounding the tubules (arrows) (Masson's trichrome stain; $\times 100$). [Color figure can be viewed in the online issue, which is available at www.anatomy.org.tr]

glomerulus (**Figure 4b**) with a significant increased area percentage compared to the control group ($p < 0.05$; **Figure 5**). The treated kidneys showed minimal fibrosis within the renal corpuscle and surrounding the tubules (**Figure 4c**) with a significant decrease in the area percentage as compared to the diabetic group ($p < 0.05$; **Figure 5**).

Toluidine blue stained semithin sections in the control group showed normal renal corpuscles and glomeruli with mesangial cells and podocytes, capillaries and intact basement membrane. The renal tubule cells showed basal striations, vesicular nuclei, and apparent brush borders (**Figure 6a**). The diabetic kidneys showed glomeruli with podocytes, mesangial cells, renal tubules with absent of basal striation, lost brush border and areas of cytoplasmic vacuolation (**Figure 6b**). The treated kidneys showed the glomeruli with intact mesangial cells and podocytes. The renal tubule cells restored the basal striations and the apparent brush borders (**Figure 6c**).

TEM examination was performed to detect the ultrastructural changes of the renal tissues. For the glomeruli, ultrathin sections of the control group showed regular basement membrane, fenestrated endothelial cells and apparent podocytes of the foot processes (**Figure 7a**). The diabetic group showed significantly thickened basement membrane, a fusion of the foot processes and degenerated podocytes (**Figure 7b** and **7c**) compared to the control group. The treated group displayed regular basement membrane and apparent podocytes of the foot processes with a significant decrease in the basement membrane

thickness compared to the diabetic group ($1.6 \mu\text{m}$, $p < 0.05$) (**Figure 7d**, **Table 5**).

For proximal convoluted tubules, ultrathin sections of the control group showed proximal tubular cells with a regular basement membrane, apical microvilli, oval euchromatic nucleus, mitochondria, and apparent autophagic vacuoles (**Figure 8a**). The diabetic group showed thickened basement membrane, distorted apical microvilli, pyknotic nucleus. The cytoplasm showed vacuoles and swollen mitochondria (**Figure 8b**). The treated group showed normal nucleus, mitochondria, apparent microvilli, and autophagic vacuoles (**Figures 8c** and **8d**). The number of autophagic vacuoles was significantly less in the diabetic

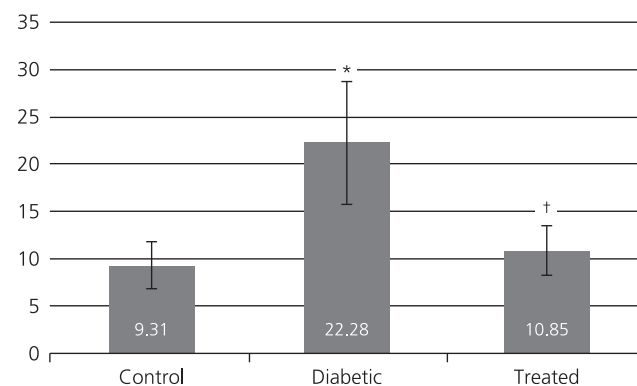


Figure 5. The mean fibrosis area in control, diabetic and treated groups (mean \pm SD; $n=12$). * $p < 0.05$ compared to the control group; † $p < 0.05$ compared to the diabetic group.

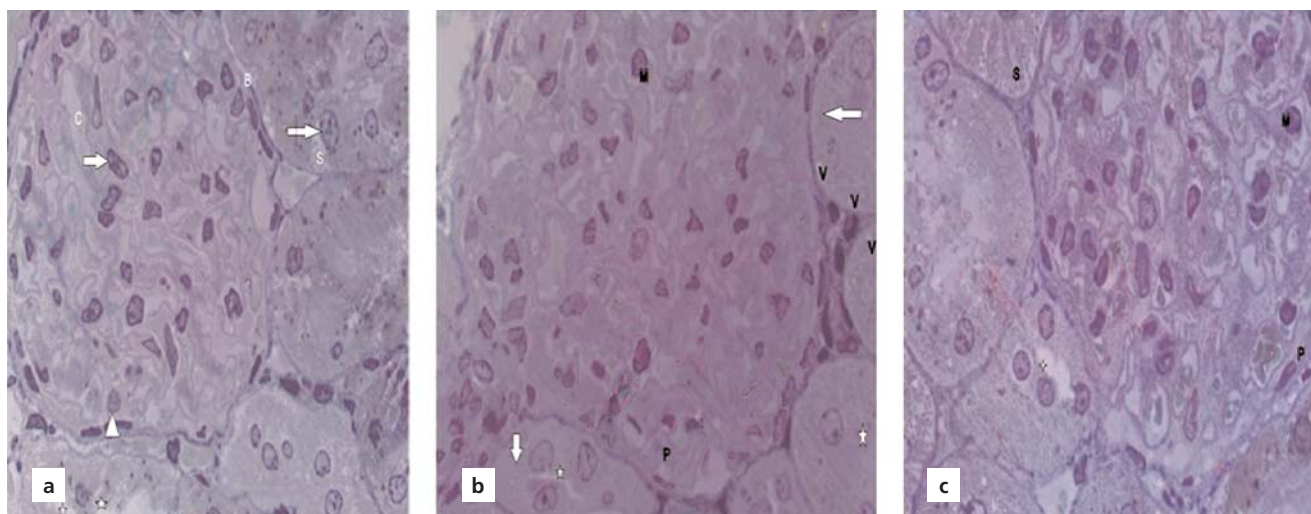


Figure 6. Photomicrographs of semithin sections of the renal cortex. (a) The control group shows normal renal corpuscle containing a glomerulus, with mesangial cells (arrow), podocytes (arrowhead), capillaries and intact basement membrane. The tubules' shows cells basal striations, apparent brush borders (*) and large vesicular nuclei (crossed arrow); (b) The diabetic kidney shows glomerulus with podocyte, mesangial cells, renal tubules with absent basal striation (arrow), lost brush border (*), areas of cytoplasmic vacuolation. (c) The treated kidney shows the glomerulus, with mesangial cells and podocytes. The tubules cells shows restored basal striations, restored apparent brush borders (*). C: capillaries; m: mesangial cells; P: podocytes; S: basal striations; V: cytoplasmic vacuoles (Toluidine blue stain, $\times 1000$). [Color figure can be viewed in the online issue, which is available at www.anatomy.org.tr]

group as compared to both control and treated groups ($p < 0.05$; Table 5).

Discussion

The present study provided evidence that empagliflozin induces an efficient, but not complete protection against DN. This conclusion is supported by our results which demonstrated that empagliflozin prevented kidney injuries occurred after 4 weeks in streptozotocin-nicotinamide-induced type 2 diabetic rat model. Empagliflozin significantly lowered the increased blood glucose, BUN, serum creatinine, and oxidative stress biomarkers that are known to be elevated in DN. Furthermore, it reduced renal tissue degeneration, fibrosis, and glomerular space; however, it did not reduce the increased kidney index and glomerular size. Beside the amelioration of ultrastructure

changes occurred in the renal cortex, we reported for the first time that empagliflozin enhanced autophagy in renal tubular cells which was indicated by increased number of autophagic vacuoles.

Approximately half of cases with type 2 diabetes and one third of cases with type 1 diabetes develop DN.^[27] Recent reports ensure that ten years mortality rates of cases with DN equal mortality rates of all cancers.^[28,29] Therefore, there is an urgent motivation to develop effective medication to slow the progression of DN.

Early intensive glycemic control is a critical strategy for prevention and delay of DN progression. However, the currently used hypoglycemic drugs fail to achieve optimum blood glucose levels and are associated with hypoglycemia and weight gain.^[30] Therefore, there is a need for new drugs that control the blood glucose level and have protective pathways. The SGLT2 inhibitors have recently being used widely.^[31] Based on their insulin-independent action and effect in losing weight, SGLT2 inhibitors would be expected to be more beneficial than the current therapies of DM. Empagliflozin, one of selective SGLT2 inhibitors, attenuates DN^[32] and cardiovascular diseases in patients with type 2 DM.^[33]

A series of experimental studies have shown that empagliflozin exerts renoprotective benefits (Table 6). It was reported to decrease blood glucose and albuminuria and ameliorate glomerular hypertrophy, mesangial expan-

Table 5

Comparison of the glomerular basement membrane thickness, and the number of autophagy vacuoles in the proximal renal tubules (mean \pm SD; n=12).

	Control	Diabetic	Treated
Thickness (μm)	1.47	2.83*	1.6 [†]
Number of autophagy vacuoles	.7/100 μm^2	.4/100 μm^2 *	.6/100 μm^2 [†]

* $p < 0.05$ compared to the the control group; [†] $p < 0.05$ compared to the diabetic group.

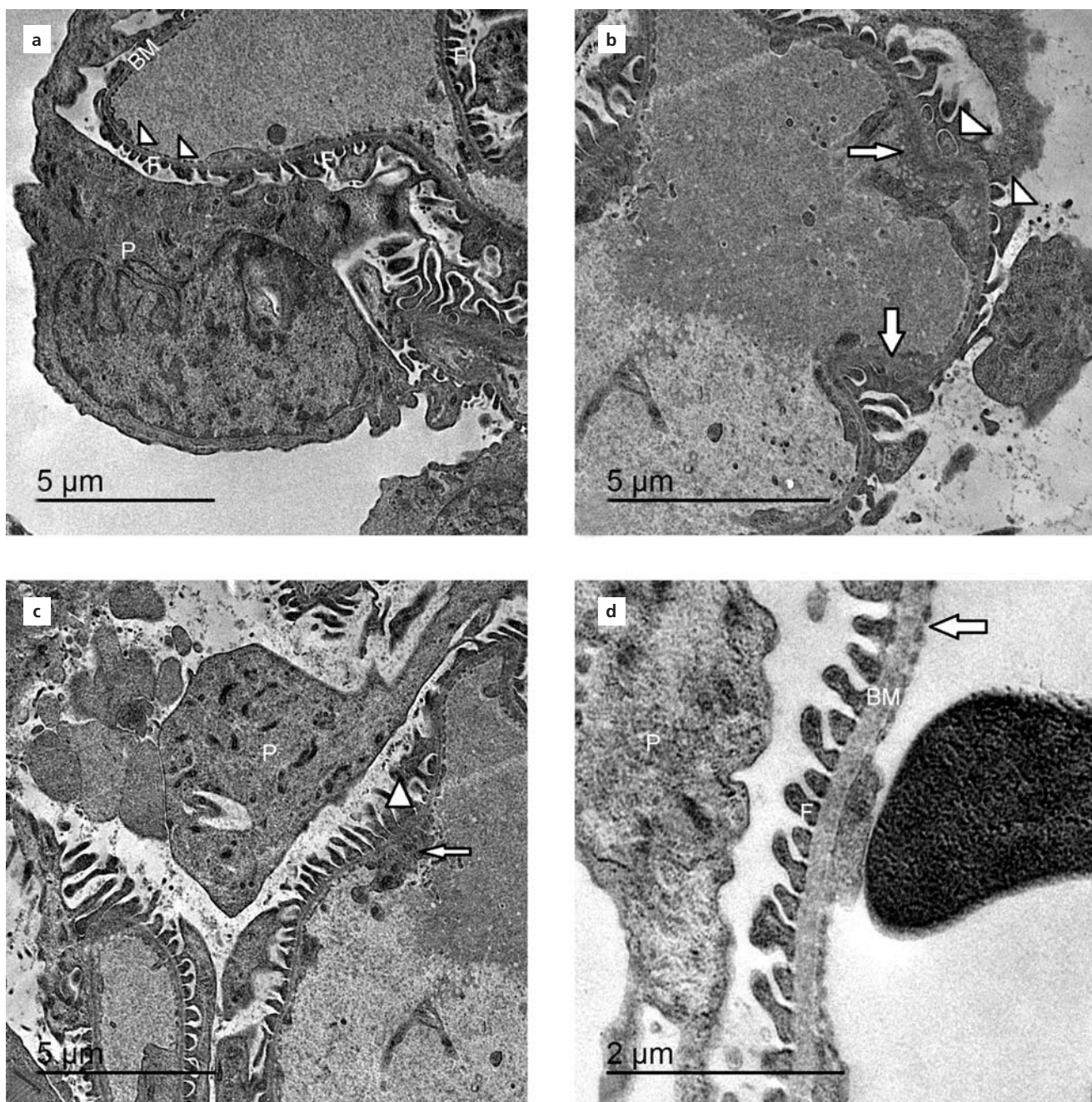


Figure 7. Photomicrographs of ultrathin section of the glomerulus. (a) The control group shows normal fenestrated endothelial cell (arrowhead); (b, c) Regular basement membrane, podocytes, foot processes of podocytes. The diabetic group shows areas of fusion of the foot processes (arrowheads) with thickened basement membrane (arrows) and degenerated podocytes. (d) The treated group shows regular basement membrane, foot processes of normal podocytes, intact endothelial lining (arrow). BM: basement membrane; F: foot processes of podocytes; P: podocytes.

sion, renal fibrosis, inflammatory and oxidative stress markers in different diabetic animal models.^[16,25,30,34,35] However, none of these previous studies have demonstrated the protective effect of empagliflozin at the ultrastructural level. A summary of the effects of empagliflozin on experimental DN is shown in **Table 7**.

In agreement with the previous studies, the present work demonstrated maintenance of body weight, significant reduction in blood glucose, and improvement in the kidney function after 4 weeks empagliflozin treatment. The only exception is the study of Lee et al.^[30] who demonstrated significant reduction in body weight after 24 weeks

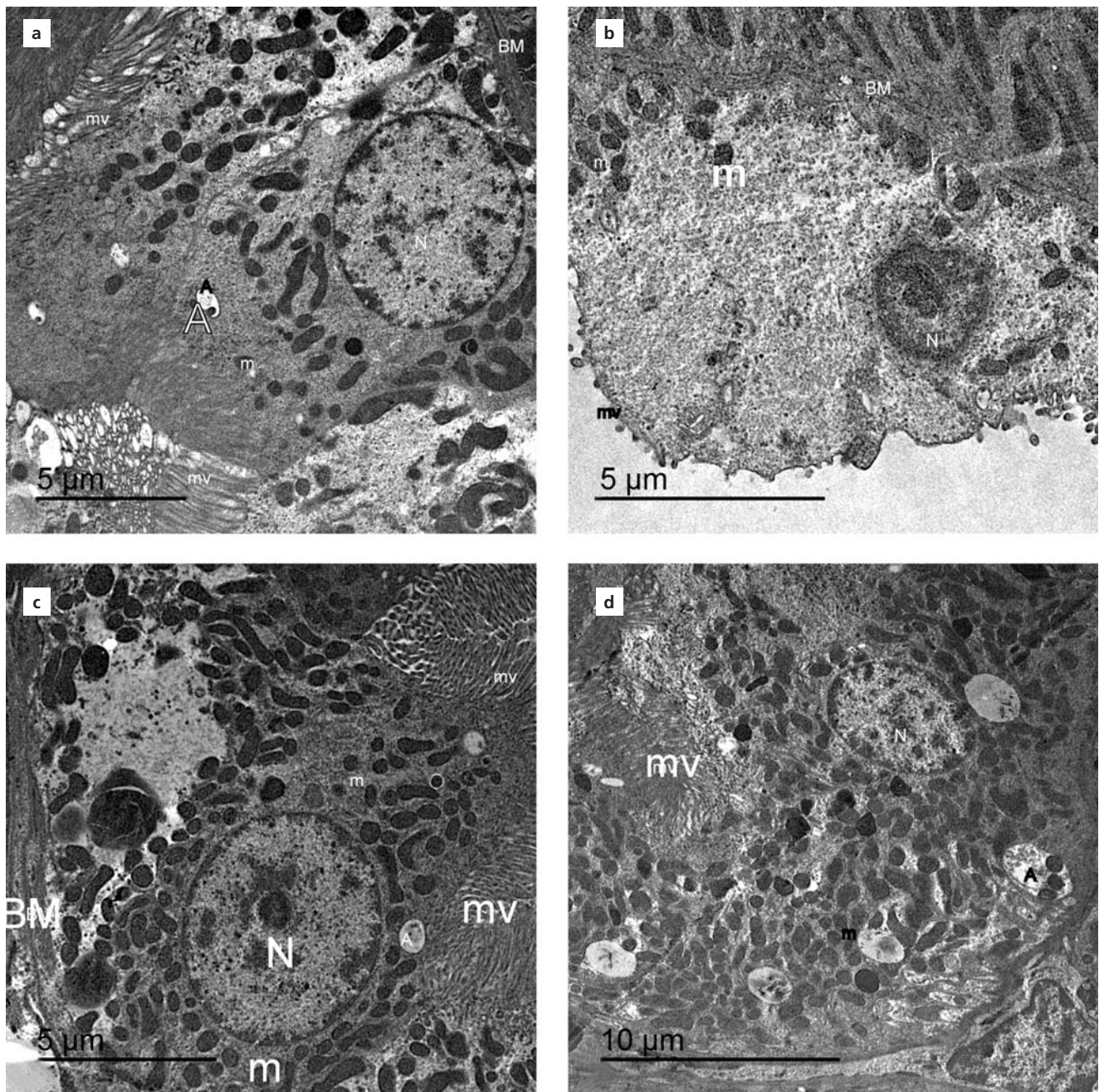


Figure 8. Photomicrographs of ultrathin sections of the proximal convoluted tubules. (a) The control group shows normal proximal tubular cells, regular basement membrane, apical microvilli, the nucleus appeared rounded and euchromatic, numerous mitochondria and autophagy vacuoles; (b) The diabetic group shows thickened basement membrane, distorted apical microvilli, pyknotic nucleus, the cytoplasm with vacuoles and swollen mitochondria; (c, d) The treated group shows thin basement membrane, normal nucleus, mitochondria, apparent microvilli and autophagic vacuoles. A: autophagy vacuoles; BM: basement membrane; m: mitochondria; mv: microvilli; N: nucleus.

empagliflozin treatment compared to the diabetic group. This may be related to longer duration of their study.

The present study also demonstrated improvement in renal histology indicated by decreased renal tubular degeneration and glomerular space in the empagliflozin

treated group. However, in contrast with the previous studies,^[34-36] we couldn't demonstrate a reduction in the increased glomerular size or kidney index after 4 weeks of empagliflozin treatment which indicated partial protection. This may be explained by shorter duration or

Table 6
Literature review of the effects of empagliflozin on experimental DN.

Experimental model	Dose of empagliflozin	Duration of study	Main effects	Study reference
BTBR ob/ob mice	Diet with 300 ppm of empagliflozin	12 weeks	= Body weight ↓ Blood glucose ↓ Albuminuria ↓ Glomerular hypertrophy ↓ Inflammation ↓ Mesangial matrix expansion	[34]
STZ-diabetic rats	10 mg/kg	4 weeks	↓ Blood glucose ↓ Oxidative stress ↓ Inflammation ↓ Fibrotic gene markers ↓ Tubular injury	[16]
Akita mice	300 mg/kg	15 weeks	↓ Glomerular hyperfiltration ↓ Albuminuria ↓ Kidney Weight ↓ Inflammation	[35]
db/db mice	10 mg/kg	10 weeks	= Body weight ↓ Kidney weight ↓ Blood glucose = Albuminuria ↓ Profibrotic gene markers ↓ Collagen IV ↓ TGF-β	[36]
STZ-diabetic rats	3 mg/kg	24 weeks	= Blood glucose ↓ Body weight ↓ Albuminuria = Glomerulosclerosis = Mesangial matrix expansion	[30]
	10 mg/kg	24 weeks	↓ Blood glucose ↓ Body weight ↓ Albuminuria ↓ Glomerulosclerosis ↓ Mesangial matrix expansion	[30]

smaller dose in our study, as well as the different animal model.

Another mechanism that may explain the nephroprotective effect of SGLT-2 inhibitor is the improvement of renal hypoxia in diabetic kidneys.^[37] It was reported that hyperglycaemia-induced changes in intracellular metabolism, like glycation end products accumulation, and free radical are main factors in the development of DN.^[31]

In agreement with Ojima et al.^[16] the present study demonstrated significant reduction in oxidative stress marker MDA in empagliflozin treated group compared to the diabetic group. This could be explained by increased glucose uptake in the kidney in diabetes which leads to increase intracellular glucose levels and in turn

stimulates reactive oxygen species (ROS) production.^[38,39] Also, proximal convoluted tubule is the site of reabsorption of organic solutes and electrolytes, which are oxygen dependent processes that cause a reduction of oxygen tension in the kidney tissue. SGLT-2 inhibitors decrease the reabsorption of sodium and glucose and therefore reduce tubular work load and improve renal oxygenation, resulting in improvement of tubular structure and function.^[40]

Inflammation, fibrosis and oxidative stress are involved in the initiation and progression of kidney disease.^[41,42] The present work demonstrated significant reduction in surface area of Masson's stained collagen fibers in the empagliflozin treated group. This finding

was in agreement with Gallo et al.^[36] and other studies which linked SGLT-2 inhibitors with reduction in anti-oxidant and antifibrotic markers.^[43]

Another cellular insult from hyperglycaemia is altered autophagic response due to cellular stress which is supposed to have a fundamental role in initiation and progression of DN.^[44] Autophagy is a highly regulated lysosomal pathway involved in the removal of damaged organelles and protein aggregates to keep cell integrity.^[45] It acts as an important role in maintenance of glomerular and tubular hemostasis. Therefore, insufficient autophagy against stresses such as hyperglycaemia may cause renal cells injuries.^[31] Recent studies highlighted the role of autophagy in the pathogenesis of DN.^[46-48] Reduction of autophagy results in podocyte degeneration, glomerular endothelial changes and increased collagen deposition.^[49]

Until the current study, whether empagliflozin exerted any ameliorating effect in the autophagy of diabetic kidney was unknown. To address this question, we used TEM to monitor the appearance of autophagosomes and check changes in renal tubular and glomerular structures.

In agreement with the previous studies,^[26,50] ultrastructural examination of diabetic kidney revealed degenerated renal tubular cells with occasional autophagic vacuoles, pronounced podocyte foot process fusion and GBM thickening. On the other hand, the tubular and podocyte injuries were greatly improved, thickness of the GBM was markedly reduced, and a significant higher number of autophagic vacuoles were detected in the proximal tubular cells in the empagliflozin treated group. Similarly, administration of another SGLT2 inhibitor, dapagliflozin, to db/db mice resulted in reduction podocyte foot process diameter by 44.9% and GBM thickness by 37.7%.^[22] It is worth mentioning that Vallon et al.^[51] demonstrated that a lack of SGLT2 gene resulted in reduced renal accumulation of p62 which is an indicator of active autophagy in SGLT2-deficient diabetic mice.

In hyperglycaemia, there is increased mTORC1 expression in podocytes and decreased autophagic activity with renal injury and fibrosis. So, activation of autophagy in the tubular cells could maintain the cellular homeostasis, stress resistance, prevents tubulointerstitial fibrosis. Therefore, the autophagy improvement may be a novel therapy for the suppression of DN.^[31]

In the light of our results, it seems that empagliflozin might be protective against DN through the restoration of autophagy activity in diabetic kidneys. This will stimulate further studies in the future to declare this cellular pathway as a new pathway where SGLT2 inhibitor empagliflozin is involved in renal protection.

Conclusion

The use of new anti-diabetic SGLT2 inhibitors creates a new era of DM treatment and reduction of its complications. Our experimental model revealed that treatment with empagliflozin significantly improved renal function and ameliorated the tubular and glomerular changes induced by diabetes in NA-STZ-treated rats. We hypothesize that its protective effect is related to reduction of hyperglycemia and improvement of cellular defense mechanisms by other effects of high glucose such as oxidative stress and autophagy induction.

References

1. Molitch ME, DeFronzo RA, Franz MJ, Keane WF, Mogensen CE, Parving HH, Steffes MW. Nephropathy in diabetes. *Diabetes Care* 2004;27:79–83.
2. Ruggenenti P, Cravedi P, Remuzzi G. The RAAS in the pathogenesis and treatment of diabetic nephropathy. *Nat Rev Nephrol* 2010;6:319–30.
3. Liu WJ, Huang WF, Ye L, Chen RH, Yang C, Wu HL, Pan QJ, Liu HF. The activity and role of autophagy in the pathogenesis of diabetic nephropathy. *Eur Rev Med Pharmacol* 2018;22:3182–9.
4. Kawanami D, Matoba K, Takeda Y, Nagai Y, Akamine T, Yokota T, Sango K, Utsunomiya K. SGLT2 inhibitors as a therapeutic option for diabetic nephropathy. *Int J Mol Sci* 2017;18. pii: E1083.
5. Shen Z, Fang Y, Xing T, Wang F. Diabetic nephropathy: from pathophysiology to treatment. *J Diabetes Res* 2017;2379432.
6. Rubinsztein DC, Marino G, Kroemer G. Autophagy and aging. *Cell* 2011;146:682–95.
7. Gonzalez CD, Lee MS, Marchetti P, Pietropaolo M, Towns R, Vaccaro MI, Watada H, Wiley JW. The emerging role of autophagy in the pathophysiology of diabetes mellitus. *Autophagy* 2011;7:2–11.
8. Yang C, Kaushal V, Shah SV, Kaushal GP. Autophagy is associated with apoptosis in cisplatin injury to renal tubular epithelial cells. *Am J Physiol Renal Physiol* 2008;294:F777–87.
9. Hartleben B, Godel M, Meyer-Schwesinger C, Liu S, Ulrich T, Kobler S, Wiech T, Grahmmer F, Arnold SJ, Lindenmeyer MT, Cohen CD, Pavenstadt H, Kerjaschki D, Mizushima N, Shaw AS, Walz G, Huber TB. Autophagy influences glomerular disease susceptibility and maintains podocyte homeostasis in aging mice. *J Clin Invest* 2010;120:1084–96.
10. Jung CH, Jang JE, Park JY. A novel therapeutic agent for type 2 diabetes mellitus: SGLT2 inhibitor. *Diabetes Metab J* 2014;38:261–73.
11. Syed SH, Gosavi S, Shami W, Bustamante M, Farah Z, Teleb M, Abbas A, Said S, Mukherjee D. A review of sodium glucose co-transporter inhibitors canagliflozin, dapagliflozin and empagliflozin. *Cardiovasc Hematol Agents Med Chem* 2015;13:105–12.
12. Takakura S, Toyoshi T, Hayashizaki Y, Takasu T. Effect of ipragliflozin, an SGLT2 inhibitor, on progression of diabetic microvascular complications in spontaneously diabetic Torii fatty rats. *Life Sci* 2016;147:125–31.
13. Fioretto P, Zambon A, Rossato M, Busetto L, Vettor R. SGLT2 inhibitors and the diabetic kidney. *Diabetes Care* 2016;39:165–71.
14. Miller EM. Elements for success in managing Type 2 diabetes with SGLT-2 inhibitors: role of the kidney in glucose homeostasis: implications for SGLT-2 inhibition in the treatment of type 2 diabetes mellitus. *J Fam Pract* 2017;66:S3–S5.

15. Baker W, Smyth L, Riche D, Bourret E, Chamberlin K, White WB. Effects of sodium-glucose co-transporter 2 inhibitors on blood pressure: a systematic review and meta-analysis. *J Am Soc Hypertens* 2014; 8:262–75.
16. Ojima A, Matsui T, Nishino Y, Nakamura N, Yamagishi S. Empagliflozin, an inhibitor of sodium-glucose cotransporter 2 exerts anti-inflammatory and antifibrotic effects on experimental diabetic nephropathy partly by suppressing AGEs-receptor axis. *Horm Metab Res* 2015;47:686–92.
17. Shirwaikar A, Rajendran K, Barik R. Effect of aqueous bark extract of *Garuga pinnata Roxb* in streptozotocin-nicotinamide induced type-II diabetes mellitus. *J Ethnopharmacol* 2006;107:285–90.
18. Mokhtare B, Cetin M, Ozakar RS, Bayrakceken H. *In vitro* and *in vivo* evaluation of alginate and alginatechitosan beads containing metformin hydrochloride. *Trop J Pharm Res* 2017;16:287–96.
19. Ma ZN, Li YZ, Li W, Yan XT, Yang G, Zhang J, Zhao LC, Yang LM. Nephroprotective effects of saponins from leaves of *Panax quinquefolius* against cisplatin-induced acute kidney injury. *Int J Mol Sci* 2017;18:1407.
20. Bancroft JD, Gamble M. Theory and practice of the histological techniques. 5th ed. London: Churchill Livingstone; 2002. p.125–39.
21. Chen Y, Yu Q, Cang-Bao X. A convenient method for quantifying collagen fibers in atherosclerotic lesions by Image software. *International Journal of Clinical Experimental Medicine* 2017;10:14904–10.
22. Han E, Shin E, Kim G, Lee JY, Lee YH, Lee BW, Kang ES, Cha BS. Combining SGLT2 Inhibition with a thiazolidinedione additively attenuate the very early phase of diabetic nephropathy progression in type 2 diabetes mellitus. *Front Endocrinol (Lausanne)* 2018;9:412.
23. Johora F, Nurunnabi ASM, Shahriah S, Ahmed R, Ara S. Histomorphometric study of the glomeruli of the kidney in Bangladeshi population. *Journal of Bangladesh Society of Physiologist* 2014;9:11–16.
24. Dallak M, Bin-Jalilah I, Al-Hashem F, Kamar SS, Abdel Kader DH, Amin SH, Haidara MA, Al-Ani B. Metformin pretreatment ameliorates diabetic nephropathy induced by a combination of high fat diet and streptozotocin in rats. *International Journal of Morphology* 2018;36:969–74.
25. Abdel-Dayem MM, Hatem MM, Elgendy MS. Histological and immunohistochemical study on nitric oxide synthase and effects of angiotensin receptor blockade in early phase of diabetes in rat kidney. *British Journal of Medicine & Medical Research* 2014;4:3317–38.
26. Geng Y, Chen G, Mao X, Wei X, Li X, Fan K, Lu Y, Liu C. Low-protein calorie-restricted diet attenuates renal injury and facilitates podocyte autophagy in type 2 diabetic rats. *International Journal of Clinical and Experimental Medicine* 2018;11:9343–52.
27. Reutens AT. Epidemiology of diabetic kidney disease. *Med Clin North Am* 2013;97:1–18.
28. Afkarian M, Sachs MC, Kestenbaum B, Hirsch IB, Tuttle KR, Himmelfarb J, de Boer IH. Kidney disease and increased mortality risk in type 2 diabetes. *J Am Soc Nephrol* 2013;24:302–308.
29. Quaresma M, Coleman MP, Rachet B. 40-year trends in an index of survival for all cancers combined and survival adjusted for age and sex for each cancer in England and Wales, 1971–2011: a population-based study. *Lancet* 2015;385:1206–18.
30. Lee KA, Jin HY, Lee NY, Kim YJ, Park TS. Effect of empagliflozin, a selective sodium glucose cotransporter 2 inhibitor, on kidney and peripheral nerves in streptozotocin induced diabetic rats. *Diabetes Metab* 2018;42:338–42.
31. Rola N, Elias K, Farid N, Inbal D, Farber E, Anam H, Nakhoul N. Sodium-glucose transporter inhibitors and diabetic nephropathy in humans and animal model. *J Clin Exp Nephrol* 2018;3:2–10.
32. Wanner C, Inzucchi SE, Lachin JM, Fitchett D, von Eynatten M, Mattheus M, Johansen OE, Woerle HJ, Broedl UC, Zinman B. Empagliflozin and progression of kidney disease in type 2 diabetes. *N Engl J Med* 2016;375:323–34.
33. Zinman B, Wanner C, Lachin JM, Fitchett D, Bluhmki E, Hantel S, Mattheus M, Devins T, Johansen OE, Woerle HJ, Broedl UC, Inzucchi SE. Empagliflozin, cardiovascular outcomes, and mortality in type 2 diabetes. *N Engl J Med* 2015;373:2117–28.
34. Gemhardt F, Bartaun C, Jarzebska N, Mayoux E, Todorov VT, Hohenstein B, Hugo C. The SGLT2 inhibitor empagliflozin ameliorates early features of diabetic nephropathy in BTBR ob/ob type 2 diabetic mice with and without hypertension. *Am J Physiol Ren Physiol* 2014;307:F317–25.
35. Gallo LA, Ward MS, Fotheringham AK, Zhuang A, Borg DJ, Flemming NB, Harvie BM, Kinneally TL, Yeh SM, McCarthy DA, Koepsell H, Vallon V, Pollock C, Panchapakesan U, Forbes JM. Once daily administration of the SGLT2 inhibitor, empagliflozin, attenuates markers of renal fibrosis without improving albuminuria in diabetic db/db mice. *Sci Rep* 2016;6:26428.
36. Vallon V. The mechanisms and therapeutic potential of SGLT2 inhibitors in diabetes mellitus. *Annu Rev Med* 2015;66:255–70.
37. Sano M, Takei M, Shiraishi Y, Suzuki Y. Increased hematocrit during sodium-glucose cotransporter 2 inhibitor therapy indicates recovery of tubulointerstitial function in diabetic kidneys. *J Clin Med Res* 2016;8:844–47.
38. Garg MC, Ojha S, Bansal DD. Antioxidant status of streptozotocin diabetic rats. *Indian J Exp Biol* 1996;34:264–66.
39. Ha H, Lee HB. Reactive oxygen species amplify glucose signalling in renal cells cultured under high glucose and in diabetic kidney. *Nephrology (Carlton)* 2005;10:S7–10.
40. Dekkers CCJ, Gansevoort RT, Heerspink HJL. New diabetes therapies and diabetic kidney disease progression: the role of SGLT-2 inhibitors. *Curr Diab Rep* 2018;18:27.
41. Wolkow PP, Niewczas MA, Perkins B, Ficociello LH, Lipinski B, Warram JH, Krolewski AS. Association of urinary inflammatory markers and renal decline in microalbuminuric type 1 diabetics. *J Am Soc Nephrol* 2008;19:789–97.
42. Sangoi MB, de Carvalho JA, Tatsch E, Hausen BS, Bollick YS, Londero SW, Duarte T, Scolari R, Duarte MMMF, Premaor MO, Comim FV, Moretto MB, Moresco RN. Urinary inflammatory cytokines as indicators of kidney damage in type 2 diabetic patients. *Clin Chim Acta* 2016;460:178–83.
43. Salim HM, Fukuda D, Yagi S, Soeki T, Shimabukuro M, Sata M. Glycemic control with ipragliflozin, a novel selective SGLT2 inhibitor, ameliorated endothelial dysfunction in streptozotocin-induced diabetic mouse. *Front Cardiovasc Med* 2016;3:43.
44. Kimura T, Takabatake Y, Takahashi A, Kaimori JY, Matsui I, Namba T, Kitamura H, Niimura F, Matsusaka T, Soga T, Rakugi H, Isaka Y. Autophagy protects the proximal tubule from degeneration and acute ischemic injury. *J Am Soc Nephrol* 2011;22:902–13.
45. Klionsky DJ, Emr SD. Autophagy as a regulated pathway of cellular degradation. *Science* 2000;290:1717–21.
46. Yasuda-Yamahara M, Kume S, Tagawa A, Maegawa H, Uzu T. Emerging role of podocyte autophagy in the progression of diabetic nephropathy. *Autophagy* 2015;11:2385–6.

47. Tagawa A, Yasuda M, Kume S, Yamahara K, Nakazawa J, Chin-Kanasaki M, Araki H, Araki SI, Koya D, Asanuma K, Kim EH, Haneda M, Kajiwara N, Hayashi K, Ohashi H, Ugi S, Maegawa H, Uzu T. Impaired podocyte autophagy exacerbates proteinuria in diabetic nephropathy. *Diabetes* 2016;65:755–67.
48. Yang D, Livingston MJ, Liu Z, Dong G, Zhang M, Chen JK, Dong Z. Autophagy in diabetic kidney disease: regulation, pathological role and therapeutic potential. *Cell Mol Life Sci* 2018;75:669–88.
49. Fang L, Zhou Y, Cao H, Wen P, Jiang L, He W, Dai C, Yang J. Autophagy attenuates diabetic glomerular damage through protection of hyperglycemia-induced podocyte injury. *PLoS One* 2013;8:e60546.
50. Miko M, Jakubovsky J, Vrabceva M, Varga. Ultrastructural changes of kidney in diabetic rats. *Bratisl Lek Listy* 2016;117:161–5.
51. Vallon V, Rose M, Gerasimova M, Satriano J, Platt KA, Koepsell H, Cunard R, Sharma K, Thomson SC, Rieg T. Knockout of Na-glucose transporter SGLT2 attenuates hyperglycemia and glomerular hyperfiltration but not kidney growth or injury in diabetes mellitus. *Am J Physiol Ren Physiol* 2013;304:F156–67.

ORCID ID:

M. Abd El-kader 0000-0002-3975-8586;
H. A. Hashish 0000-0003-4245-7650



Correspondence to: Hagar A. Hashish, MD

Department of Anatomy and Embryology, School of Medicine,
Mansoura University, 35516, Mansoura, Egypt
Phone: +201006392728
e-mail: dr.hagar1979@gmail.com

Conflict of interest statement: No conflicts declared.

This is an open access article distributed under the terms of the Creative Commons Attribution-NonCommercial-NoDerivs 3.0 Unported (CC BY-NC-ND3.0) Licence (<http://creativecommons.org/licenses/by-nc-nd/3.0/>) which permits unrestricted noncommercial use, distribution, and reproduction in any medium, provided the original work is properly cited. *Please cite this article as:* Abd El-kader M, Hashish HA. Potential role of empagliflozin in prevention of nephropathy in streptozotocin-nicotinamide-induced type 2 diabetes: an ultrastructural study. *Anatomy* 2019;13(3):137–148.

Comparison of macerations with dermestid larvae, potassium hydroxide and sodium hypochlorite in Wistar rat crania

Daniela Botero-González , Marcela Agudelo 

School of Biomedical Sciences, Universidad del Valle, Cali, Colombia

Abstract

Objectives: The aim of this study was to determine the most effective maceration method to remove soft tissue without altering bone tissue conformation.

Methods: A comparison was made between maceration with insects and chemical maceration performed on heads of Wistar rats. The sample consisted of 18 biomodels, six of which were macerated by dermestid larvae and the remaining 12 divided into two groups for chemical maceration, one with potassium hydroxide and the other with sodium hypochlorite. In chemical maceration, 1%, 5% and 10% concentrations were used with varying exposure times and temperature.

Results: The ideal method for soft tissue maceration, preserving all bone components, was shown to be maceration with insects. Potassium hydroxide was effective in the removal of soft tissue. However, being a highly corrosive chemical agent, it altered the integrity of the bone tissue. Sodium hypochlorite did not meet the maceration objective.

Conclusion: This research is relevant in its contribution to discussions on appropriate maceration techniques for small bone structures.

Keywords: bone; bone tissue integrity; chemical maceration; dermestid; maceration; osteology; skull; soft tissue maceration; tissue dissolution

Anatomy 2019;13(3):149–154 ©2019 Turkish Society of Anatomy and Clinical Anatomy (TSACA)

Introduction

Maceration provides bone pieces on which morphological and morphometric studies can be carried out. In the fields of anatomy and morphology, it has proved to be a powerful tool to produce analysis on morphometry of bone structures, which is not only qualitative but also quantitative. For this reason, maceration is an important technique for visualizing the bone component.

Various maceration techniques provide removal of the soft tissue adhered to bone structures. The most common maceration techniques are use of inorganic chemical agents and insects. The length of time required to carry out the different techniques vary according to the size of the specimen, the ambient temperature and the technique itself.^[1] In this study, three types of maceration on Wistar rat skulls were compared with the objective of establishing the most effective method to remove soft tissue, while

keeping the hard connective tissues in optimal condition: maceration using potassium hydroxide (KOH), sodium hypochlorite (NaClO) and dermestid larvae.

Materials and Methods

This research was part of a project entitled “Evaluation of the effect of obesity on craniofacial morphology in Wistar rats in the neonatal (p21), preadolescent (p38) and young adult (p77) stages”, approved by the Human and Animal Ethics Committee of the Faculty of Health in the Universidad del Valle, Cali, Colombia (Internal code: 013–017). The biomodels were used in accordance with the international principle of the 3Rs, (Replacement, Reduction and Refinement), once the aforementioned research had ended.

Maceration was carried out on 18 adult rats (*Rattus norvegicus*) of the Wistar strain from the Intermediate

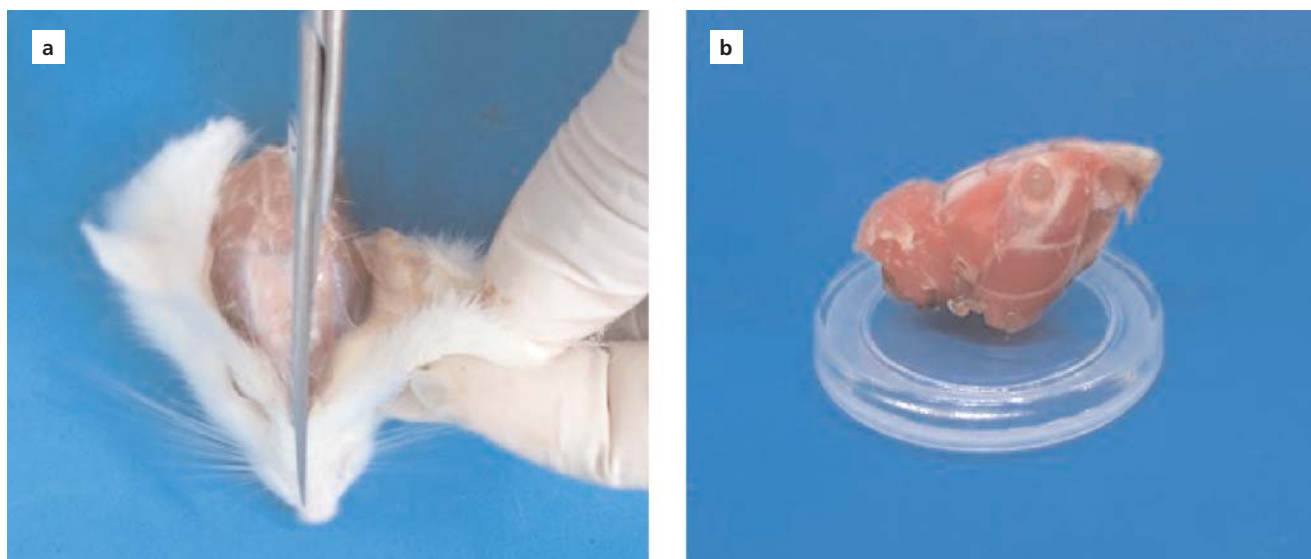


Figure 1. Wistar rat biomodel: (a) removal of the skin; (b) head removed. [Color figure can be viewed in the online issue, which is available at www.anatomy.org.tr]

Laboratory of Preclinical and Animal Testing Research (LABBIO) of the Universidad del Valle in Cali, Colombia. Six of the biomodels were subjected to maceration by dermestid larvae while the remaining 12 to maceration with chemicals. The latter were euthanized with pentobarbital (390 mg/ml) and diphenylhydantoin sodium (50 mg/ml) applied intramuscularly (IM).

Subsequently, modifying the sampling protocol of Gage et al.,^[2] all biomodels were cross-sectioned at the fifth cervical vertebra to obtain the head and the skin removed ventrally and dorsally towards the nose (**Figure 1**). During maceration with chemicals, written and photographic

records were made during the first three days and on days 9 and 27. The heads were assigned randomly to the various maceration types. Each head was weighed on a calibrated electronic scale, Radwag brand, model WLC 2 / A2 (**Table 1**).

Maceration by Dermestid Larvae

For this study, one group of maceration was performed using dermestid larvae, which feed on dry animal material, primarily during the larval stage. The colony belonged to the Zoology Department of the Faculty of Biology at the Universidad del Valle. The beetle colony was maintained at an average temperature of 25°C with indirect natural

Table 1
Maceration type, biomodel number used (n), average weight (gr) and temperature.

Groups	Maceration	Biomodel (n)	Weight (gr)	Temperature
Group 1	Dermestid larvae	13 to 18	13.16	Room temperature
Group 2	KOH at 1%	3	15.40	Oven
	KOH at 1%	8	13.93	Room temperature
	KOH at 5%	4	12.81	Oven
	KOH at 5%	9	16.14	Room temperature
	KOH at 10%	10	13.96	Room temperature
	KOH at 10%	11	14.30	Oven
Group 3	NaClO at 1%	7	14.16	Room temperature
	NaClO at 1%	12	13.41	Oven
	NaClO at 5%	1	11.00	Oven
	NaClO at 5%	6	14.01	Room temperature
	NaClO at 10%	2	11.07	Oven
	NaClO at 10%	5	12.80	Room temperature



Figure 2. Maceration by dermestid larvae: (a) external base of cranium as viewed from above; (b) external base of skull as viewed from below; (c) jaw. [Color figure can be viewed in the online issue, which is available at www.anatomy.org.tr]

light. For this maceration, the biomodel was euthanized with inhaled isoflurane; the technique used on the other 12 biomodels could not be performed in this case as exposure to chemicals intramuscularly in the specimen results in rejection of the tissue by the dermestid colony. Once the heads were obtained and the skin removed as detailed in the chemical macerations, the tongue, eyes and brain were removed to facilitate handling in the colony. The heads were put in an oven (Thermo Fisher Scientific Inc, Waltham, MA, USA; model 6528) for drying the soft tissue at a temperature of 56°C for 12 hours before being taken to the colony where it remained for eight days.

Maceration with KOH

Six KOH solutions were prepared in glass containers, two for each concentration. The solutions were 1% (1 g of KOH/100 ml of distilled water), 5% (5 g of KOH/100 ml of distilled water) and 10% (10 g of KOH/100 ml of distilled water). Six heads were selected at random and divided into two equal groups: Group A: Heads were subjected to heat in an oven (Precision Scientific Co, Tamil Nadu, India, model 16), at a temperature that ranged between 37°C and 45.5°C; Group B: Heads were kept at room temperature which ranged between 21.5°C and 25.4°C. The

distribution of concentrations for each group is shown in **Table 1**.

Maceration with NaClO

Six NaClO solutions were prepared in plastic containers, two for each concentration. The solutions were 1% (7.7 ml of NaClO/92.3 ml of distilled water), 5% (38.4 ml of NaClO/61.6 ml of distilled water) and 10% (76.9 ml of NaClO/23.1 ml of distilled water). Six heads were selected at random and divided into two equal groups: Group A: Heads were subjected to heat in an oven (Precision Scientific Co, Tamil Nadu, India, model 16), at a temperature that ranged between 37°C and 45.5°C; Group B: Heads were kept at room temperature which ranged between 21.5°C and 25.4°C. The distribution of concentrations for each group is shown in **Table 1**.

Results

Soft tissue maceration was achieved in two of the three methods evaluated. The dermestid larvae completely macerated the soft tissue, while preserving the bone tissue intact (**Figure 2**). KOH eliminated the majority of soft tissue. However, it disarticulated some bones and caused

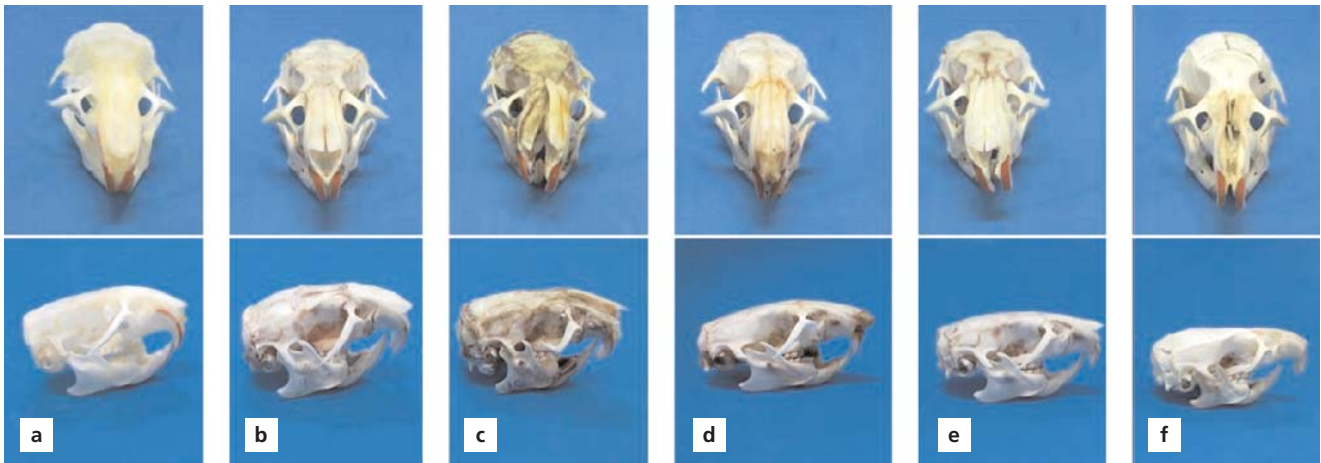


Figure 3. Results of maceration with (a) 1% KOH at room temperature; (b) 5% KOH at room temperature; (c) 10% KOH at room temperature; (d) 1% KOH at oven temperature; (e) 5% KOH at oven temperature; (f) 10% KOH at oven temperature. [Color figure can be viewed in the online issue, which is available at www.anatomy.org.tr]

some bone loss in others (**Figure 3**). NaClO did not meet the objective of macerating the soft tissue (**Figure 4**).

Discussion

The experiments showed that maceration by dermestid larvae was the most effective method as the hard tissue did not present any type of alteration and the soft tissue

was removed in its entirety, preserving the bone piece in excellent condition. However, it is essential that the bio-model has not been exposed to any chemical agent or substance that emanates odor, so that it can be processed by these larvae. Taking into account the weight of the biomodel, the time required to obtain the desired final result was eight days.

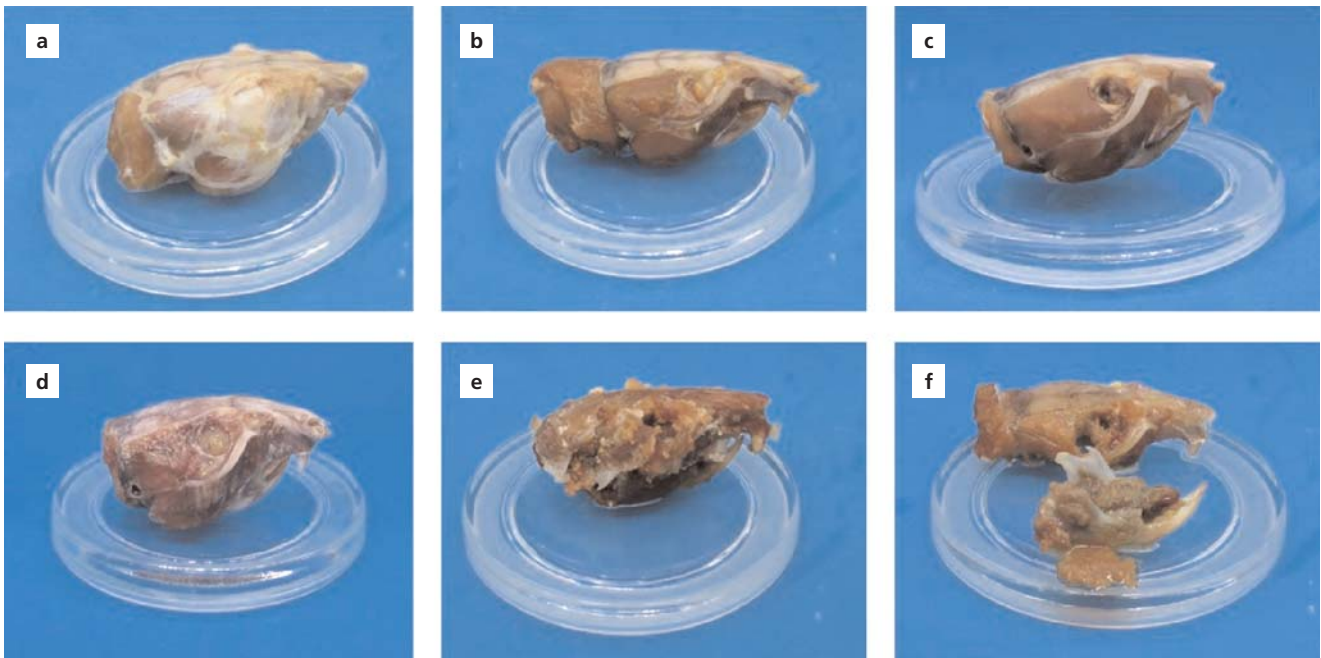


Figure 4. Results of maceration with NaClO: (a) 1% at room temperature; (b) 5% at room temperature; (c) 10% at room temperature; (d) 1% at oven temperature; (e) 5% at oven temperature; (f) 10% at oven temperature. [Color figure can be viewed in the online issue, which is available at www.anatomy.org.tr]

Authors such as Ajayi et al.,^[3] reported that dermestid larvae are useful as a technique to clean bones, especially for parts that are difficult to dissect. Ator et al.,^[4] indicated that the dermestid beetles in larval stage (those used in this experiment) have high appetite and achieve excellent maceration of small pieces.

Yet Couse et al.^[5] and King et al.^[6] stated that in order to implement maceration by dermestids, the laboratory requires a colony, something that in itself involves significant maintenance. Given that forensic science is not typically profitable, the additional costs associated with maintaining a colony could be a limiting factor for employing this type of maceration. This disadvantage is minor, however, when compared to the risk of escape for such beetles, due to the potentially destructive capacity of the species. In addition, the overexposure of a piece can also be harmful, since the beetles can begin to feed on the mineralized tissue, making daily monitoring necessary. King et al.^[6] showed that the duration of the procedure ranged from weeks to months. This period of time can be further extended due to the beetles' preference for dry tissues over fresh.

The maceration by 1% KOH and 5% KOH at room temperature completely eliminated the soft tissue and required a time of 27 days and 45 hours, respectively. However, 1% KOH caused the loss of the right and left zygomatic bone. A whiter coloration was observed when compared to the rest, indicating a possible lower bone density and, therefore, greater fragility of the bone tissue. The skull submerged in 5% KOH showed disarticulation of the nasal bones, incisors and the scaly portion of the left temporal bone. In addition, the loss of the right and left zygomatic bone was observed.

Miller and Tarpley^[7] obtained effective macerations with 3% KOH concentrations at room temperature with continuous agitation during the cycle, unlike this study in which the samples were not stirred. The same authors reported that increasing the concentration of KOH led to the loss of samples, while eliminating the agitation or decreasing the concentration of KOH produced an incomplete maceration.

The maceration by 10% KOH at room temperature in a period of 18 hours failed to completely remove the soft tissue. Remnants were observed in the inner part of the mandibular branches and around the petrous portion of the left temporal bone. Likewise, it generated disarticulation of the nasal bones and left incisor, loss of the right and left zygomatic bone and of the petrous portion of the right temporal bone. A darker coloration was obtained when compared with the rest of the pieces.

Gibb^[1] reported that the size and physical characteristics of the sample, the concentration of the chemical

agent and the temperature at which the procedure is carried out should be taken into account in macerations with KOH. The process performed at night and at room temperature is generally adequate for most specimens; samples that resisted heat required longer periods at higher temperatures. However, Renaud et al.^[8] and Gelfand et al.^[9,10] advised caution when handling the chemical, because it is highly corrosive and therefore constitutes a disadvantage for an inexperienced operator, although an advantage for the technique.

Maceration with 1% and 5% KOH in the oven was carried out for five and four hours, respectively. The 1% KOH preserved soft tissue around the petrous portion of the temporal bone and lingual part of the molars and preserved the nasal cartilage but generated loss of the right and left zygomatic bone. The 5% KOH preserved soft tissue in the lingual part of the molars and eliminated the right and left zygomatic bone. Unlike the previous concentrations, 10% KOH required two hours and 30 minutes to completely eliminate the soft tissue. Loss of the right and left zygomatic bones and disarticulation of the interparietal bone, nasal and mandibular symphysis were observed. In his book, Boyde^[11] explained that small bones could be treated with strong solutions of KOH at 50°C, which eliminated all soft tissues and the matrix at night. However, with the use of the oven in our experiment, the same effect was achieved in a few hours.

King and Birch^[6] showed that maceration with chemicals is fast, depending on the size of the specimens. However, chemical products can be difficult to control, because prolonged exposure can demineralize the bone, leading to fragility and loss of bone integrity. Renaud et al.^[8] used glass containers, observing an incomplete maceration process, similar to that found in our experiment where all macerations with KOH presented hard tissue damage.

The maceration with NaClO in different concentrations and temperatures in a period of 27 days did not meet the maceration criteria, and soft, adherent, dehydrated tissue of firm consistency was observed. Dutta and Saunders^[12] used concentrations of 1.36% and 4.65% which, after 60 minutes of exposure to the substance, did not show dissolution of the soft tissue. However, Fuente et al.^[13] used NaClO for nine hours at a concentration of 35% and immersed specimens in boiling water, obtaining positive results. Mann and Berryman^[14] used concentrations of 3% to 6% of NaClO and concluded that it is a fast, safe and effective method for exposing bone tissue.

Steadman et al.^[15] stated that NaClO is an easy-to-use, accessible and economical chemical maceration method that allows rapid bone cleaning. They used 10%

NaClO plus 3% hydrogen peroxide and recorded that the procedures that lacked heat were substantially slower than the techniques in which hot or water brought to boiling point was used. Furthermore, the pieces gave off stronger smells and did not necessarily produce better quality bone tissue. They recommended concentrations that did not exceed 10%. Hildebrand^[16] in his book proposed NaClO in concentrations of 1% to 2% at 50°C for five days for small pieces.

Conclusion

The results of this study showed that maceration by insects is an ideal method for soft tissue maceration, preserving all bone components. Maceration by KOH was an effective, but aggressive method for the bone tissue. Conducting further studies in which the chemical agent is agitated during this type of maceration is recommended. It was not possible to achieve a successful maceration with NaClO; immersing the pieces in boiling water first was another recommendation.

Acknowledgements

The authors of this study would like to thank the Department of Morphology at Universidad del Valle for authorization to use the laboratory, reagents and bio-models. Many thanks to Professor Oscar Murillo in the zoology section of the Department of Biology of Universidad del Valle for his time and help with the dermestid colony.

References

- Gibb T. Equipping a diagnostic laboratory In: Gibb T, editor. Contemporary insect diagnostics. Waltham (MA): Academic Press Elsevier; 2014. p. 9–50.
- Gage GJ, Kipke DR, Shain W. Whole animal perfusion fixation for rodents. *J Vis Exp* 2012;65:3564.
- Ajayi A, Edjomariogwe O, Iselaiye OT. A review of bone preparation techniques for anatomical studies. *Malaya Journal of Biosciences* 2016;3:76–80.
- Ator GA, Andrews JC, Maxwell DS. Preparation of the human skull for skull base anatomic study. *Skull Base Surg* 1993;3:1–6.
- Couse T, Connor M. A comparison of maceration techniques for use in forensic skeletal preparations. *Journal of Forensic Investigation* 2015;3:1–6.
- King C, Birch W. Assessment of maceration techniques used to remove soft tissue from bone in cut mark analysis. *J Forensic Sci* 2015;60:124–35.
- Miller DM, Tarpley J. An automated double staining procedure for bone and cartilage. *Biotech Histochem* 1996;71:79–83.
- Renaud R, Brettes P, Castanier C, Loubiere R. Placental bilharziasis. *Int J Gynaecol Obstet* 1972;10:24–30.
- Gelfand M, Ross CM, Blair DM, Castle WM, Weber MC. Schistosomiasis of the male pelvic organs. Severity of infection as determined by digestion of tissue and histologic methods in 300 cadavers. *Am J Trop Med Hyg* 1970;19:779–84.
- Gelfand M, Ross DM, Blair DM, Weber MC. Distribution and extent of schistosomiasis in female pelvic organs, with special reference to the genital tract, as determined at autopsy. *Am J Trop Med* 1971;20:846–9.
- Boyde A. Scanning electron microscopy of bone. In: Idris, AI, editor. Bone research protocols. Methods in molecular biology. New York: Humana Press; 2012. p. 365–400.
- Dutta A, Saunders WP. Comparative evaluation of calcium hypochlorite and sodium hypochlorite on soft-tissue dissolution. *J Endod* 2012;38:1395–8.
- Fuente del Campo A, Martinez Elizondo M, Melloni Magnelli L, Salazar Valadez A, Saavedra Ontiveros A. Craniofacial development in rats with early resection of the zygomatic arch. *Plast Reconstr Surg* 1995;95:486–95.
- Mann RW, Berryman HE. A method for defleshing human remains using household bleach. *J Forensic Sci* 2012;57:440–2.
- Steadman DW, Diantonio LL, Wilson JJ, Sheridan KE, Tammariello SP. The effects of chemical and heat maceration techniques on the recovery of nuclear and mitochondrial DNA from bone. *J Forensic Sci* 2006;51:11–7.
- Hildebrand M Dry skeletons. Hildebrand M (ed). Anatomical preparations. Berkeley (CA): University of California Press; 1968. p.16–42.

ORCID ID:

D. Botero-González 0000-0002-0156-4997;
M. Agudelo 0000-0002-3571-5255



Correspondence to: Daniela Botero-González, Dt, MSc
School of Biomedical Sciences, Universidad del Valle, 4B # 36 – 00
760043, Santiago de Cali, Colombia
Phone: +57 310 392 46 06
e-mail: daniela.botero.gonzalez@correounivalle.edu.co

Conflict of interest statement: No conflicts declared.

This is an open access article distributed under the terms of the Creative Commons Attribution-NonCommercial-NoDerivs 3.0 Unported (CC BY-NC-ND3.0) Licence (<http://creativecommons.org/licenses/by-nc-nd/3.0/>) which permits unrestricted noncommercial use, distribution, and reproduction in any medium, provided the original work is properly cited. *Please cite this article as:* Botero-González D, Agudelo M. Comparison of macerations with dermestid larvae, potassium hydroxide and sodium hypochlorite in Wistar rat crania. *Anatomy* 2019;13(3):149–154.

The underestimated role of a somatosensory neural network on thyroid gland morphology: an experimental subarachnoid hemorrhage model study

Cengiz Öztürk¹ , Mehmet Nuri Koçak² , Tuba Demirci³ , İsmail Malkoç⁴ ,
Mehmet Dumlu Aydın⁵ 

¹Department of Anatomy, School of Medicine, Erzurum Atatürk University, Erzurum, Turkey

²Department of Neurology, School of Medicine, Erzurum Atatürk University, Erzurum, Turkey

³Department of Histology and Embryology, School of Medicine, Erzurum Atatürk University, Erzurum, Turkey

⁴Department of Anatomy, School of Medicine, Düzce University, Düzce, Turkey

⁵Department of Neurosurgery, School of Medicine, Erzurum Atatürk University, Erzurum, Turkey

Abstract

Objectives: Innervation of the thyroid gland has been attributed to the autonomic nervous system. Although peripheral sympathetic and parasympathetic innervations of the thyroid gland are well known, little is known about the somatosensory innervation of the thyroid gland. In this study, alterations on the somatosensory neural network of the thyroid gland following an experimental subarachnoid hemorrhage were investigated in rabbits.

Methods: Experiments were conducted on 23 rabbits under no medical intervention. Five rabbits were used as control group. Five rabbits were used as the sham group and serum physiologic (SF) was injected into their cisterna magna. The remaining 13 animals were used as the subarachnoid hemorrhage (SAH) group; their own blood (1 ml) was re-injected into the cisterna magna. Thyroid hormone levels of animals were measured at the end of one month. Then, histological sections of the middle parts of the thyroid glands were stained with haematoxylin-eosin (H&E) for investigation of SAH-related damage. The total follicle volume (TFV) per cubic millimeter of the thyroid gland was estimated by stereological methods. Comparison of degenerated neuronal density (DND) in the C4 dorsal root ganglia (DRG) was examined bilaterally using H&E and TUNEL stainings.

Results: Following SAH, neuronal degeneration in the cervical DRG caused somatic innervation deficiency, follicular atrophy and thyroid hormone depletion in the thyroid gland. T3 and T4 hormone levels of the SAH group (T3: 61±8 µg/dl; T4: 1.01±0.12 µg/dl) were significantly ($p<0.005$) lower than those of control (T3: 103±6 µg/dl, T4: 1.37±0.36 µg/dl) and sham (T3: 94±10 µg/dl; T4: 1.24±0.87 µg/dl) groups. In control groups, mean TFV was 41% / mm³ and DND of C4 DRG was 6±2 / mm³. These values were significantly lower than those in sham (TFV: 35%/mm³ and DND: 22±7/mm³) and experimental SAH (TFV: 23%/mm³ and DND: 253±49/mm³) groups ($p<0.0005$ and $p<0.0001$, respectively).

Conclusion: Thyroid follicle growth and its secretory activity are under the control of a quite complex, multi-originated, yet incompletely understood innervation pattern. We propose the presence of an underestimated role of a somatosensory neural network - an interganglionic link between the superior cervical, thyroid, laryngeal, nodose, trigeminal and dorsal root ganglia - on thyroid gland morphology.

Keywords: cisterna magna; dorsal root ganglion; rabbit; subarachnoid hemorrhage; thyroid gland

Anatomy 2019;13(3):155–162 ©2019 Turkish Society of Anatomy and Clinical Anatomy (TSACA)

Introduction

The bulk of the parenchymal tissue of the thyroid gland is composed of the follicular cells, producing the thyroid hormones, generally under the control of the suprathalamic

nucleus.^[1] A small portion of the parenchyma is parafollicular cells which have their origins in the ultimobranchial bodies derived from epithelial clusters of the

fourth pharyngeal pouches invaded by the neural crest cells. The distribution and origin of the nerve fibers innervating the thyroid gland of rats arise from the cell bodies in the thyroid, laryngeal, superior cervical, jugular-nodose, trigeminal and dorsal root ganglia (DRGs) of C2-C5 spinal nerves.^[2] Removal of the superior cervical ganglia network causes several neuroendocrine dysfunctions.^[3,4] Aging process reduces thyroid hormone levels secondary to sympathetic hypofunction.^[5] The thyroid gland and blood vessels have dual innervation arising from the sympathetic and parasympathetic fibers.^[6] They are located around blood vessels, under the fibrous capsule and in the close vicinity to the secretory vesicles.^[7] Follicular cells are not as enriched with sympathetic nervous system fibers as with cholinergic fibers.^[8] There may be an undescribed interganglionic link among superior cervical, thyroid, laryngeal, nodose, dorsal root and trigeminal ganglia. Parasympathetic innervation of the thyroid gland is managed by the inferior laryngeal branches of the vagal nerve. Stimulation of the parasympathetic nerves increases the blood flow of the thyroid gland by dilating thyroidal vessels. Parasympathetic vasodilation has supplementary role in both regulation of the secretion of thyroid hormone and alteration of the thyroidal blood flow.^[9,10] Extirpation of the nodose ganglion results in decrease of parasympathetic activity of the thyroid gland.^[11] Sympathetic innervation of the thyroid gland on the other hand is provided by the superior cervical ganglion,^[12] which contributes to enlargement of the gland and might modulate tissue and hormone (TSH) interactions.^[13] Unilateral superior cervical ganglion section leads to a decrease in the size of thyroid gland. The superior cervical ganglion projects to the pineal and other glands such as the salivary glands. Postganglionic nerve transection relies on various histomorphological abnormalities in the related glands.^[14] Acute superior cervical ganglionectomy leads to significant depression of the thyroid economy.^[15] The middle and/or inferior cervical ganglia also send their axons through external carotid nerve to the thyroid.^[16] Hypothalamo-hypophyseal and pineal gland injuries may result in decreased thyroid hormone levels secondary to follicular atrophy.^[17] Since the somatic innervation should have major roles on the formation and continuation of thyroid gland morphology, functions and the prevention of thyroid gland pathologies, in the current study, we aimed to investigate the alterations in the somatosensory innervation of the thyroid gland following subarachnoidal hemorrhage in rabbits.

Materials and Methods

The study protocol was approved by the Ethics Committee for Animal Experiments, Atatürk University School of Medicine, Erzurum, Turkey. The care of the animals and

the experiments were conducted according to the guidelines set forth by the same ethics committee. The animals were kept in individual metal cages at room temperature with 12 h of light per day and 50% relative humidity under veterinary supervision. They were fed with standard laboratory diet and water *ad libitum*. The animals were randomly assigned into three groups. After anesthesia isoflurane applied using a face mask, 0.2 ml/kg of the anesthetic combination (Ketamine HCL, 150 mg/1.5 ml; Xylazine HCl, 30 mg/1.5 ml in distilled water) was injected subcutaneously before surgery. A balanced, injectable analgesic was used to reduce pain and mortality.

Five rabbits were selected as the control group (Group 1, n=5). In the sham group, 1 ml saline was injected into the cisterna magna (Group 2, n=5). To induce experimental subarachnoid hemorrhage, autologous blood (1 ml) was taken from the auricular artery. While the head of the animal was held in a hyperflexed position, the posterior notch of the foramen magnum was identified and CSF was aspirated from the cisterna magna. After the confirmation of the cisterna magna, 1 ml of autologous blood was injected by using a 22-gauge needle for over one minute.

Following the injection, all animals were observed for one month without any medical treatment. Animals that developed severe ischemia were chosen for the SAH group (Group 3, n=13), and their vital findings were monitored for ten minute-periods, two times a week. Their hormone levels were examined weekly during the experiments. After formalin perfusion under the general anesthesia, the thyroid glands, cervical spinal cords and C4 DRGs were carefully removed for histologic examination. The extracted tissues were passed through a graded alcohol series, and then embedded in liquid paraffin. Tissue sections from each block were collected on glass slides for haematoxylin-eosin (H&E) and TUNEL stainings to examine SAH-related damage under light microscopy.

The thyroid glands were sectioned at 5 μm thickness with 30 μm intervals. Every 30th and 31st sections were sampled for quantification of the follicles. The total number of follicles in the thyroid gland was estimated by the fractionator method. For the analysis of C4 DRG sections, the spinal cord specimens together with their extensions were longitudinally embedded in paraffin blocks in order to observe all the roots during the histologic examination. For the stereological analysis, the first pair of sampled sections was selected randomly from a starting point within the first 30 section interval. Thereafter, every 30th section and its neighbor was sampled. The section sampling fraction (f1) was therefore $f1=1/30$. Section pairs not containing the thyroid tissue and vagal nuclei were discarded. This

sampling fraction yielded on average 10 to 11 section pairs. Area of sampling fraction, f_2 , was 1/1. We preferred to use physical dissector method to evaluate the numbers of thyroid follicles; because, this method is intuitively simple, free from assumptions about particle shape, size and orientation, and the particle number can be readily estimated and unaffected overprotection and truncation. Two consecutive sections (dissector pairs) obtained from tissue samples were mounted on each slide. Reference and look-up sections were reversed in order to double number of dissector pairs without taking new sections. The number of counted follicles was designated ΣQ . The total numbers of thyroid follicles (N), in thyroid glands were estimated from the equation:

$$N = \Sigma Q \times 1/f_1 \times 1/f_2.$$

After counting procedure, total follicle volume (TFV) was estimated via summation of each vesicle volumes. Since the shape of thyroid follicles resembled as ellipsoid, their volumes were estimated by using the following formula: $V_n = 4/3\pi r_n^3$.

The TFV was estimated as: $TFV = \sum_{N=1}^N N \times V_n$.

$$\sum_1^n V_f = \sum_{f=1}^n n \left[\frac{4}{3} \pi < \frac{a+b+c}{3} >^3 \right]^*$$

The physical dissector method was used to evaluate the numbers of living and degenerated neurons in C4 DRG. Two consecutive sections (dissector pairs) obtained from reference tissue samples were mounted on each slide. The paired reference sections were reversed in order to double the number of dissector pairs without having to cut new sections.

The mean numerical density of the C4 DRG (N_v/G_v) per mm^3 was estimated using the following formula.

$$N_v/G_v = \Sigma Q / \Sigma A \times d$$

Where ΣQ -N is the total number of counted neurons appearing only in the reference sections, d is the section thickness, and A is the area of the counting frame. The most effective way of estimating ΣA for the set of dissector is via $\Sigma A = \Sigma P \cdot a$. ΣP is the total number of counting set frames points and a is a constant area associated set point. The total volume of each specimen were estimated by the Cavalieri volume estimation method. Then, the total number of neurons was calculated by multiplication of the volume (mm^3) and the numerical density of neurons in each ganglion.

The differences between the thyroid follicle densities per unit volume of the thyroid gland and degenerated neuron densities in the C4 DRG were analyzed using a commercially available statistics software package (SPSS® for Windows, version 12.0, Chicago, IL, USA). In all the

groups, the numbers of follicles did not show normal distribution according to Kolmogorov-Smirnov and Shapiro-Wilk test. Therefore, data analysis consisted of the Kruskal-Wallis and Mann-Whitney U tests. Differences were considered to be significant at $p < 0.05$. The p value used for multiple comparisons were calculated by dividing 0.05 with six for Bonferroni correction and considered as statistically significant for ≤ 0.0083 .

Results

In control animals, the average heart rate was 280 ± 15 /min, the respiratory rate was 35 ± 9 /min and the blood oxygen concentration was $95 \pm 7\%$. In experimental animals, soon after inducing SAH, the heart rate decreased to 150 ± 30 /min, the mean respiratory rate to 18 ± 5 /min, and the mean blood oxygen concentration to $78 \pm 10\%$. Considerable electrocardiographic changes were observed such as ventricular extra systoles, ST depression, QRS separation, bigeminal or trigeminal extra systoles and fibrillations. Four animals in the SAH group and one animal in the SHAM group were dead within the seven days of surgery. Neck stiffness, unconsciousness, convulsive attacks, fever, apnea, cardiac arrhythmia, and breathing disturbances were observed in all hypothermic animals. However, in the late phase of fatality-inducing SAH, the heart rate increased to 350 ± 40 /min. When analyzing respiratory parameters, both decreased respiration frequency (bradypnea) (14 ± 3) and increased respiratory amplitudes were observed in the first hours following SAH. Conversely, at longer intervals following SAH, increased respiration frequency (tachypnea) and decreased respiration amplitude were observed, resulting in shortened inspiration, a longer expiration time, apnea-tachypnea attacks, diaphragmatic breath and respiratory arrest. Massive subarachnoid hemorrhage was observed in the basal cisterns of GIII animals. They showed meningeal irritation signs, cardiorespiratory dysrhythmia.

Average thyroid hormone levels of animals are shown in **Table 1** and statistical comparisons of groups in **Table 2**. T3 and T4 hormone levels of the SAH group (T3= 61 ± 8 $\mu\text{g/dl}$; T4= 1.01 ± 0.12 $\mu\text{g/dl}$) were significantly lower than those of control (T3= 103 ± 6 $\mu\text{g/dl}$; T4= 1.37 ± 0.36 $\mu\text{g/dl}$) and sham (T3= 94 ± 10 $\mu\text{g/dl}$; T4= 1.24 ± 0.87 $\mu\text{g/dl}$) groups. On the other hand, TSH levels were higher than 0.5 ng/dl in sham and SAH groups (**Table 1**).

While mean TFV was $41\%/mm^3$ in control groups, it was significantly decreased in sham ($35\%/mm^3$) and SAH ($23\%/mm^3$) groups (**Tables 1** and **2**). The significance level was more prominent between control and SAH groups ($p < 0.00005$) than those of control and sham groups ($p < 0.001$) as displayed in **Table 2**.

Similarly, density of degenerated neurons in C4 DRG was significantly higher in SAH group ($253 \pm 49/\text{mm}^3$) than those of control ($6 \pm 2/\text{mm}^3$) and sham ($22 \pm 7/\text{mm}^3$) operated groups, respectively (Table 1). Comparisons of the groups that displayed a significance level was more prominent between control and SAH groups ($p < 0.00001$) than those of control and sham groups ($p < 0.001$; Table 2).

Postmortem gross morphological and histopathological investigations of the tissues in the central nervous system of the rabbits showed brain edema, stiffness and enhanced leptomeningeal thickness in animals with SAH. The brain swelling and increased brain weight were seen in all animals who developed hyperthermia. In general, the basal cisterns and rarely the fourth and the lateral ventricles were filled with blood. Arachnoid membranes of the lower cranial parts were stuck to the lower cranial nerve roots.

Histology of the normal thyroid gland, follicles (F1-n) and the volume estimation method of follicles are shown in Figure 1. In sham rabbits, partially atrophic and lessened thyroid follicles were evident in the thyroid gland under light microscopy (Figure 2). On the other hand, size of the thyroid glands decreased dramatically in SAH animals. Acinar cell loosening, decreased number of hormone filled vesicles, total volume reduction of thyroid follicles, ductal epithelial cell injury related ductal closing, degenerative changes of extra thyroidal parasympathetic ganglia neurons and apoptotic changes in the acinar cells, tubular cells and supporting cells were detected in the histological sections of their thyroid glands stained with H&E (Figure 3).

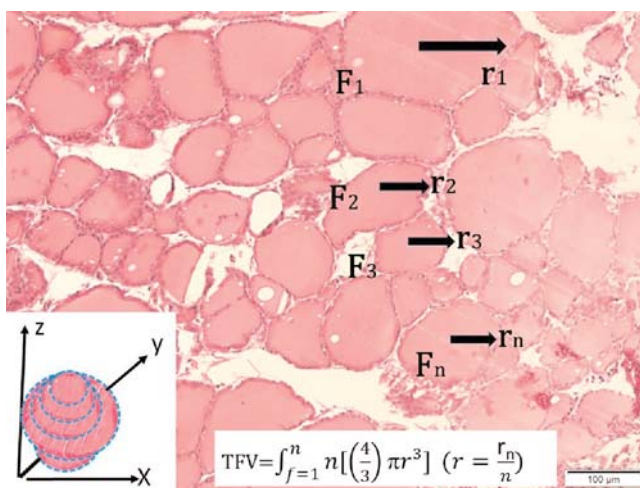


Figure 1. Thyroid gland follicles (F1-n) in control animals and stereological method used for follicle volume estimation (H&E stain; scale bar=100 μm). [Color figure can be viewed in the online issue, which is available at www.anatomy.org.tr]

Table 1
Thyroid hormone levels, quantitative analyses of thyroid follicles and DRG neurons for control (Group 1), sham (Group 2) and SAH (Group 3).

	Group 1/ Group 2	Group 1/ Group 3	Group 2/ Group 3
T4	$p < 0.001$	$p < 0.0001$	$p < 0.0005$
TFV	$p < 0.001$	$p < 0.00005$	$p < 0.0001$
DND in C4 DRG	$p < 0.001$	$p < 0.00001$	$p < 0.0001$

DND: degenerated neuron density; DRG: dorsal root ganglion; TFV: thyroid follicle volume.

Table 2
Statistical comparisons for control (Group 1), sham (Group 2) and SAH (Group 3) groups.

	Group 1	Group 2	Group 3
T3 (μg/dl)	103 ± 6	94 ± 1	61 ± 8
T4 (μg/dl)	1.37 ± 0.36	1.24 ± 0.87	1.01 ± 0.12
TSH I (ng/dl)	0.5	>0.5	>0.5
Mean TFV /mm ³	41%	35%	23%
DND of C4 DRG/mm ³	6 ± 2	22 ± 7	253 ± 49

DND: degenerated neuron density; DRG: dorsal root ganglion; TFV: thyroid follicle volume.

Histology of the cervical spinal cord with C4 DRG is shown in Figure 4. Cytoplasmic condensation, nuclear shrinking, cellular angulations and peri-cytoplasmic halo formation were accepted as neuronal degeneration crite-

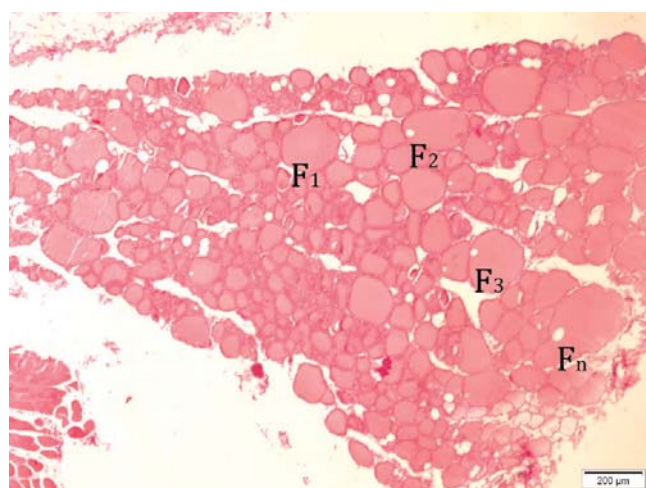


Figure 2. Thyroid gland and normal follicles in sham operated rabbit (H&E stain; scale bar=200 μm). [Color figure can be viewed in the online issue, which is available at www.anatomy.org.tr]

ria. Degenerating neuronal profiles and apoptotic neuronal changes were apparently more abundant in DRG of the animal with SAH. Especially, the arteries supplying nerve roots and ganglia were more vasospastic in SAH rabbits. Therefore, the ratio of arterial wall surface to lumen surface accepted as vasospasm index (VSI), which can be calculated by using the (R^2-r^2/r^2) formula, displayed alterations in animals following SAH (Figure 4) in comparison to control animals (Figure 5).

Discussion

In this study, we used a SAH model in rabbits to investigate alterations in the thyroid gland cytoarchitecture and somatosensory neural network. Our results displayed significant changes in the total volume of thyroid follicles and enhanced degeneration in the cervical DRG neurons innervating the thyroid gland. SAH accounts for approximately 5% of all strokes, with an incidence of 5–10 per 100,000 in most populations.^[18] This life-threatening condition interrupts the productivity of an individual by causing major disabilities and a severe socio-economic impact with the estimated life time costs more than double that of ischemic stroke.^[19] Small laboratory animals, such as rats and mice can be used as model to induce SAH. In these animal models, different surgical methods are used to create an effective degree of vasospasm. However, many traditional SAH animal models do not adequately mimic the acute pathophysiological changes seen in human and have been criticized for missing delayed cerebral ischemia.^[20]

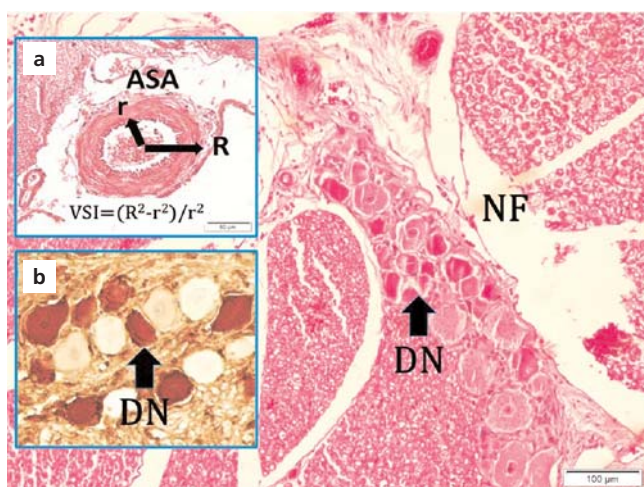


Figure 4. (a) Cervical spinal cord with constructed anterior spinal artery (ASA) and vasospasm index calculation method. (b) Degenerated apoptotic neurons (DN) in C4; TUNEL stain. Nerve fibers (NF) are shown with H&E staining (black arrow). Scale bar=100 μm. [Color figure can be viewed in the online issue, which is available at www.anatomy.org.tr]

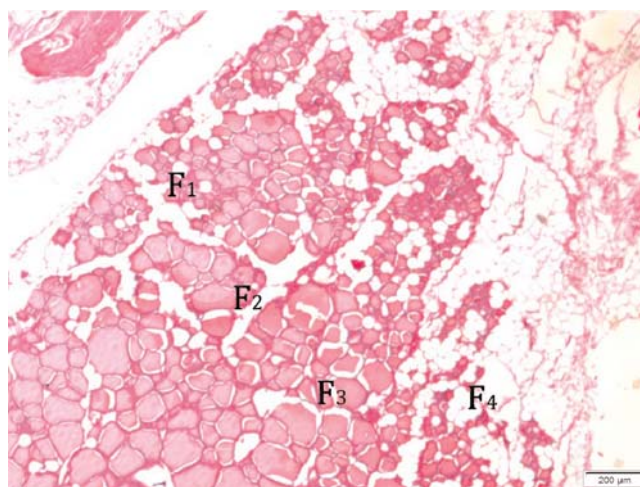


Figure 3. Thyroid gland and partially atrophic follicles in a rabbit with SAH (H&E stain; scale bar=200 μm). [Color figure can be viewed in the online issue, which is available at www.anatomy.org.tr]

Although more fitting animal models for this purpose seem like bigger experimental animals such as dogs and primates, it is very difficult to use these animal models due to ethical and financial problems. Instead, injection of a single standard volume of blood (1 ml) into the cisterna magna of a rabbit has been shown as a useful and reliable animal model of SAH. This model exerts biphasic pattern of vasospasm and vasoconstriction and morphological alterations in the arteries display similarities to changes observed in humans.^[21]

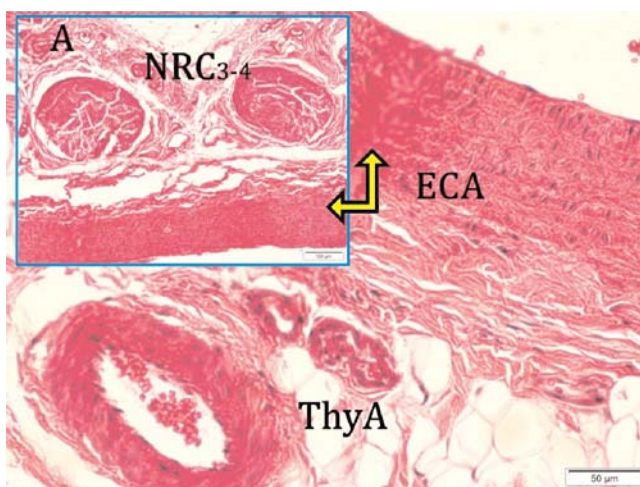


Figure 5. Thyroid gland with constructed thyroidal artery (ThyA) and a branch of external carotid artery (ECA). (A): Cervical 3-4 nerve roots (NRC3-4) stained with H&E. Scale bar=50 μm. [Color figure can be viewed in the online issue, which is available at www.anatomy.org.tr]

In humans, although about 70% of patients may develop focal arterial vasospasm, and only 30% will manifest neurological deficits. Vasospasm of the major cerebral arteries is usually focal, but it also might be diffuse usually with the onset on day 3 after SAH, maximal at days 6–8, and lasting for 2–3 weeks.^[22] Symptomatic vasospasm is characterized by the insidious onset of confusion and decreased level of consciousness, followed by focal motor and/or speech impairments. In the surviving patients, secondary insults caused by the cerebral vasospasm results in various complications. In this study, we detected alterations in the ratio of arterial wall surface to lumen surface of the thyroidal arteries in animals following SAH. We thought that changes in the perivascular nerves might be responsible for the observed outcomes in the thyroid gland.

The distribution and origin of the nerve fibers innervating the thyroid gland were studied comprehensively in rats by immunohistochemistry, retrograde tracing and denervation experiments. Different subpopulations of nerve fibers containing noradrenaline (NA), neuropeptide Y (NPY), vasoactive intestinal peptide (VIP), galanin (GAL), substance P (SP), and calcitonin gene-related peptide (CGRP) have been shown around the blood vessels and thyroid follicles. Injection of a retrograde tracer, True Blue into the thyroid gland labelled cell bodies in the thyroid, laryngeal, superior cervical, the jugular-nodose, C2-C5 DRG and trigeminal ganglia.^[2] In the light of the number of retrogradely labelled cell bodies, it seems like the most of the innervation of the gland is supported by the superior cervical and thyroid ganglia while the contribution of the laryngeal and trigeminal ganglia is the least. Denervation studies showed that neurons located in the superior cervical ganglion provide all NA-containing and the majority of NPY-containing nerve fibers to the thyroid gland. On the other hand, all VIP- and a minor population of NPY- and GAL-containing fibers in the thyroid gland originate from the thyroid ganglion. Whereas, SP and/or CGRP containing nerve fibers derive from the jugular, cervical dorsal root and/or trigeminal ganglia. These results emphasize the importance of multiple sources of innervation arriving to the thyroid gland and their different neuropeptide expression in regulation of the activity of thyroid follicles.^[2]

Innervation of the thyroid gland and control of thyroid activity occur mostly via the superior cervical ganglia, intrathyroidal ganglia of vagal nerves as well as the trigeminal ganglia and cervical DRG.^[2] Extirpation of the nodose ganglion decreases of parasympathetic activity on thyroid gland.^[11] Bilateral inferior laryngeal nerve section causes

reduction in circulating T4 for up to four weeks after surgery, while unilateral section causes a transient T4 decrease one week after surgery. In contrast, electrical stimulation of parasympathetic activity in the superior laryngeal nerve increases the thyroid blood flow via dilatation of the blood vessels. Thus, parasympathetic vasodilation has a supplementary role in regulating both the secretion of thyroid hormones and alteration in the thyroid blood flow.^[9]

Sympathetic innervation of thyroid gland is provided by the superior cervical ganglion^[12] which contributes to the enlargement of gland and might modulate the tissue and hormone (TSH) interactions.^[13,16] In addition, middle and/or inferior cervical ganglia send their axons through the external carotid nerve to the thyroid gland.^[16] Neuron numbers especially in the superior cervical ganglion are important in regulating sympathetic activity of the thyroid gland.^[14] The sympathoadrenal system also closely interacts with thyroid hormone levels. Exaggerated responses to catecholamines or exposure to cold trigger thyroidal sympathetic activity and dominate the manifestations of thyrotoxicosis.^[23] In contrast, unilateral transection of the superior cervical ganglion leads to decrease in the size of thyroid gland and reduction of follicle volume.^[24] Acute superior cervical ganglionectomy causes significant depression in the thyroid economy.^[15] It is important to highlight that superior cervical ganglion also project to the pineal and other salivary glands in the head.^[25] Therefore, postganglionic nerve transection causes various histomorphological abnormalities on the related glands.

Beside the sympathetic and parasympathetic innervation, several studies draw special attention to the role of the serotonergic system in the modulation of the thyroid gland functions. It has been shown that serotonin might inhibit the secretion of thyrotropin by the pituitary gland, but has a direct stimulatory effect on thyrocytes mediated by the serotonin 5-HT₂ receptors.^[26] In hypothyroidism, synthesis and metabolism of serotonin in the brain are slowed down. In depression, reduction in the concentration of serotonin is accompanied by inhibition of the enzyme activity deiodinase type 2. Activation of 5-HT₁ receptor lead to increased levels of intracellular calcium, causing inhibition of the promoter of CGRP.

CGRP has a special importance among neuropeptides, because it is one of the most potent microvascular vasodilators identified to date. Its vascular relaxation effects are mediated via activation of a G protein-coupled receptor, called as calcitonin receptor-like receptor.

Vasoconstriction has been shown to be associated with a decrease in CGRP levels in nerves and an increase in CGRP levels in draining blood, suggesting that CGRP is released from nerves to oppose the vasoconstriction.^[27] This might be an important mechanism in the pathogenesis of vasospasm after SAH; because, similar to the thyroid gland, the cerebral arteries also have sympathetic, parasympathetic, and sensory innervation. It is quite possible that SAH causes an imbalance in the neuronal regulatory mechanisms, which in turn leads to vascular smooth muscle contraction.^[28] In humans, reduced levels of CGRP in the cerebral perivascular nerves have been associated with vasoconstriction and an enhancement in CGRP levels in blood draining from the external jugular vein, suggesting that CGRP is released antidromically from trigeminal sensory perivascular nerves to oppose the vasoconstriction.^[29]

Conclusion

In combination with the knowledge from the literature and findings of the current study, we suggest that control of thyroid follicle growth and its secretory activity is under the control of quite complex, multi-originated, yet incompletely understood innervation pattern. We postulated that underestimated role of an interganglionic link among superior cervical, thyroid, laryngeal, nodose, trigeminal and dorsal root ganglia might be important in the etiopathogenesis and/or treatment of SAH-associated vasospasm. Further immunohistochemical labeling of somatosensitive fibers in the thyroid gland following SAH will shed light into these issues.

References

- Kalsbeek A, Fliers E, Franke AN, Wortel J, Buijs RM. Functional connections between the suprachiasmatic nucleus and the thyroid gland as revealed by lesioning and viral tracing techniques in the rat. *Endocrinology* 2000;141:3832–41.
- Sundler F, Grunditz T, Håkanson R, Uddman R. Innervation of the thyroid. A study of the rat using retrograde tracing and immunocytochemistry. *Acta Histochem Suppl* 1989;37:191–8.
- Melander A. Aminergic regulation of thyroid activity: importance of the sympathetic innervation and of the mast cells of the thyroid gland. *Acta Med Scand* 1977;201:257–62.
- Onen MR, Yilmaz I, Ramazanoglu L, Aydin MD, Keles S, Baykal O, Aydin N, Gundogdu C. Uncovering the forgotten effect of superior cervical ganglia on pupil diameter in subarachnoid hemorrhage: an experimental study. *Turk Neurosurg* 2018;28:48–55.
- Melander A, Sundler F, Westgren U. Sympathetic innervation of the thyroid: variation with species and with age. *Endocrinology* 1975;96:102–6.
- Diamantis E, Farmaki P, Savvanis S, Athanasiadis G, Troupis T, Damaskos C. Sympathetic nerve injury in thyroid cancer. *Acta Medica (Hradec Králové)* 2017;60:135–9.
- Baryla J, Greniuk G, Lakomy M. The adrenergic and cholinergic innervation of the thyroid chicken gland. *Folia Morphol (Warsz)* 2003;62:247–9.
- Van Sande J, Dumont JE, Melander A, Sundler F. Presence and influence of cholinergic nerves in the human thyroid. *J Clin Endocrinol Metab* 1980;51:500–2.
- Ito H, Matsuda K, Sato A, Tohgi H. Cholinergic and VIPergic vasodilator actions of parasympathetic nerves on the thyroid blood flow in rats. *Jpn J Physiol* 1987;37:1005–17.
- Stern JE, Sarmiento MI, Cardinali DP. Parasympathetic control of parathyroid hormone and calcitonin secretion in rats. *J Auton Nerv Syst* 1994;48:45–53.
- Grunditz T, Ekman R, Håkanson R, Rerup C, Sundler F, Uddman R. Calcitonin gene-related peptide in thyroid nerve fibers and C cells: effects on thyroid hormone secretion and response to hypercalcemia. *Endocrinology* 1986;119:2313–24.
- Jallageas M, Mas N, Saboureaux M, Roussel JP, Lacroix A. Effects of bilateral superior cervical ganglionectomy on thyroid and gonadal functions in the edible dormouse *Glis glis*. *Comp Biochem Physiol Comp Physiol* 1993;104:299–304.
- Young JB, Bürgi-Saville ME, Bürgi U, Landsberg L. Sympathetic nervous system activity in rat thyroid: potential role in goitrogenesis. *Am J Physiol Endocrinol Metab* 2005;288:E861–7.
- Flett DL, Bell C. Topography of functional subpopulations of neurons in the superior cervical ganglion of the rat. *J Anat* 1991;177:55–66.
- Boado RJ, Romeo HE, Chuluyan HE, Cageao L, Cardinali DP, Zaninovich AA. Evidence suggesting that the sympathetic nervous system mediates thyroidal depression in turpentine-induced nonthyroidal illness syndrome. *Neuroendocrinology* 1991;53:360–4.
- Romeo HE, González Solveyra C, Vacas MI, Rosenstein RE, Barontini M, Cardinali DP. Origins of the sympathetic projections to rat thyroid and parathyroid glands. *J Auton Nerv Syst* 1986;17:63–70.
- Cardinali DP, Vacas MI, Gejman PV, Pisarev MA, Barontini M, Boado RJ, Juvenal GJ. The sympathetic superior cervical ganglia as “little neuroendocrine brains”. *Acta Physiol Lat Am* 1983;33:205–21.
- de Rooij NK, Linn FHH, Van der Plas JA, Algra B, Rinkel GJE. Incidence of subarachnoid haemorrhage: a systematic review with emphasis on region, age, gender and time trends. *J Neurol Neurosurg Psychiatry* 2007;78:1365–72.
- Dirnagl U, Macleod MR. Stroke research at a road block: The streets from adversity should be paved with meta-analysis and good laboratory practice. *Br J Pharmacol* 2009;157:1154–6.
- Marbacher S, Grüter B, Schöpf S, Croci D, Nevzati E, D’Alonzo D, Lattmann J, Roth T, Bircher B, Wolfert C, Muroi C, Dutilh G, Widmer HR, Fandino J. Systematic review of in vivo animal models of subarachnoid hemorrhage: species, standard parameters, and outcomes. *Translat Stroke Res* 2019;10:250–8.
- Chan RC, Durity FA, Thompson GB, Nugent RA, Kendall M. The role of the prostacyclin-thromboxane system in cerebral vasospasm following induced subarachnoid hemorrhage in the rabbit. *J Neurosurg* 1984;61:1120–8.
- Wilkins RH. Cerebral vasospasm. *Crit Rev Neurobiol* 1990;6:51–77.
- Silva JE, Bianco SD. Thyroid-adrenergic interactions: physiological and clinical implications. *Thyroid* 2008;18:157–65.
- Zerek-Melen G, Lewinski A. Influence of sympathetic denervation of the thyroid by superior cervical ganglionectomy on the growth

- processes in the gland in basal conditions and after hemithyroidectomy. *Acta Physiol Pharmacol Latinoam* 1988;38:377–87.
25. Cardinali DP, Vacas MI, Gejman PV. The sympathetic superior cervical ganglia as peripheral neuroendocrine centers. *J Neural Transm* 1981;52:1–21.
26. Lychkova AE. Nervous regulation of thyroid function. *Vestn Ross Akad Med Nauk* 2013;6:49–55.
27. Cardinali DP, Sartorio GC, Ladizesky MG, Guillén CE, Soto RJ. Changes in calcitonin release during sympathetic nerve degeneration after superior cervical ganglionectomy of rats. *Neuroendocrinology* 1986;43:498–503.
28. Edvinsson L, Ekman R, Jansen I, McCulloch J, Mortensen A, Uddman R. Reduced levels of calcitonin gene-related peptide-like immunoreactivity in human brain vessels after subarachnoid haemorrhage. *Neurosci Lett* 1991;121:151–4.
29. Kokkoris S, Andrews P, Webb DJ. Role of calcitonin gene-related peptide in cerebral vasospasm, and as a therapeutic approach to subarachnoid hemorrhage. *Front Endocrinol (Lausanne)* 2012;3:135.

ORCID ID:

C. Öztürk 0000-0002-2000-4952; M. N. Koçak 0000-0003-0828-520X;
T. Demirci 0000-0002-8814-9648; I. Malkoç 0000-0002-9221-510X;
M. D. Aydın 0000-0002-0383-9739



Correspondence to: Mehmet Dumlu Aydın, MD

Erzurum Atatürk University, Department of Neurosurgery,
School of Medicine, Erzurum, Turkey
Phone: +90 532 322 83 89
e-mail: nmda11@hotmail.com

Conflict of interest statement: No conflicts declared.

This is an open access article distributed under the terms of the Creative Commons Attribution-NonCommercial-NoDerivs 3.0 Unported (CC BY-NC-ND3.0) Licence (<http://creativecommons.org/licenses/by-nc-nd/3.0/>) which permits unrestricted noncommercial use, distribution, and reproduction in any medium, provided the original work is properly cited. *Please cite this article as:* Öztürk C, Koçak MN, Demirci T, Malkoç İ, Aydın MD. The underestimated role of a somatosensory neural network on thyroid gland morphology: an experimental subarachnoid hemorrhage model study. *Anatomy* 2019;13(3):155–162.

Estimation of sex using mandibular canine index in a young Nepalese population

Sunil Shrestha¹ , Rojina Shakya² , Dil Islam Mansoor² , Dilip Kumar Mehta² ,
Shamsher Shrestha¹ 

¹Department of Human Anatomy, B.P. Koirala Institute of Health Sciences, Dharan, Nepal

²Department of Anatomy, Kathmandu University School of Medical Sciences, Dhulikhel, Nepal

Abstract

Objectives: Tooth size standards based on odontometric investigations can be used in age and sex determination in forensic investigations and natural disasters such as tsunami, earthquakes etc. where bones are frequently fragmented. In such cases, mandibular canines are found to exhibit the highest degree of sexual dimorphism. This study aimed to assess the usefulness of mandibular canine for sex identification.

Methods: The present study was conducted based on measurements of mandibular canine teeth of 160 students (80 males and 80 females; aged 17–24 years) in Kathmandu University, Dhulikhel, Nepal.

Results: Mandibular canine index for right and left canines was found to be significantly different in males and females. The identification of sex correctly using right mandibular canine index was 53.75% in males and 41.25% in females; and using left mandibular canine index was 61.25% in males and 38.75% in females. The sex can be predicted correctly using a mandibular canine index: being higher in males (57.5%) than females (45.62%). The mean mesiodistal width of the right and left mandibular canines and intercanine distance were significantly greater in males than females. Sexual dimorphism in right mandibular canine was higher (8.29%) than that of the left mandibular canine (6.12%).

Conclusion: Sex can be predicted correctly using mandibular canine index. Right mandibular canine teeth are more sexually dimorphic than left. This may be influenced by gender, heredity, cultural, environmental and racial factors mostly influenced by Y chromosomes.

Keywords: canine; canine teeth; dimorphism; intercanine distance; mandibular canine index

Anatomy 2019;13(3):163–167 ©2019 Turkish Society of Anatomy and Clinical Anatomy (TSACA)

Introduction

Teeth are the hardest and chemically most stable tissue found in the body with the composition of enamel and dentine, and 11 other elements such as calcium, phosphorus, sodium, magnesium and aluminium in higher concentrations. Due to this, teeth are known to resist post-mortem, mechanical and physical stresses, and from chemical destruction. Sexual dimorphism represents a group of morphological characteristics that differentiate males and females such as differences in size, stature and appearance that can be applied to dental identification, because no two mouths are alike.^[1–4]

Bossert and Marks^[5] stated that the study of the permanent mandibular and maxillary canine teeth offer certain advantages *i.e.* least used in the oral cavity and less

affected by periodontal diseases and referred as cornerstone of dental arches with single-pointed cusps. The shape of the crowns with their single-pointed cusps, location in the mouth, strongly developed roots, anchorage in the alveolar process of the jaws makes mandibular canine teeth most stable in mouth and crown portions of the canines are shaped in the manner that promotes self-cleansing quality preserve these teeth throughout life.^[3] Tooth size standards based on odontometric studies can be used in age and sex determination and its morphology is influenced by gender, heredity, cultural, environmental and racial factors. This remarkable capability of canine teeth for determining individual sex is based on the influence of the Y chromosomes which do not exhibit uniform influence on all teeth and the thickness of the dentin,

whereas the X chromosomes play a role in the thickness of the enamel and its relative uniformity.^[6,7]

In sex determination studies from forensic medicine and mass graves where bones are frequently fragmented, mandibular canines exhibited the highest degree of sexual dimorphism with a mean age of eruption of 10.87 years and last teeth extracted with age.^[8] Gender determination of skeletal remains is part of archaeological and many medicolegal examinations, but bones belonging to one single person cannot be found during exhumations of bodies from mass graves. This makes teeth and the skulls the only real material for identification, but the accurate result is only obtained from DNA technique.^[9,10] Therefore, mandibular canine index (MCI) was employed in numerous studies on large populations, because it is simple, reliable, inexpensive and easy to perform; and the canine teeth were considered as key teeth for the personal identification.^[8] As no such study has been performed in Nepal yet, the present study attempted to find the correlation between gender and MCI in a young Nepalase population.

Materials and Methods

The present study was conducted in 160 students (80 males and 80 females; min. 17 – max. 24 years of age) from Kathmandu University, Dhulikhel, Nepal and approved by Kathmandu University School of Medicine Institutional Review Committee (approval number: 16/14). Right and left mandibular canine mesiodistal width and mandibular intercanine distance were measured using a digital vernier calliper by the same person in a clean and well-illuminated room under aseptic precautions (Figures 1 and 2). Individuals with healthy gingiva and periodontium, caries-free teeth, normal overjet and overbite and absence of spacing in the anterior teeth were

included in the study. Individuals with any pathological condition of canines, broken canines or any malformed canines were excluded. The data were analyzed using the Statistical Package for Social Sciences (SPSS for Windows, version 16.0, Chicago, IL, USA).

The observed and standard MCI were calculated using the following formula adapted from Kaushal et al.:^[4,11]

$$\text{Observed MCI} = \frac{\text{Mesiodistal crown width of mandibular canine (mm)}}{\text{Intercanine distance (mm)}}$$

$$\text{Observed MCI} = \frac{(\text{mean male MCI} - \text{SD}) + (\text{mean female MCI} + \text{SD})}{2}$$

If the observed MCI for the individual was higher than the standard MCI, the individual was considered to be male, and if lower or equal to standard MCI as female.

Sexual dimorphism represents a group of morphological characteristics that differentiate male and females such as differences in size, stature and appearance and calculated with the following formula adapted from Ibeachu et al.^[12]

Sexual dimorphism = $\left[\frac{X_m}{X_f} - 1 \right] \times 100$ (X_m = mean mesiodistal canine width in male; X_f = mean mesiodistal canine width in female)

Results

Mesiodistal width of right and left mandibular canine teeth, intercanine distance and right and left MCI are shown in Table 1. The value of the standard MCI for the right and left sides was 0.24. The observed right and

Table 1

The result of mesiodistal width of right and left mandibular canine teeth, intercanine distance, right and left MCI.*

Parameters	Sex	Range (mm)	Mean±SD (mm)	Variance	p-value
Mesiodistal width of RMC	Male	5.71–7.83	6.63±0.41	0.17	0
	Female	5.18–7.30	6.12±0.5	0.25	
Mesiodistal width of LMC	Male	5.09–7.24	6.52±0.4	0.16	0
	Female	4.19–7.40	6.14±0.61	0.38	
Intercanine distance	Male	24.04–33.66	27.76±2.07	4.30	0
	Female	21.57–31.66	25.15±1.98	3.92	
RMCI	Male	0.19–0.29	0.23±0.012	0.00041	0.17
	Female	0.17–0.30	0.24±0.02	0.00048	
LMCI	Male	0.15–0.26	0.23±0.02	0.00049	0.02
	Female	0.17–0.31	0.24±0.02	0.00071	

LMC: left mandibular canine; LMCI: Left mandibular canine index; RMC: right mandibular canine; RMCI: right mandibular canine index. *p>0.05.

left MCI in 160 students was calculated and categorized as above the standard MCI and equal and less than standard MCI. According to Kaushal et al.,^[4] if the observed MCI for the individual is higher than the standard MCI, then the individual is predicted to be male and if lower or equal to standard MCI female. The frequency of standard and observed MCIs are shown in **Table 2**. MCI for right and left canines were found to be significantly different for males and females. The percentage of cases correctly identified using right MCI was 53.75% in males and 41.25% in females. This value is 61.25 % in males and 50% in females for the left MCI (**Table 3**). Thus, sex can be predicted correctly 57.5% higher in males compared to 45.62% in females using MCI.

The mean mesiodistal width of right and left mandibular canines teeth were found to be highly significant in male and female. The mean mesiodistal right mandibular canine (RMC) width for males 6.63 (range: 5.71–7.83) mm was higher than that of females 6.12 (range: 5.18–7.3) mm. The mean RMC mesiodistal width of males as 6.63 (range: 5.71–7.83) mm was higher than mean left mandibular canine mesiodistal width (LMC) in males as 6.52 (range: 5.09–7.24) mm. The mean LMC mesiodistal width in males as 6.12 mm was found to be nearly equal or greater than mean mesiodistal width of RMC in females as 6.14 (range: 5.18–7.3) mm. The mean intercanine distance (ICD) was 27.76 (range: 24.04–33.66) mm in males which is higher than the females 25.15 (range: 21.57–31.66) mm (**Table 1**).

Sexual dimorphism was calculated for the right mandibular canine as 8.29%, more dimorphic than the left mandibular canine (6.12%).



Figure 1. Measurement of mesiodistal width of mandibular canine.

Table 2
Standard MCI and observed RMCI and LMCI values for males and females.

Parameters	Standard MCI	RMCI	LMCI
Male	>0.24	43	49
	≤0.24	37	31
Female	>0.24	47	40
	≤0.24	33	40

LMCI: Left mandibular canine index; RMCI: Right mandibular canine index.

Table 3
Percentage of sex correctly predicted using standard MCI value.

Sex	Parameter	Number	%	Correctly predicted sex (%)
Male	RMCI	43	53.75%	57.50%
	LMCI	49	61.25%	
Female	RMCI	33	41.25%	45.62%
	LMCI	30	50%	

LMCI: Left mandibular canine index; RMCI: Right mandibular canine index.

Discussion

The present study reports the estimation of sex using MCI in a young Nepalese population. The sex could be predicted correctly higher in males (57.5%) than females (45.62%) using MCI which was approximately similar to the results of the Al-Rifaiya et al.^[13] (55.07%). However, studies of Yadav et al.^[14] (72%) and Rao et al.^[15] (male=



Figure 2. Measurement of mandibular intercanine distance.

84.3%; female=85.7%) in a Southern Indian population, Reddy et al.^[9] (82%) in a Northern Indian population had comparatively higher sex prediction rates than that of the present study. These differences are attributable to the regional differences in the tooth size. Similarly, the percentage of females correctly predicted in studies by Rao et al.,^[15] Ahmed,^[16] Hosmani's et al.^[17] was higher than the present study. For studies conducted for male sex prediction by Ahmed^[16] in an Iraqi population, Acharya's et al.^[18] and Hosmani's et al.^[17] in an Indian population were lower than the present study (57.50%). The possible reason for low accuracy can be assumed as evolutionary change, genetic factors and ethnic background.

The study also showed that value of RMC was significantly different between males and females. This is similar to the findings of Ahmed,^[16] Muhamedagic and Sarajlic,^[10] Grover et al.,^[6] and Ibeucu's et al.^[12] However, the results of the present study for mean mesiodistal of RMC and LMC for males and females was lower than those by Ayoub et al.,^[19] Vishwakarma and Guha^[8] and Khan et al.^[7] There are few differences in mesiodistal width of mandibular canine, which may be probably accounted for the racial variations in tooth size, as studies have been conducted in different populations and different countries. Therefore, evaluation and comparison of present data with the previous studies revealed several differences as well as similarities.

Mean ICD was higher in males in the present study, which is highly significant and in accordance with the findings of Ahmed,^[16] Ayoub et al.,^[19] Bakkannavar et al.,^[5] Muller et al.,^[20] and Kaushal et al.^[4] and in controversy with the findings of Vishwakarma and Guha.^[8] The mean ICD for males in the present study was 27.76±2.08 mm, which is approximately equal to the findings of Ayoub et al.^[19] (27.62 mm) and Sherufudin et al.^[21] (27.36 mm). The mean ICD distance was 25.16±1.98 mm in females, approximately equal to the findings of Muller's^[20] (25.03 mm) and Kaushal's study^[11] (25.07 mm).

This study also showed that the sexual dimorphism was more in right mandibular canine teeth (8.29%) than the left (6.12%). This finding supports the results of earlier studies by Vishwakarma and Guha^[8] and Srivastava.^[22] The value of sexual dimorphism for RMC (8.26%) was approximately equal to the findings of Reddy et al.^[9] (8.78%), Kaushal et al.^[4] (7.95%), Grover et al.^[6] (RMC=9.43%), and Ayoub et al.^[19] (RMC=9.7%). The controversial findings of the present study may be attributed to racial, environmental and nutritional factors of the study population.

Conclusion

Tooth size standards based on odontometric investigations can be used in age and sex determination and is known to be influenced by gender, heredity, cultural, environmental and racial factor mostly influenced by Y chromosomes. Y chromosomes control the thickness of the dentin but do not exhibit a uniform influence on all teeth, whereas X chromosomes play a role in the thickness of enamel and its relative uniformity. In this study, we have found the mean mesiodistal width of RMC, LMC, and intercanine distance higher in males, and concluded that sex can be predicted correctly 57.50% higher in males compared to 45.62% in females, and the MCI of right mandibular canine teeth was more sexually dimorphic than that of the left side.

References

1. Standring S (ed). Gray's anatomy: the anatomical basis of clinical practice. 40th ed. London: Churchill Livingstone Elsevier; 2013. p. 1–1551.
2. Zenóbio Madelon AF, Nogueira Maria S, Zenobio Elton G. Chemical composition of human enamel and dentin. Preliminary results to determination of the effective atomic number. Proceedings of the 12nd International Congress of the International Radiation Protection Association (IRPA12), 2008;42:1–6.
3. Nelson SJ. Wheeler's dental anatomy, physiology, and occlusion. 10th ed. St. Louis, MO: Elsevier, Saunders, 2014. p. 1–350.
4. Kaushal S, Patnaik V, Agnihotri G. Mandibular canines in sex determination. Journal of Anatomical Society of India 2003;52:119–24.
5. Bakkannavar SM, Manjunath S, Nayak VC, Kumar GP. Canine index – a tool for sex determination. Egyptian Journal of Forensic Sciences 2015;5:157–61.
6. Grover M, Bai RG, Ram T, Puri PM, Ghodke KR. An odontologist's key to sex determination: study analysis of mandibular canine teeth in South Indian population. Journal of Orofacial Research 2013;3:157–60.
7. Khan SH, Hassan GS, Rafique T, Hasan N, Russell SH. Mesiodistal crown dimensions of permanent teeth in Bangladeshi population. Bangabandhu Sheikh Mujib Medical University Journal 2011;4:81–7.
8. Vishwakarma N, Guha R. A study of sexual dimorphism in permanent mandibular canines and its implications in forensic investigations. Nepal Medical College Journal 2011;13:96–9.
9. Reddy VM, Saxena S, Bansal P. Mandibular canine index as a sex determinant? A study on the population of western Uttar Pradesh. Journal of Oral and Maxillofacial Pathology 2008;12:56–9.
10. Muhamedagic B, Sarajlic N. Sex determination of the Bosnian-Herzegovinian population based on odontometric characteristics of permanent lower canines. Journal of Health Sciences 2013;3:164–9.
11. Bindu A, Vasudeva K, Subash K, Usha C, Sanjay S. Gender based comparison of intercanine distance of mandibular permanent canine in different populations. Journal of Punjab Academy of Forensic Medicine and Toxicology 2008;8:6–9.
12. Ibeachu PC, Didia BC, Orish CN. Sexual dimorphism in mandibular canine width and intercanine distance of University of Port-

- Harcourt student, Nigeria. *Asian Journal Medical Sciences* 2012;2:166-9.
13. Al-Rifaiy MQ, Abdullah MA, Ashraf I, Khan N. Dimorphism of mandibular and maxillary canine teeth in establishing identity. *The Saudi Dental Journal* 1997;9:17-20.
 14. Yadav S, Nagabhushana D, Rao B, Mamatha G. Mandibular canine index in establishing sex identity in establishing sex identity. *Indian Journal of Dental Research* 2002;13:143-6.
 15. Rao NG, Rao NN, Pai ML, Kotian MS. Mandibular canine index – a clue for establishing sex identity. *Forensic Sci Int* 1989;42:249-54.
 16. Ahmed HMA. Genders identification using mandibular canines (Iraqi study). *Journal of Baghdad College of Dentistry* 2014;26:150-3.
 17. Hosmani JV, Nayak RS, Kotrashetti VS, S P, Babji D. Reliability of mandibular canines as indicators for sexual dichotomy. *J Int Oral Health* 2013;5:1-7.
 18. Acharya AB, Angadi PV, Prabhu S, Nagnur S. Validity of the mandibular canine index (MCI) in sex prediction? Reassessment in an Indian sample. *Forensic Sci Int* 2011;204:207.e1-4.
 19. Ayoub F, Shamseddine L, Rifai M, Cassia A, Diab R, Zaarour I, Saadeh M, Rouhana G. Mandibular canine dimorphism in establishing sex identity in the Lebanese population. *Int J Dent* 2014;2014:235204.
 20. Muller M, Lupi-pegurier L, Quatrehomme G, Bolla M. Odontometrical method useful in determining gender and dental alignment. *Forensic Sci Int* 2001;121:194-7.
 21. Sherfudhin H, Abdullah M, Khan N. A cross-sectional study of canine dimorphism in establishing sex identity: comparison of two statistical methods. *J Oral Rehabil* 1996;23:627-31.
 22. Srivastava PC. Correlation of odontometric measures in sex determination. *J Indian Academy of Forensic Medicine* 2010;32:56-61.

ORCID ID:

Su. Shrestha 0000-0002-3094-5035; R. Shakya 0000-0002-2028-1466;
D. I. Mansoor 0000-0001-5958-0423; D. K. Mehta 0000-0002-9408-9469;
Sh. Shrestha 0000-0002-0547-7823



Correspondence to: Sunil Shrestha, MSc

Department of Human Anatomy, B.P. Koirala Institute of Health Sciences,
Dharan, Nepal
Phone: +97 79803911259
e-mail: sunilmanshrestha@gmail.com

Conflict of interest statement: No conflicts declared.

This is an open access article distributed under the terms of the Creative Commons Attribution-NonCommercial-NoDerivs 3.0 Unported (CC BY-NC-ND3.0) Licence (<http://creativecommons.org/licenses/by-nc-nd/3.0/>) which permits unrestricted noncommercial use, distribution, and reproduction in any medium, provided the original work is properly cited. *Please cite this article as:* Shrestha Su, Shakya R, Mansoor DI, Mehta DK, Shrestha Sh. Estimation of sex using mandibular canine index in a young Nepalese population. *Anatomy* 2019;13(3):163-167.

Macroscopic footprint of the glenoid labrum

Mehmet Emin Şimşek¹ , Mustafa Akkaya² , Safa Gürsoy² , Özgür Kaya³ ,
Nihal Apaydın⁴ , Murat Bozkurt² 

¹Department of Orthopedics and Traumatology, School of Medicine, Lokman Hekim University, Ankara, Turkey

²Department of Orthopedics and Traumatology, School of Medicine, Ankara Yıldırım Beyazıt University, Ankara, Turkey

³Department of Orthopedics and Traumatology, Lokman Hekim Etlik Hospital, Ankara, Turkey

⁴Department of Anatomy, School of Medicine, Ankara University, Ankara, Turkey

Abstract

Objectives: Glenoid labrum lesions are one of the main causes of traumatic shoulder dislocations. Arthroscopic or open repair using suture anchors is commonly used to treat labral lesions. Proper placement of suture anchors in order to replace the normal ligamentous restraint is essential to restore normal anatomy that determines the final location of the repaired labrum. Yet, the most efficient and safest location of the glenoid bone has not been precisely described. Therefore, this study aimed to describe the macroscopic footprint of the glenoid labrum in order to depict the ideal anchor placement location precisely.

Methods: Twenty-two shoulders from 11 cadavers were dissected to reveal glenoid labrum. Clock positions were determined on glenoid labrum circumferentially to evaluate the footprint of the glenoid labrum. The distance between the bony edge of the glenoid rim and the edge of the labrum was measured.

Results: The mean distance from the glenoid labrum to the bony glenoid rim was measured as 5.1 mm (3 o'clock position), 6.2 mm (6 o'clock position), 5.1 mm (9 o'clock position) and 4.1 mm (12 o'clock position) in the anterior, inferior, posterior and superior aspects, respectively. 29.3% of the specimens had a completely defective anterior labrum.

Conclusion: Location of the labrum with respect to the bony glenoid rim should be considered for proper suture placements in treatment of labral tears. It is suggested that the most important step in the stabilization of joint laxity is appropriate placement of the sutures in the anterior and inferior aspects of the glenoid labrum.

Keywords: anatomy; footprint; glenoid labrum

Anatomy 2019;13(3):168–173 ©2019 Turkish Society of Anatomy and Clinical Anatomy (TSACA)

Introduction

The glenoid labrum is a ring of fibrocartilage that lies around the margin of the glenoid cavity. The articular cavity is deepened by the labrum and the labrum also protects the bone edges and facilitates lubrication of the joint.^[1,2] Synovium lines the inner surface of the labrum, whereas the outer surface is continuous with the scapular neck periosteum and attaches to the capsule. Edges of the glenoid fossa become more flexible since the shape of the labrum changes to contain the rotation of the humeral head. The labrum represents a fold of the capsule that serves as an attachment for glenohumeral ligaments.^[3,4]

In general, traumatic shoulder dislocation is the main cause of extensive glenoid labrum lesions. Labral tears are

typically divided into two categories according to the location of the lesion. Anterior labral tears or Bankart lesions, posterior labral tears or reverse Bankart lesions, and superior labral tears or superior labrum anterior and posterior (SLAP) lesions are among such tears.^[5,6]

Today, the best method to reattach the labrum and the capsule to the glenoid is to place suture anchors. The degree of capsulolabral detachment determines the number of suture anchors that will be used. For instance, in a standard Bankart repair in the right shoulder, 3 or 4 anchors would be placed at the 5 o'clock, 4 o'clock, 3 o'clock and 2 o'clock positions.^[7,8] The repair performed by placing suture anchors is conducted from the inferior to the superior aspect. Posterior labral repair is conducted

with 3 anchors from the inferior aspect to the mid-glenoid posteriorly, after placing an anchor placement guide through the infraspinatus muscle. Then, the same technique is used to repair the anterior labrum. The anchor placement guide is placed through the subscapularis muscle so as to place the anchors. Starting from the inferior aspect, three anchors are placed until the anterior labrum.^[9]

The repair of soft tissue detachments highly relies on suture anchors. Recurrent instability, which is one of the most frequent complications of glenoid repair, can be encountered due to improper suture anchor placement or problems during insertion. Such a problem can also be observed due to pathological laxity or inadequate capsular tension.^[10,11]

Today, it is suggested to place the anchors 2–3 mm onto the articular surface on the chondral rim of the glenoid. The safest and most effective location of labral reattachment on the glenoid rim should be depicted well, since surgical failure has been associated with improper surgical technique. Today, this is referred to as the “art of repair” by surgeons. The aim of this study is to describe the macroscopic footprint of the glenoid labrum in order to depict the ideal anchor placement location precisely.

Materials and Methods

Twenty-two shoulders from 11 cadavers were dissected for this study. The age and sex of the cadavers and the side from which specimens were collected were recorded. Of these, 12 were females and 10 males. The mean age of the cadavers was 67 years (min. 57 – max. 78 years). 9 specimens were collected from the left side and 13 specimens from the right side (**Figure 1**). There was no history of



Figure 1. Dissection of the glenoid, left shoulder. [Color figure can be viewed in the online issue, which is available at www.anatomy.org.tr]

significant trauma or upper extremity surgery in any of the specimens. First, the skin was removed from the scapula, and the specimen was cleared of subcutaneous tissue and muscular connections. Then, the capsule was removed at the capsulolabral junction. In general practice, clock positions were used to depict the location and extent of labral tears and in the course of surgical treatment. Therefore, same clock positions were used to evaluate the morphological characteristics of the glenoid labrum and its footprint. Moreover, the relationship between the capsular ligaments and glenoid labrum was also evaluated using clock positions. The distance between the bony edge of the glenoid fossa and the edge of the labrum was measured in order to evaluate the footprint of the glenoid labrum. Efforts were made not to disrupt the labrum and the cartilage covering the glenoid. The apex of the line passing through the midglenoid in parallel to the scapular edge plane was marked as 12 o'clock and the clock plane was placed on the glenoid in order to determine 12 measurement points with 1-hour intervals. 12 o'clock was designated as the superior edge; 1 and 2 o'clock as the antero-superior; 3, 4 and 5 o'clock as the anterior; 6 o'clock as the inferior; 7, 8 and 9 o'clock as the posterior; 10 and 11 o'clock as the posterosuperior edge (**Figure 2**). There was severe glenohumeral arthrosis with significant degenerative changes in three specimens, which were not suitable for measurement. Accordingly, 19 cadaveric specimens were used for performing measurements in the study. Microcalipers (General Tools, New York, NY) were used for all measurements and the mean values were recorded. 3 experienced specialist orthopedic surgeons conducted all measurements on images and a double-blind setup was used to minimize inter- and intraobserver errors.

SPSS software package (Version 25.0, SPSS Inc., Chicago, IL, USA) was used for statistical analysis. Normal distribution of the continuous variables were evaluated using the Kolmogorov Smirnov and Shapiro-Wilk tests and histograms. Numerical variables were expressed with mean \pm SD, median values (minimum-maximum) or with proportions. Intergroup comparisons were performed using Student's t-test for normally distributed data and Mann-Whitney U test for data that did not have a normal distribution. $p < 0.05$ was considered statistically significant. Relative intra- and interobserver reliabilities were determined using the intra-class correlation coefficient (ICC) model 2.1.

The specimens used in the present study were unclaimed bodies obtained from the forensic medicine according to official regulations. Conducting scientific studies on cadavers or cadaveric body parts do not require ethical approval in our institution.

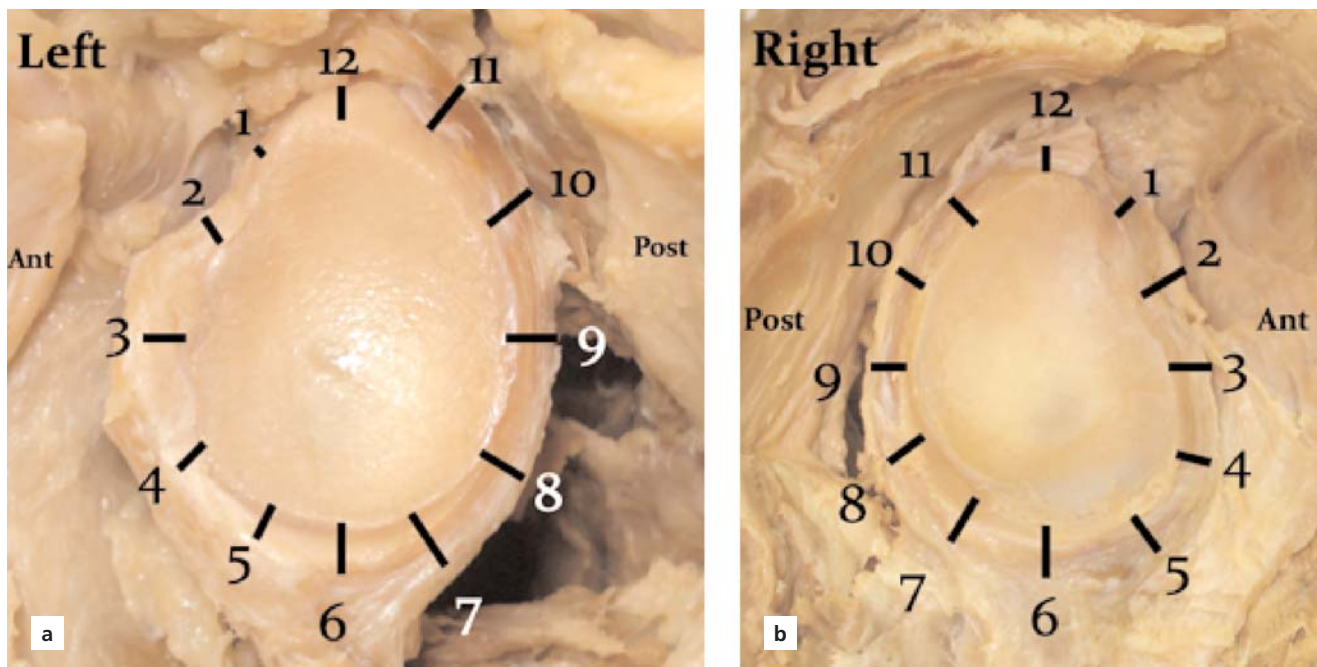


Figure 2. Clock positions of the left (a) and right (b) glenoid labrum. [Color figure can be viewed in the online issue, which is available at www.anatomy.org.tr]

Results

The dissections revealed that the morphology of the superior labrum was significantly different than that of the inferior labrum. It had a meniscal pattern and a loose attachment to the glenoid process. Moreover, the anterior part was completely missing in 29.3% of the specimens. The anterosuperior part of the labrum inserted into the fibers of the middle or inferior glenohumeral ligament, rather than to the actual glenoid margin. The mentioned meniscal pattern was also observed in the posterosuperior part of the labrum with a loose attachment to the glenoid rim. The inferior portion of the labrum was rounded and fibrous and appeared like an immobile extension of articular cartilage.

Starting at the 12 o'clock position, the mean distance from the bony edge in hourly intervals was 4.86 ± 0.87 mm at 12 o'clock, 4.20 ± 1.5 mm at 1 o'clock, 4.41 ± 1.2 mm at 2 o'clock, 5.23 ± 1.28 mm at 3 o'clock, 5.52 ± 1.23 mm at 4 o'clock, 6.25 ± 1.02 mm at 5 o'clock, 6.10 ± 0.86 mm at 6 o'clock, 5.98 ± 0.82 mm at 7 o'clock position of glenoid labrum; and 5.71 ± 0.91 mm at 8 o'clock, 5.52 ± 0.85 mm at 9 o'clock, 5.14 ± 0.98 mm at 10 o'clock and 5.52 ± 0.73 mm at 11 o'clock position of glenoid labrum (Table 1). The inter- and intraobserver variability of the measurements did not exceed 0.1 mm (Table 2).

According to the statistical analysis, there was a trend towards the differences between different locations on the glenoid face, but it was not statistically significant. The greatest difference between the measurements were observed between the 6 and 11, 12, 1 and 2 o'clock positions (Figure 3).

Table 1

Distance from macroscopic edge of the glenoid labrum to bony edge of the glenoid for the measured regions and positions.

Region	Position	Mean \pm SD (mm)
Anterosuperior	1 o'clock	4.20 ± 1.15
	2 o'clock	4.41 ± 1.20
Anterior	3 o'clock	5.23 ± 1.28
	4 o'clock	5.52 ± 1.23
	5 o'clock	6.25 ± 1.02
Inferior	6 o'clock	6.10 ± 0.86
	7 o'clock	5.98 ± 0.82
Posterior	8 o'clock	5.71 ± 0.91
	9 o'clock	5.52 ± 0.85
Posterosuperior	10 o'clock	5.14 ± 0.98
	11 o'clock	5.52 ± 0.73
Superior	12 o'clock	4.86 ± 0.87

Table 2
Intraobserver and interobserver reliabilities for the measured regions of the glenoid labrum.

Region	Position	Intraobserver reliability % CI	p	Interobserver reliability % CI	p
Antero-superior	1 o'clock	0.97 (0.96–0.99)	0.214	0.99 (0.98–0.99)	0.141
	2 o'clock	0.98 (0.96–0.99)	0.128	0.98 (0.96–0.99)	0.126
Anterior	3 o'clock	0.96 (0.95–0.97)	0.168	0.93 (0.87–0.97)	0.168
	4 o'clock	0.98 (0.98–0.99)	0.099	0.98 (0.98–0.99)	0.099
	5 o'clock	0.96 (0.95–0.97)	0.210	0.91 (0.92–0.97)	0.210
Inferior	6 o'clock	0.97 (0.96–0.99)	0.157	0.98 (0.98–0.99)	0.152
Posterior	7 o'clock	0.95 (0.93–0.97)	0.238	0.93 (0.87–0.97)	0.168
	8 o'clock	0.85 (0.71–0.94)	0.147	0.85 (0.71–0.94)	0.147
	9 o'clock	0.92 (0.82–0.96)	0.164	0.91 (0.82–0.96)	0.154
Postero-superior	10 o'clock	0.98 (0.97–0.99)	0.456	0.98 (0.97–0.99)	0.470
	11 o'clock	0.94 (0.90–0.96)	0.188	0.93 (0.90–0.96)	0.178
Superior	12 o'clock	0.987 (0.96–0.99)	0.504	0.98 (0.97–0.99)	0.907

Discussion

Pathomorphological changes may initially be observed at three different locations in traumatic anterior dislocations of the shoulder: at the capsule, at its origin or insertion. Typically, the injury is in the form of an avulsion of the capsule and labrum from the glenoid.^[12] The normal glenohumeral joint restraints can be recreated by anatomic

restoration of the glenoid labrum following a traumatic detachment.^[13]

Anchor placement is of vital importance to achieve successful outcomes in labral repairs.^[14] Recent studies suggest to start 5 o'clock and use the 4 and 3 o'clock position for an anchor placement,^[15–17] because these locations provide the strongest anchor placement to gle-

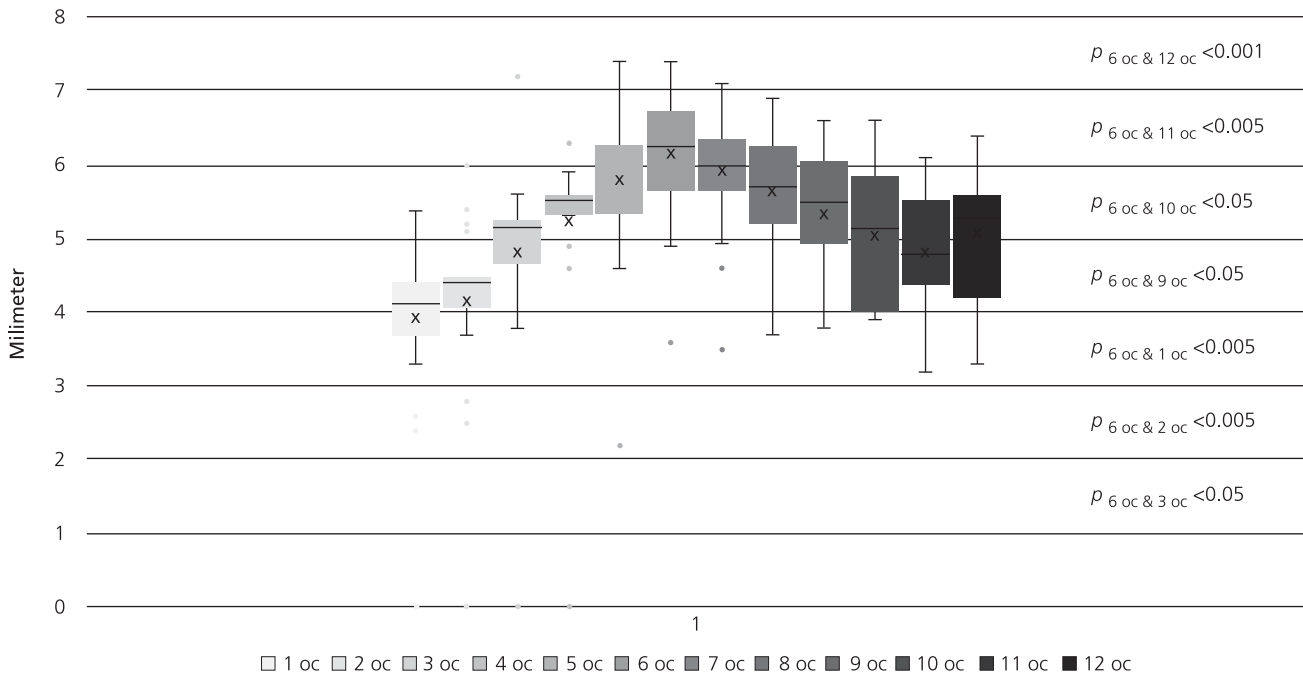


Figure 3. Labrum measurements at 12 different clock positions.

noid labrum. There were some conflicts about the ideal site of fixation in the past. Some surgeons asserted that the anchors should be placed on articular surface in order to enhance stability.^[18,19] However, anchor placement right on the edge of articular surface did not cause any changes in stability and even prevented potential arthropathies on the glenohumeral joint surface.^[20-22]

According to the results of the present study, the insertion of the glenoid labrum was observed at a variable distance from the bony edge of the glenoid. It is required to place the suture anchor on the glenoid face at the articular margin in order to perform the anatomic reconstruction of the detached labrum. During anatomic dissections, we observed that the macroscopic edge of the labrum, described as the visible line of transition between the labrum and articular cartilage, was significantly more medial to the edge of the glenoid bone than expected.^[7,9,23]

A smooth transition from the cartilaginous surface to the labrum is necessary for the translation of the glenohumeral joint. Therefore, a suture anchor should be placed in the vicinity of the glenohumeral articulation with caution.

The most important causes of glenohumeral arthropathy after an open or arthroscopic shoulder surgery were associated with anchor placement, regardless of the anchor type, i.e. metallic or biodegradable in recent studies.^[24-28] With this perspective, knowing the anatomy of the labrum and glenoid is important and it should be kept in mind that the anatomy may be different in each person.

The limitations of this study were as follows: open surgical visualization was performed and there were no arthroscopic evaluations in the study. Arthroscopic visualization of the macroscopic edge of the glenoid labrum could be different in comparison to open surgical visualization. Moreover, other parameters concerning glenoid variability were not measured, which made it impossible to make any further associations with glenoid morphology.

Conclusion

The results of this study suggest that insertion of the glenoid labrum onto the bony face of the glenoid occurs at a variable distance. Reattachment of the capsule and labrum to the glenoid articular surface essentially relies on suture anchors. In suture placement, location of the labrum with respect to the bony glenoid rim should be considered. It is suggested that the most important step in stabilizing joint laxity is proper placement along the anterior and inferior side of the glenoid labrum.

References

- Cooper DE, Arnoczky SP, O'Brien SJ, Warren RF, DiCarlo E, Allen AA. Anatomy, histology, and vascularity of the glenoid labrum. An anatomical study. *J Bone Joint Surg Am* 1992;74:46-52.
- Barthel T, König U, Böhm D, Loehr JF, Gohlke F. Anatomy of the glenoid labrum. [Article in German] *Orthopäde* 2003;32:578-85.
- Tischer T, Putz R. Anatomy of the superior labrum complex of the shoulder. [Article in German] *Orthopäde* 2003;32:572-7.
- Alashkham A, Alraddadi A, Felts P, Soames R. Histology, vascularity and innervation of the glenoid labrum. *J Orthop Surg (Hong Kong)* 2018;26:2309499018770900.
- Sailer J, Imhof H. Shoulder instability. [Article in German] *Radiologe* 2004;44:578-90.
- Antonio GE, Griffith JF, Yu AB, Yung PS, Chan KM, Ahuja AT. First-time shoulder dislocation. High prevalence of labral injury and age-related differences revealed by MR arthrography. *J Magn Reson Imaging* 2007;26:983-91.
- Valis P, Nydrle M. Arthroscopic stabilization of the shoulder using anchors. *Acta Chir Orthop Traumatol Cech* 2003;70:233-36.
- Zarzycki W. Arthroscopic Bankart repair. [Article in Polish] *Chir Narzadow Ruchu Ortop Pol* 2006;71:309-11.
- Lehtinen JT, Tingart MJ, Apreleva M, Ticker JB, Warner JJ. Anatomy of the superior glenoid rim. Repair of superior labral anterior to posterior tears. *Am J Sports Med* 2003;31:257-60.
- Rowe CR, Zarins B, Ciullo JV. Recurrent anterior dislocation of the shoulder after surgical repair. Apparent causes of failure and treatment. *J Bone Joint Surg Am* 1984;66:159-68.
- Zhu W, Lu W, Zhang L, Han Y, Ou Y, Peng L, Liu H, Wang D, Zeng Y. Arthroscopic findings in the recurrent anterior instability of the shoulder. *Eur J Orthop Surg Traumatol* 2014;24:699-705.
- Wiedemann E, Jäger A, Nebelung W. Pathomorphology of shoulder instability. [Article in German] *Orthopäde* 2009;38:16-20, 22-3.
- Slabaugh MA, Friel NA, Wang VM, Cole BJ. Restoring the labral height for treatment of Bankart lesions: a comparison of suture anchor constructs. *Arthroscopy* 2010;26:587-91.
- Koulalis D, Kendoff D, Citak M, O'Loughlin PF, Pearle AD. Freehand versus navigated glenoid anchor positioning in anterior labral repair. *Knee Surg Sports Traumatol Arthrosc* 2011;19:1554-7.
- Carreira DS, Mazzocca AD, Oryhon J, Brown FM, Hayden JK, Romeo AA. A prospective outcome evaluation of arthroscopic Bankart repairs: minimum 2-year follow-up. *Am J Sports Med* 2006;34:771-7.
- Boileau P, Ahrens P. The TOTS (temporary outside traction suture): a new technique to allow easy suture placement and improve capsular shift in arthroscopic bankart repair. *Arthroscopy* 2003;19:672-7.
- Tischer T, Vogt S, Imhoff AB. Arthroscopic stabilization of the shoulder with suture anchors with special reference to the deep anterior-inferior portal (5.30 o'clock). *Oper Orthop Traumatol* 2007;19:133-54.
- Gartsman GM, Roddey TS, Hammerman SM. Arthroscopic treatment of anterior-inferior glenohumeral instability. Two to five-year follow-up. *J Bone Joint Surg Am* 2000;82-A:991-1003.
- Mazzocca AD, Brown FM Jr, Carreira DS, Hayden J, Romeo AA. Arthroscopic anterior shoulder stabilization of collision and contact athletes. *Am J Sports Med* 2005;33:52-60.

20. Yamamoto N, Muraki T, Sperling JW, Steinmann SP, Itoi E, Cofield RH, An KN. Does the “bumper” created during Bankart repair contribute to shoulder stability? *J Shoulder Elbow Surg* 2013; 22:828–34.
21. Thal R. A knotless suture anchor. Technique for use in arthroscopic Bankart repair. *Arthroscopy* 2001;17:213–8.
22. Wolf EM. Arthroscopic capsulolabral repair using suture anchors. *Orthop Clin North Am* 1993;24:59–69.
23. Lehtinen JT, Tingart MJ, Apreleva M, Ticker JB, Warner JJ. Variations in glenoid rim anatomy: implications regarding anchor insertion. *Arthroscopy* 2004;20:175–8.
24. McNickle AG, L’Heureux DR, Provencher MT, Romeo AA, Cole BJ. Postsurgical glenohumeral arthritis in young adults. *Am J Sports Med* 2009;37:1784–91.
25. Dines JS, Elattrache NS. Horizontal mattress with a knotless anchor to better recreate the normal superior labrum anatomy. *Arthroscopy* 2008;24:1422–5.
26. Kaar TK, Schenck RC Jr, Wirth MA, Rockwood CA Jr. Complications of metallic suture anchors in shoulder surgery: a report of 8 cases. *Arthroscopy* 2001;17:31–7.
27. Athwal GS, Shridharani SM, O’Driscoll SW. Osteolysis and arthropathy of the shoulder after use of bioabsorbable knotless suture anchors. A report of four cases. *J Bone Joint Surg Am* 2006;88:1840–5.
28. Ekelund A, Ahmed M, Bjurholm A, Nilsson O. Neuropeptides in heterotopic bone induced by bone matrix in immunosuppressed rats. *Clin Orthop Relat Res* 1997;(345)229–38.

ORCID ID:

M. E. Şimşek 0000-0002-8081-0550; M. Akkaya 0000-0002-2694-4208;
S. Gürsoy 0000-0003-4466-9657; Ö. Kaya 0000-0003-2033-9020;
N. Apaydın 0000-0002-7680-1766; M. Bozkurt 0000-0001-8160-5375

deomed®

Correspondence to: Mustafa Akkaya, MD

Department of Orthopedics and Traumatology, School of Medicine,
Ankara Yıldırım Beyazıt University, Ankara, Turkey
Phone: +90 312 578 20 00
e-mail: makkaya@outlook.com

Conflict of interest statement: No conflicts declared.

This is an open access article distributed under the terms of the Creative Commons Attribution-NonCommercial-NoDerivs 3.0 Unported (CC BY-NC-ND3.0) Licence (<http://creativecommons.org/licenses/by-nc-nd/3.0/>) which permits unrestricted noncommercial use, distribution, and reproduction in any medium, provided the original work is properly cited. *Please cite this article as:* Şimşek ME, Akkaya M, Gürsoy S, Kaya Ö, Apaydın N, Bozkurt M. Macroscopic footprint of the glenoid labrum. *Anatomy* 2019;13(3):168–173.

Clinical significance of the relationship between 3D analysis of the distal femur and femoral shaft anatomy in total knee arthroplasty

Mehmet Emin Şimşek¹ , Murat Bozkurt² 

¹Department of Orthopedics and Traumatology, Lokman Hekim University, Ankara, Turkey

²Department of Orthopedics and Traumatology, Ankara Yıldırım Beyazıt University, Ankara, Turkey

Abstract

Objectives: A proper morphometric analysis of the anatomy of the distal femur is of utmost importance for providing correct alignment for the survival of total knee arthroplasty (TKA). Herein, we aimed to conduct a detailed morphometric analysis of the distal femur, including the differences between men and women. We also aimed to determine landmarks in the sagittal and coronal planes for positioning of the femoral component during TKA and demonstrate the data that may affect clinical outcome.

Methods: Two-hundred adult femurs from the collection of anatomy department were enrolled in this study. Three-dimensional reconstruction of computed tomography scans were performed on these femurs. Differences between the reference axes and lines in the sagittal and coronal planes were obtained from the images, and correlation coefficients of the collected data were analyzed. All measurements were compared between men and women.

Results: The calculated mean angles between the sagittal mechanical axis, anterior cortical axis and distal medullary axis were found as $5.14 \pm 1.67^\circ$ and $4.12 \pm 2.41^\circ$, respectively, and the mean angle difference between the posterior condylar line (PCL) and the epicondylar axis (EA) was $4.37 \pm 2.18^\circ$. The angle difference between PCL and EA was higher in females ($p=0.047$).

Conclusion: In addition to the gender-dependent anthropomorphic differences between the distal femurs of females and males, differences between the measurements used as reference in conventional TKA techniques may affect the post-operative alignment.

Keywords: distal femur; femoral bowing; morphometry; total knee arthroplasty

Anatomy 2019;13(3):174–182 ©2019 Turkish Society of Anatomy and Clinical Anatomy (TSACA)

Introduction

One of the best treatment methods for advanced arthrosis of the knee is total knee arthroplasty (TKA).^[1] Achieving correct postoperative alignment is one of the most important factors for success following TKA.^[2] Malalignment of the prosthesis can lead to complications such as wear and aseptic loosening that could require early revision. Thus, components should be implanted according to the mechanical axes during knee arthroplasty. However, the landmarks used for the femoral alignment are not always distinct enough to determine these axes due to its complex structure.^[3,4]

Various axes and reference landmarks used during femoral implantation were mainly determined in the coronal plane since the prosthesis that provides a neutral alignment in the coronal plane has been demonstrated to have a higher long-term survival success.^[5,6] However, the situation in sagittal alignment, which is as important as coronal alignment, was not demonstrated. The inability to achieve suitable alignment in the sagittal plane and placement of the femoral component in flexion lead to loss of extension and posterior polyethylene wear, whereas placement in extension with respect to the mechanical axis can result in anterior notching leading to periprosthetic fracture.^[7–9]

In addition to the sagittal morphometry of the distal femur, there are other factors that affect prosthesis survival and knee functions after primary and revision surgeries. Rotation of the femoral component and one of its important determinants, *i.e.*, posterior condylar structures; femoral bowing; medullary canal diameters in the distal femur; and anteroposterior (AP) and mediolateral (ML) width of the distal femur are some of the factors.^[6,10]

Nearly two-thirds of the patients who undergo TKA are females. Moreover, studies have revealed variations in the morphometry of the distal femur based on factors such as gender and race. Thus, there is a need to develop different designs considering all these variables to obtain desired results after TKA.^[11]

Possible challenges that can be encountered by surgeons in anatomic alignment of the mechanical axis of the lower extremity during TKA are now easier to overcome with the use of computer-assisted orthopedic surgery techniques. Identifying the reference points and angles to be used during femoral implantation and, furthermore, identifying the differences thereof according to an important variable such as gender would increase the success of surgery while using conventional knee prosthesis techniques, still being commonly used throughout the world.^[12,13]

In this study, we aimed to conduct a detailed morphometric analysis of the anatomy of the distal femur, including many variables in the coronal and sagittal planes, to determine the differences among genders, and to demonstrate the data that could be associated with clinical outcomes.

Materials and Methods

A total of 200 adult femurs were randomly selected from the collection of Department of Anatomy of Ankara University School of Medicine. The bones with deformity, fracture, tumor, and other such changes were excluded. The bones were then assigned to two groups (100 females and 100 males) of unknown age. 115 bones were right side, and 85 were from the left. Each bone was assigned a number for identification. Computed tomography (CT) scans were performed on each femur in the coronal, sagittal, and axial planes to encompass the entire femur, with a slice thickness of 0.6 mm (256-slice multidetector scanner; Siemens®, Erlangen, Germany). Each CT scan of the femurs was analyzed with the femur rotated fully in AP position and lateral position on three-dimensional (3D) reconstructions obtained by Leonardo Dr/Dsa Va30a software (Siemens®, Erlangen, Germany) in a digital environment (**Figure 1**). Measurements for each parameter were

carried out from the obtained images by three different observers (MES, SG, MA), with the intra- and inter-observer differences being determined. Measurements done for the morphometric analysis of the distal femur were as follows:

Measurements in the Sagittal Plane

- **Femoral length:** distance from the most superior point of the femoral head to the most distal point of the medial epicondyle (ME)
- **Bowing angle:** the angle between the vertical lines passing through the midpoint of the line drawn at the level of the flair point and the transverse line drawn below the lesser trochanter. The flair point is the point at which condyles start to expand in the distal part. This angle was determined as the tip of bowing and AP - ML medullary diameter measurements done at this level; the distance of the tip to the Blumensaat line (BL) was determined as the bowing tip distance (**Figure 2**).
- **Anterior cortical axis (ACA):** the line that connects the points drawn at 5 cm and 10 cm proximal to the distal joint line (JL) on the anterior cortex^[14] (**Figure 3**).
- **Distal medullary axis (DMA):** the line drawn between 1 cm anterior to the BL end point and the midpoint



Figure 1. Anteroposterior (a) and lateral (b) images of the femur after 3D reconstruction of the CT images obtained by Leonardo Dr/Dsa Va30a software (Siemens®, Erlangen, Germany). [Color figure can be viewed in the online issue, which is available at www.anatomy.org.tr]

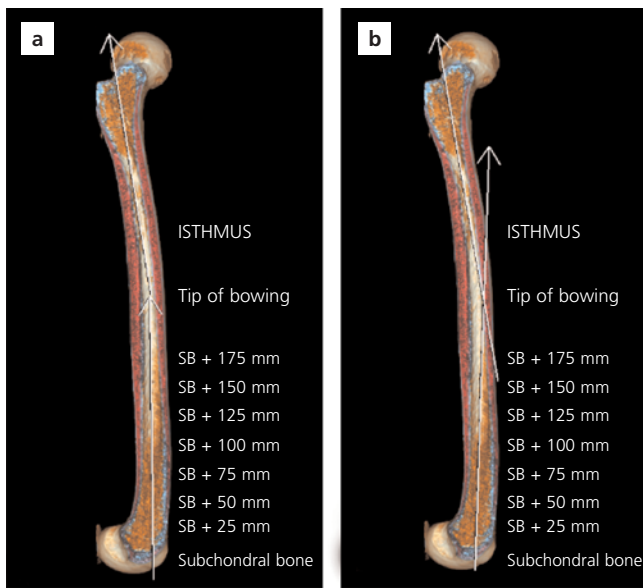


Figure 2. Determination of the tip of femoral bowing (a) and bowing tip distance measurement (b). [Color figure can be viewed in the online issue, which is available at www.anatomy.org.tr]

of the medullary canal at 20 cm proximal to the JL (Figure 3).

- **Sagittal mechanical axis (sMA):** the line that connects the center of the femoral head and the midpoint of the epicondylar axis (EA)^[15] (Figure 3).

Measurements in the Coronal and Axial Planes

- **Medial epicondyle (ME) and lateral epicondyle (LE) distance:** the distance from the most prominent

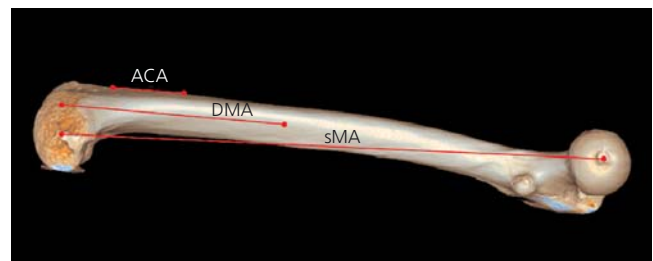


Figure 3. Reference angles of the distal femur in the sagittal plane. ACA: Anterior cortical axis; the line that connects the points drawn at 5 cm and 10 cm proximal to the distal joint line on the anterior cortex. DMA: distal medullary axis; the line drawn between 1 cm anterior of the BL and the midpoint of the medullary canal at 20 cm proximal to the joint line. sMA: sagittal mechanical axis; the line that connects the center of the femoral head and the midpoint of the epicondylar axis. [Color figure can be viewed in the online issue, which is available at www.anatomy.org.tr]

point of the medial and lateral epicondyles to the JL in the coronal plane (Figure 4).

- **Epicondylar axis (EA):** the line that connects the most prominent points of the medial and lateral epicondyle (Figure 4).
- **Posterior condylar line (PCL):** the line that connects the posterior borders of the condyles (Figure 4).
- **Medial and lateral posterior condylar offset (m-PCO and l-PCO):** the distance from the most prominent posterior point of the medial and lateral femoral condyles to the posterior femoral cortex in the sagittal plane measured from the 3D reconstruction of the PCO (Figure 4).

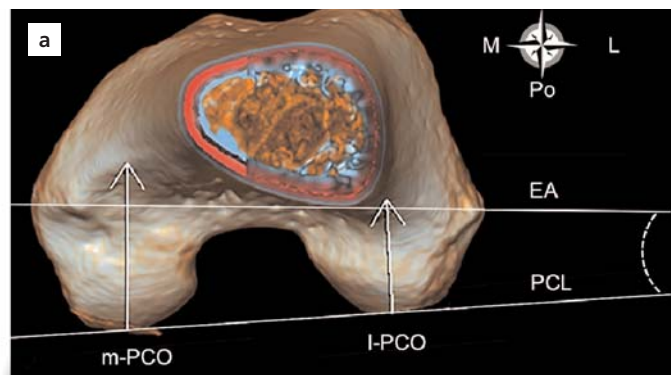
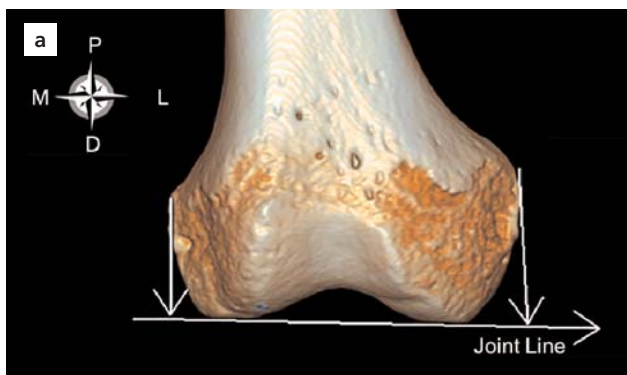


Figure 4. Medial epicondyle and lateral epicondyle distance (a), Measurement of posterior offset and reference axes (b). ME distance (MEd) and LE distance (LEd); the distance from the most prominent point of the medial and lateral epicondyle distance to the joint line. EA: epicondylar axis; the line that connects the most prominent points of the ME and LE. PCL: posterior condylar line; the line that connects the posterior borders of the condyles. m-PCO: medial posterior condylar offset; l-PCO: lateral posterior condylar offset; the distance from the most prominent posterior point of the medial and lateral femoral condyles to the posterior femoral cortex in the sagittal plane from the 3D reconstruction of the posterior condylar offset measurement (D: distal, L: lateral, M: medial, P: proximal, Po: posterior). [Color figure can be viewed in the online issue, which is available at www.anatomy.org.tr]

Additionally, AP and ML canal diameters at 25, 50, 75, 100, 125, 150, 175, and 200 mm were measured from distal to proximal starting from the BL (Figures 5 and 6).

In 5 mm slices starting from the BL, AP and ML diameters at the level with the narrowest medullary canal width was determined as the isthmus diameter and the distance of this level to the BL distal endpoint was determined as isthmus distance.

The angle between EA and PCL was measured in the coronal plane. The angle difference between the axis measurements in the sagittal plane was calculated. The correlation of the measurements with bowing and each other in the sagittal plane was analyzed. All measurements were compared between men and women.

The variables with normal distribution were analyzed with the Shapiro–Wilk test. Descriptive statistics of the variables without normal distribution were expressed as median (minimum, maximum) values. In addition, mean±standard deviation values were also provided. Mann–Whitney U test was used to analyze the differences between variables according to gender. The relationship between the specified variables was studied with the Spearman’s rho correlation coefficient. In cases with significant relationships, the correlations were interpreted as “no correlation or negligible correlation” for correlation coefficients between 0.00–0.19, as “poor (low)” for 0.20–0.39, as “moderate” for 0.40–0.69, as “strong (high)”

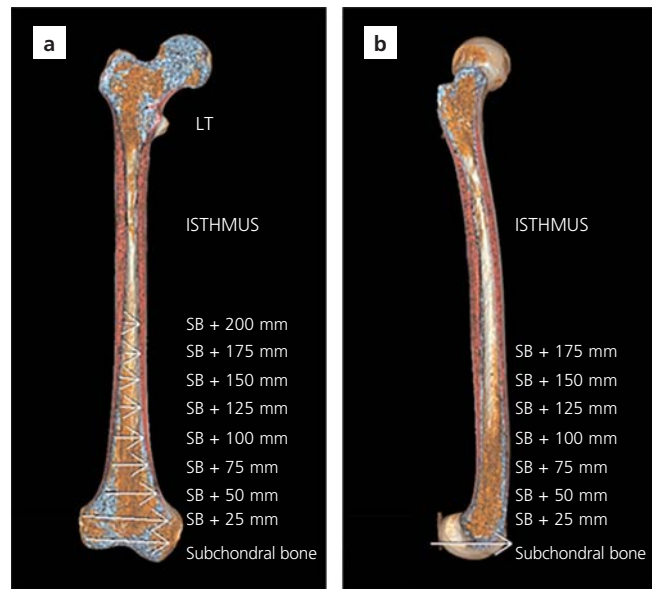


Figure 5. Measurement of canal diameters from distal end of the Blumensaat line level towards the proximal part in the coronal (a) and sagittal (b) planes. [Color figure can be viewed in the online issue, which is available at www.anatomy.org.tr]

for 0.70–0.89, and as “very strong” for those between 0.90–1.0.

IBM SPSS Statistics for Windows (Version 21, Armonk, NY, USA) and MS-Excel 2007 software were used for statistical analyses and calculations. The level of statistical significance was considered as $p < 0.05$.

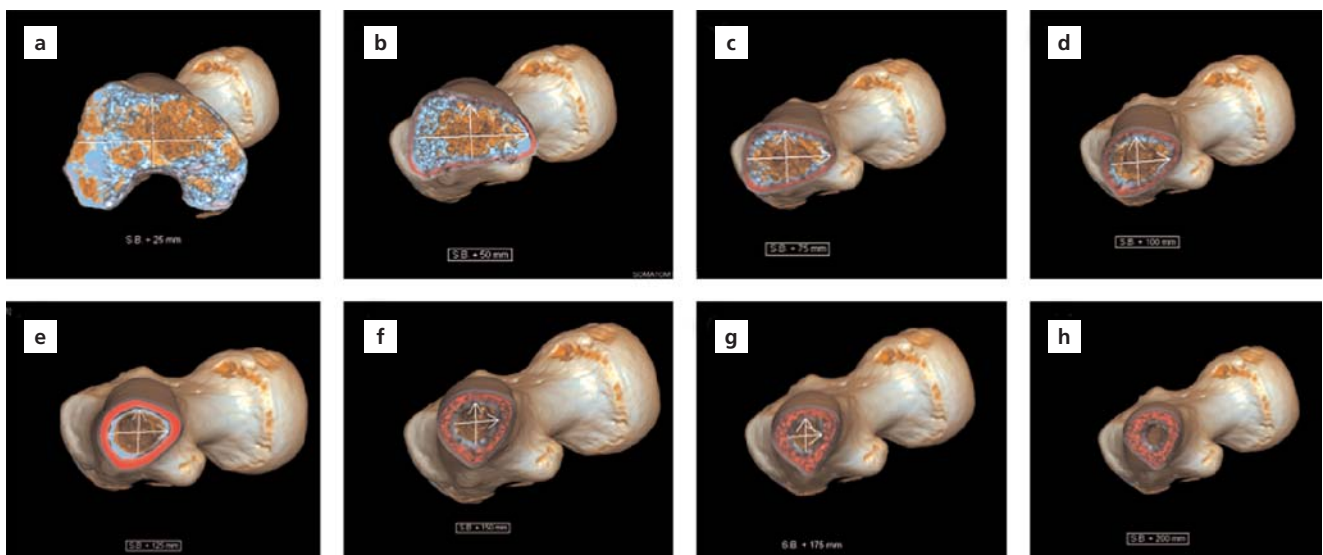


Figure 6. Examples of canal diameter measurements at different cross-section levels from distal end of the Blumensaat line level towards the proximal part. Canal diameters at 25 mm (a), 50 mm (b), 75 mm (c), 100 mm (d), 125 mm (e), 150 mm (f), 175 mm (g), and 200 mm (h). [Color figure can be viewed in the online issue, which is available at www.anatomy.org.tr]

Results

No statistically significant difference was found between genders in terms of the values for femoral length, being 41.93 ± 5.19 cm in males and 39.75 ± 5.10 cm in females ($p=0.475$). However, the distance from the tip of bowing to the BL was 17.74 ± 2.53 cm in females and 19.14 ± 2.70 cm in males, the difference being statistically significant ($p=0.017$). Moreover, the variable bowing angle exhibited a significant difference according to gender ($p=0.013$), with the mean bowing angle being $15.78 \pm 4.47^\circ$ and $13.25 \pm 4.42^\circ$ in females and males, respectively.

For comparing the medullary canal diameters of the femurs by gender, AP and ML diameters were measured at 25 mm, 50 mm, 75 mm, 100 mm, 125 mm, 150 mm, 175 mm, and 200 mm levels with respect to the BL distal endpoint. The two gender-groups had similar results in terms of the AP diameter at 200 mm and ML diameter at 25 mm; whereas, there was a statistically significant difference at all the other levels particularly being higher in males: (AP 25 mm, $p=0.05$; AP 50 mm, $p=0.036$; AP 75 mm, $p=0.041$; AP 100 mm, $p=0.049$; AP 125 mm, $p=0.045$; AP 150 mm, $p=0.037$; AP 175 mm, $p=0.05$; AP 200 mm, $p=0.051$; ML 25 mm; $p=0.052$; ML 50 mm, $p=0.043$; ML 75 mm, $p=0.032$; ML 100 mm, $p=0.04$; ML 125 mm, $p=0.038$; ML 150 mm, $p=0.024$; ML 175 mm, $p=0.049$; and ML 200 mm, $p=0.046$). The comparison of

measured values and all variables according to gender are shown in **Tables 1** and **2**.

It was observed that there was a mean difference of $5.14 \pm 1.67^\circ$ and $4.12 \pm 2.41^\circ$ between sMA and the ACA and DMA, respectively. These two parameters are commonly used in component positioning in the sagittal plane while using conventional total knee prosthesis techniques. And this difference was statistically significant in both male and female femurs ($p=0.02$ and $p=0.031$, respectively). The calculated mean angle between PCL and EA in the coronal plane was $4.37 \pm 2.18^\circ$, and it this angle between the two lines showed a statistically significant difference according to gender ($p=0.047$). Moreover, it was observed that the m- and l-PCOs were longer in male femurs as compared to female femurs, with the difference being statistically significant ($p=0.025$ and $p=0.037$, respectively).

Correlation coefficients between the variables are shown in **Table 3**. There was no statistically significant relationship between the femoral bowing tip distance and isthmus distance from the distal part ($p=0.837$). A moderate correlation was observed between the medial offset and ME-JL distance ($p<0.001$) both in female and male femurs ($p<0.001$ and $p<0.001$, respectively). On evaluating statistical relationship between the femoral length and bowing angle, it was found that the bowing angle increased in parallel with increasing femoral length

Table 1

Angle and length measurements of the parameters used for morphometric analysis of the anatomy of distal femur and the descriptive statistics of these variables according to gender (mean \pm SD).

Variables	Gender			p-value
	Male Mean \pm SD	Female Mean \pm SD	All Mean \pm SD	
Femoral length (cm)	41.93 \pm 5.19	39.75 \pm 5.10	40.84 \pm 5.23	0.475
Bowing angle	13.25 \pm 4.42 $^\circ$	15.78 \pm 4.47 $^\circ$	14.02 \pm 4.50 $^\circ$	0.013
Bowing tip distance (cm)	19.14 \pm 2.70	17.74 \pm 2.53	18.44 \pm 2.51	0.017
Bowing tip ML diameter (cm)	1.16 \pm 0.17	1.14 \pm 0.17	1.15 \pm 0.17	0.728
Bowing tip AP diameter (cm)	1.30 \pm 0.21	1.27 \pm 0.19	1.29 \pm 0.20	0.595
The angle between the anterior cortical axis and sagittal mechanical axis	4.10 \pm 1.80 $^\circ$	6.16 \pm 1.58 $^\circ$	5.14 \pm 1.67 $^\circ$	0.020
The angle between the distal medullary axis and sagittal mechanical axis	3.71 \pm 2.30 $^\circ$	4.82 \pm 2.36 $^\circ$	4.12 \pm 2.41 $^\circ$	0.031
Medial condylar offset (mm)	35.47 \pm 5.91	28.1 \pm 4.3	31.79 \pm 5.10	0.025
Lateral condylar offset (mm)	28.96 \pm 4.28	25.6 \pm 4.4	27.28 \pm 4.35	0.037
The angle between the posterior condylar line and epicondylar axis	3.60 \pm 2.10 $^\circ$	5.10 \pm 3.10 $^\circ$	4.37 \pm 2.18 $^\circ$	0.047
Lateral epicondyle distance (mm)	28.41 \pm 3.00	23.95 \pm 2.72	24.18 \pm 1.87	0.040
Medial epicondyle distance (mm)	37.1 \pm 2.8	30.88 \pm 4.14	32.97 \pm 3.49	0.003
Isthmus distance (cm)	25.41 \pm 2.89	23.31 \pm 2.04	24.36 \pm 2.96	0.022
Isthmus diameter ML (cm)	1.37 \pm 0.43	0.97 \pm 0.15	1.17 \pm 0.44	0.456
Isthmus diameter AP (cm)	1.06 \pm 0.12	1.07 \pm 0.13	1.07 \pm 0.13	0.641

Table 2

Measurement of anteroposterior and mediolateral canal diameters at 25, 50, 75, 100, 125, 150, 175, and 200 mm from the Blumensaat line distal end point towards the proximal part and the descriptive statistics of these variables according to gender.

Variables	Gender			p-value
	Male Mean±SD	Female Mean±SD	All Mean±SD	
ML at 25 mm (cm)	6.18±0.84	6.08±0.79	6.13±0.81	0.052
AP at 25 mm (cm)	3.87±0.46	3.51±0.30	3.76±0.28	0.050
ML at 50 mm (cm)	3.61±0.69	3.47±0.70	3.59±1.70	0.043
AP at 50 mm (cm)	2.72±2.45	2.16±0.40	2.48±1.40	0.036
ML at 75 mm (cm)	2.75±1.50	2.42±0.58	2.68±0.90	0.032
AP at 75 mm (cm)	2.31±0.25	1.98±0.29	2.24±0.27	0.041
ML at 100 mm (cm)	2.21±0.38	2.06±0.39	2.18±0.88	0.040
AP at 100 mm (cm)	1.86±0.25	1.66±0.97	1.71±0.26	0.049
ML at 125 mm (cm)	1.77±0.29	1.62±0.29	1.69±0.79	0.038
AP at 125 mm (cm)	1.65±0.22	1.52±0.24	1.59±0.29	0.045
ML at 150 mm (cm)	1.57±0.37	1.37±0.25	1.41±0.23	0.024
AP at 150 mm (cm)	1.53±0.25	1.28±0.29	1.49±0.35	0.037
ML at 175 mm (cm)	1.37±0.76	1.19±0.17	1.24±0.16	0.049
AP at 175 mm (cm)	1.39±0.21	1.23±0.22	1.33±0.49	0.050
ML at 200 mm (cm)	1.23±0.67	1.13±0.16	1.18±0.46	0.046
AP at 200 mm (cm)	1.22±0.18	1.14±0.19	1.18±0.19	0.051
ML at Isthmus (cm)	0.97±0.15	1.37±0.43	1.07±0.44	0.784
AP at Isthmus (cm)	1.07±0.13	1.06±0.12	1.07±0.13	0.646

AP: anteroposterior; ML: mediolateral.

in both male and female femurs ($p < 0.05$ and $p < 0.001$, respectively). Bowing angle with ACA/sMA and bowing angle with DMA/sMA were also correlated ($p < 0.01$ and $p = 0.043$, respectively), and this correlation was found to be higher in female femurs.

The inter- and intra-observer differences in the measurements were not statistically significant ($p > 0.05$).

Discussion

This study showed that significant difference between genders in terms of various parameters for the distal and medullary canal structures of males and females, with a discussion on the improvements in the femoral component and stem designs and positioning that these differences may require. In addition to the gender-dependent

Table 3

Correlation coefficients between the variables in general and according to gender.

Compared parameters	Gender					
	Male (n=100)		Female (n=100)		All (n=200)	
	rho	p-value	rho	p-value	rho	p-value
Isthmus distance - Femoral bowing tip distance	0.134	0.514	0.118	0.748	0.015	0.837
Medial epicondylar distance - Medial condylar offset	0.716	<0.001	0.633	<0.001	0.682	<0.001
Lateral epicondylar distance - Lateral condylar offset	0.089	0.379	0.065	0.522	0.071	0.262
Femoral length - Bowing angle	0.715	<0.05	0.878	0.001	0.799	<0.001
ACA/sMA - Bowing angle	0.413	<0.05	0.876	<0.001	0.517	<0.01
DMA/sMA - Bowing angle	0.489	<0.05	0.817	<0.001	0.615	0.043

ACA/sMA: the angle between the anterior cortical axis and sagittal mechanical axis; DMA/sMA: the angle between the distal medullary axis and sagittal mechanical axis.

variables, differences between the angular parameters that are commonly used in knee prosthesis during femoral implantation were also analyzed.

Previous studies have provided different suggestions for femoral component design due to the gender-dependent morphometric differences in the anatomy of the distal femur between males and females.^[16,17] Especially in revision surgeries that involve the use of long stems, not paying attention to the femoral width and bowing could lead to excessive stress and, in turn, to fractures during surgery, rapid wear and also early failure in the postoperative period. One of the important findings of this study was that the isthmus and tip of bowing measured from the distal part were at different levels in male and female femurs, and the tip of femoral bowing was closer to the joint than the isthmus. Moreover, we observed that the bowing angle was higher and that the tip of bowing was closer to the JL in female femurs as compared to the male ones. It was also found that the isthmus was closer to the joint in female femurs as compared to male femurs. It was observed that increased bowing resulted in increased flexion in the distal part of the femur, thereby causing an increase in the DMA in female femurs. Therefore, it is possible to say that using shorter femoral stems would be necessary in females with the same bowing angle, as the tip of bowing would be closer to the JL.

Today, many authors emphasize that correct component alignment in primary and revision surgeries have important effects on the survivorship and clinical success of arthroplasty.^[18] Apart from the planning in the coronal plane, planning in the sagittal plane to align the femoral component in accordance with the mechanical axis is of utmost importance for the survival of the component. The mentioned positioning can be achieved more successfully by using knee prosthesis techniques that involve navigation rather than conventional methods.^[19,20] Studies have shown that the femoral component position achieved by using DMA and ACA references with conventional techniques could be in flexion or extension with respect to the mechanical axis.^[14] Placement of the femoral component in flexion or extension can lead to many complications such as early polyethylene wear, limitation of movement, and periprosthetic fracture. In this study, ACA, DMA, and sMA axes described in the literature were measured in all the bones to reveal the differences between these axes, and it was confirmed that the mentioned differences were statistically significant. Our study showed that there was a strong correlation between the femoral bowing and ACA, DMA, and sMA.

The angles between ACA and sMA and DMA and sMA were significantly increased in parallel with increased femoral bowing in male and female femurs ($p < 0.01$ and $p = 0.043$, respectively). In a similar study, Chung et al.^[21] found that the difference between DMA and sMA according to the measurement method was highly affected by anterior bowing. The same study showed that each 1-degree increase in anterior bowing resulted in a 0.15 degree increase in DMA with respect to sMA. Our study has shown that the mentioned increment exhibited a higher variation in female femurs as compared to male femurs. A distal bowing in addition to the mentioned bowing can be relevant in females since the deviation between DMA, ACA, and the sagittal mechanical axis exhibits a higher increment with the change in bowing angle in females as compared to the males who have the same bowing angle. Knowing the differences between these reference points used during femoral component implantation in systems that do not involve navigation would ensure that the intramedullary and extramedullary guides are correctly routed and interpreted, thereby helping the positioning of the component closer to the desired mechanical axis.

Suitable rotation of the femoral component is one of the most important parameters for the survival of the prosthesis and functional outcomes. Malrotation of the femoral component is associated with many complications such as patellofemoral mal-tracking, limitation of movement and stiffness, and early loosening.^[22,23] In the presence of normal condylar anatomy, PCL is at 3–4° internal rotation with respect to EA, and this angle difference is the main parameter that determines the amount of resection. In our study, m- and l-PCO values were smaller in female femurs as compared to male femurs ($p = 0.025$ and $p = 0.037$, respectively). Moreover, in female femurs, the l-PCO value exhibited a higher decrease with respect to the medial value, in comparison to male femurs, and the angle between PCL and EA was higher in female femurs ($p = 0.047$). Therefore, having a shorter resection in the lateral aspect as compared to the medial aspect in femoral posterior chamfer and posterior offset resections would provide a femoral component rotation more consistent with the EA in comparison to the knee replacement implant systems that use a standard resection with 3°.

Bellemans et al.^[24] were the first to describe the concept of PCO. They suggested that the maximum flexion following TKA was limited to the angle from the posterior edge of the tibia to its contact point on the posterior edge of the femur. In our study, considering the rela-

tionship between ME and LE–JL distance and l- and m-PCOs, the only linear correlation observed was for the medial aspect. Therefore, we suggest that l- and m-PCOs should be evaluated separately to adjust the ideal offset. Although it is thought that increasing PCO with TKA would increase flexion, according to a study by Mitsuyasu et al.,^[25] posterior tissue tension increases due to enlarged posterior femoral component, thereby tightening the extension gap. To prevent this instability, m- and l-PCO measurements should be conducted separately using CT, considering the triangular structure of the distal femur, and it should be kept in mind that conventional x-rays could lead to faulty measurement results.

Conclusion

Since there is a wide range of gender-dependent anthropomorphic differences between the distal femurs of males and females, as well as a wide range of variables from the measurement of each morphological structure around the knee; it is necessary to have various implants with different designs. Size and morphologic measurements exhibit differences not only between genders but also within the same gender. Therefore, there is no standard value. Further studies are necessary to evaluate the effect of using designs based on the relevant variables on the clinical outcomes in individuals who undergo TKA.

Acknowledgement

The authors gratefully acknowledge those who donated their bodies to medical research and their families.

References

- Garriga C, Murphy J, Leal J, Price A, Prieto-Alhambra D, Carr A, Arden NK, Rangan A, Cooper C, Peat G, Fitzpatrick R, Barker K, Judge A. Impact of a national enhanced recovery after surgery programme on patient outcomes of primary total knee replacement: an interrupted time series analysis from “The National Joint Registry of England, Wales, Northern Ireland and the Isle of Man”. *Osteoarthritis Cartilage* 2019;27:1280–93.
- Ritter MA, Faris PM, Keating EM, Meding JB. Postoperative alignment of total knee replacement. Its effect on survival. *Clin Orthop Relat Res* 1994;(299):153–6.
- Bargren JH, Blaha JD, Freeman MA. Alignment in total knee arthroplasty. Correlated biomechanical and clinical observations. *Clin Orthop Relat Res* 1983;(173):178–83.
- Berend ME, Ritter MA, Meding JB, Faris PM, Keating EM, Redelman R, Faris GW, Davis KE. Tibial component failure mechanisms in total knee arthroplasty. *Clin Orthop Relat Res* 2004;(428):26–34.
- Larose G, Fuentes A, Lavoie F, Aissaoui R, de Guise J, Hagemester N. Can total knee arthroplasty restore the correlation between radiographic mechanical axis angle and dynamic coronal plane alignment during gait? *Knee* 2019;26:586–94.
- Kim CW, Lee CR. Effects of femoral lateral bowing on coronal alignment and component position after total knee arthroplasty: a comparison of conventional and navigation-assisted surgery. *Knee Surg Relat Res* 2018;30:64–73.
- O’Rourke MR, Callaghan JJ, Goetz DD, Sullivan PM, Johnston RC. Osteolysis associated with a cemented modular posterior-cruciate-substituting total knee design : five to eight-year follow-up. *J Bone Joint Surg Am* 2002;84:1362–71.
- Yehyawi TM, Callaghan JJ, Pedersen DR, O’Rourke MR, Liu SS. Variances in sagittal femoral shaft bowing in patients undergoing TKA. *Clin Orthop Relat Res* 2007;(464):99–104.
- Jethanandani R, Patwary MB, Shellito AD, Meehan JP, Amanatullah DF. Biomechanical consequences of anterior femoral notching in cruciate-retaining versus posterior-stabilized total knee arthroplasty. *Am J Orthop* 2016;45:E268–72.
- Nagamine R, Inoue S, Miura H, Matsuda S, Iwamoto Y. Femoral shaft bowing influences the correction angle for high tibial osteotomy. *J Orthop Sci* 2007;12:214–8.
- Vaidya SV, Ranawat CS, Aroojis A, Laud NS. Anthropometric measurements to design total knee prostheses for the Indian population. *J Arthroplasty* 2000;15:79–85.
- Schiffner E, Wild M, Regenbrecht B, Schek A, Hakimi M, Thelen S, Jungbluth P, Schnependahl J. Neutral or natural? Functional impact of the coronal alignment in total. *Knee Arthroplasty. J Knee Surg* 2019;32:820–4.
- Okamoto Y, Otsuki S, Nakajima M, Jotoku T, Wakama H, Neo M. Sagittal alignment of the femoral component and patient height are associated with persisting flexion contracture after primary total knee arthroplasty. *J Arthroplasty* 2019;34:1476–82.
- Asada S, Mori S, Matsushita T, Hashimoto K, Inoue S, Akagi M. Influence of the sagittal reference axis on the femoral component size. *J Arthroplasty* 2013;28:943–9.
- Lustig S, Lavoie F, Selmi TA, Servien E, Neyret P. Relationship between the surgical epicondylar axis and the articular surface of the distal femur: an anatomic study. *Knee Surg Sports Traumatol Arthrosc* 2008;16:674–82.
- Booth RE Jr. Sex and the total knee: gender-sensitive designs. *Orthopedics* 2006;29:836–8.
- Ritter MA, Thong AE, Keating EM, Faris PM, Meding JB, Berend ME, Pierson JL, Davis KE. The effect of femoral notching during total knee arthroplasty on the prevalence of postoperative femoral fractures and on clinical outcome. *J Bone Joint Surg Am* 2005;87:2411–4.
- Rand JA, Coventry MB. Ten-year evaluation of geometric total knee arthroplasty. *Clin Orthop Relat Res* 1988;(232):168–73.
- Huang TW, Kuo LT, Peng KT, Lee MS, Hsu RW. Computed tomography evaluation in total knee arthroplasty: computer-assisted navigation versus conventional instrumentation in patients with advanced valgus arthritic knees. *J Arthroplasty* 2014;29:2363–8.
- Mullaji A, Kanna R, Marawar S, Kohli A, Sharma A. Comparison of limb and component alignment using computer-assisted navigation versus image intensifier-guided conventional total knee arthroplasty: a prospective, randomized, single-surgeon study of 467 knees. *J Arthroplasty* 2007;22:953–9.
- Kuriyama S, Hyakuna K, Inoue S, Kawai Y, Tamaki Y, Ito H, Matsuda S. Bone-femoral component interface gap after sagittal mechanical axis alignment is filled with new bone after cementless

- total knee arthroplasty. *Knee Surg Sports Traumatol Arthrosc* 2018;26:1478–84.
22. Tao K, Cai M, Li SH. The anteroposterior axis of the tibia in total knee arthroplasty for chinese knees. *Orthopedics* 2010;33:799.
23. Boldt JG, Stiehl JB, Hodler J, Zanetti M, Munzinger U. Femoral component rotation and arthrofibrosis following mobile-bearing total knee arthroplasty. *Int Orthop* 2006;30:420–5.
24. Bellemans J, Banks S, Victor J, Vandenuecker H, Moemans A. Fluoroscopic analysis of the kinematics of deep flexion in total knee arthroplasty. Influence of posterior condylar offset. *J Bone Joint Surg Br* 2002;84:50–3.
25. Mitsuyasu H, Matsuda S, Fukagawa S, Okazaki K, Tashiro Y, Kawahara S, Nakahara H, Iwamoto Y. Enlarged post-operative posterior condyle tightens extension gap in total knee arthroplasty. *J Bone Joint Surg Br* 2011;93:1210–6.

ORCID ID:

M. E. Şimşek 0000-0002-8081-0550;
M. Bozkurt 0000-0001-8160-5375



Correspondence to: Mehmet Emin Şimşek, MD

Department of Orthopedics and Traumatology,
Lokman Hekim University, Ankara, Turkey

Phone: +90 506 632 74 13

e-mail: mehmeteminsimsek@gmail.com

Conflict of interest statement: No conflicts declared.

This is an open access article distributed under the terms of the Creative Commons Attribution-NonCommercial-NoDerivs 3.0 Unported (CC BY-NC-ND3.0) Licence (<http://creativecommons.org/licenses/by-nc-nd/3.0/>) which permits unrestricted noncommercial use, distribution, and reproduction in any medium, provided the original work is properly cited. *Please cite this article as:* Şimşek ME, Bozkurt M. Clinical significance of the relationship between 3D analysis of the distal femur and femoral shaft anatomy in total knee arthroplasty. *Anatomy* 2019;13(3):174–182.

Effect of mesenchymal stem cells and their niche on diabetic and osteoporotic wound healing following osteogenic differentiation and bone matrix formation *in vitro*

Müge Karakayalı¹ , Tuna Önal² , İbrahim Tuğlu² 

¹Department of Medical Microbiology, School of Medicine, İzmir Democracy University, İzmir, Turkey

²Department of Histology and Embryology, School of Medicine, Celal Bayar University, Manisa, Turkey

Abstract

Objectives: Mesenchymal stem cells (MSC) and their secreted factors (*i.e.* niche) are becoming growingly popular in bone regeneration. The mechanisms of this effect can be investigated through *in vitro* models which are cost-effective methods used for determining the effectiveness of new products in experimental and clinical applications. In the present study, we established an experimental diabetic osteoporosis model in a high-glucose culture medium with no estrogen supplement to investigate the effect of MSC and their niche which their factors secreted into 24 hours medium on osteoblastic differentiation, formation of bone islets, and the wound healing model induced by scratch assay.

Methods: A culture medium of adipose-derived rat MSC (ADMSC) with no estrogen supplement was used for cell growth to assess osteoblastic differentiation and bone islet formation. A wound model was induced using the scratch assay to investigate the effect of the model on the parameters of wound healing. Cell growth and viability was assessed using MTT assay, cell migration and differentiation and the amount of wound closure were assessed based on the expression of CD44, CD45, and CD73, and osteoblast differentiation was evaluated using Alizarin Red S and von Kossa staining. Morphological observations were performed using an inverted phase-contrast microscope and h-score was assessed with immunohistochemical staining.

Results: The use of osteogenic medium with estrogen supplement led to MSC growth and migration as well as bone islet formation. The use of a high-glucose medium without estrogen supplement inhibited MSC differentiation and bone islet formation. The administration of MSC and niche promoted the wound healing initiated by the administration of the scratch assay and this promotion was significant in terms of all the parameters of wound healing.

Conclusion: The results indicated that the therapeutic effect of MSC and niche could be used as an effective treatment model in wound healing in patients with diabetic osteoporosis. Moreover, this model could be a cost-effective method for the new treatment products to be applied in dental and orthopedic practice prior to animal experiments and clinical trials.

Keywords: diabetic osteoporosis; *in vitro*; mesenchymal stem cell; niche; osteoblastic differentiation; wound healing

Anatomy 2019;13(3):183–192 ©2019 Turkish Society of Anatomy and Clinical Anatomy (TSACA)

Introduction

Mesenchymal stem cells (MSC) are important cell-based therapy products due to their regenerative properties and ability to give rise to cells of various lineages. These cells have the potential to differentiate into osteoblasts and osteocytes both *in vitro* and *in vivo*, which makes them excellent candidates for bone tissue regenerative therapy.^[1]

MSC can be easily obtained from various sources such as adipose tissue and be prepared for use after being produced in laboratories with Good Manufacturing Practice (GMP) standards. Early-phase studies of MSC in clinical conditions including ischemia, Crohn's disease, ulcerative colitis, and liver diseases have been completed and MSC therapies have been initiated thereafter.^[2] Additionally, the clinical use of MSC in numerous bone diseases has also

been initiated.^[3] MSC have the potential to differentiate into osteocytes and chondrocytes both *in vitro* and *in vivo*, which makes them excellent candidates for bone and cartilage diseases in clinical trials.^[1] Moreover, it has also been suggested that MSC can also be used in the presence of osteoporosis.^[4-6] On the other hand, long-term exposure to the high glucose effect leads to changes in bone metabolism and microarchitecture, thereby resulting in decreased healing rates in patients with chronic and non-controlled diabetes mellitus.^[7] It has also been suggested that the effect of oxidative stress, inflammation, and drug use on osteoblasts and osteoclasts produce weak bones with increased fracture risk.^[8]

MSC are pluripotent cell-based therapy products that can be derived from bone marrow, adipose tissue, placenta, amniotic fluid, and fetal tissues. MSC can be easily obtained and expand for therapeutic purposes. These cells, unlike hematopoietic stem cells (HSC), can be characterized as negative for CD34 and CD45 and positive for CD29, CD44, CD71, CD90, CD73 (SH3/SH4), CD105 (SH2), CD106, and CD124.^[9-12] Regenerative medicine has the potential to heal or replace damaged tissues and organs using biological products. Adipose-derived MSC (ADMSC) have recently emerged as popular therapeutic products in regenerative medicine, particularly in the treatment of inflammation and autoimmune diseases. These cells are considered to inhibit bacterial growth and colony formation in diseases such as osteomyelitis and cystic fibrosis. MSC and their secreted factors (*i.e.* niche) have been accepted as mainstay therapeutic products with no side effects in clinical practice and their distinct modifications continue to emerge every passing day.^[13] They have the potential to decrease inflammation in damaged tissues, thereby promoting immunomodulation and regeneration. Moreover, MSC also accelerate regeneration and provide relatively better healing in critical volume defects.^[14]

Previous study indicated that the osteoblastogenesis mineralization of rat bone marrow stromal cells is inhibited in hyperglycemic culture *via* activation of the Notch2 signaling pathway.^[15] Another study evaluated diabetic rats induced with streptozotocin (STZ) and revealed that the transplantation of CXCL13-stimulated bone marrow stromal cells (BMSC) in culture increased cell proliferation rate and *in vivo* enhanced the corresponding ALP expression in bone healing.^[16] Moreover, it has also been reported that high glucose levels may affect the bone cells in culture medium.^[17] Other studies indicated that the administration of human diabetic serum into MSC culture medium led to reduced osteogenic differentiation in association with high glucose levels and could also be an

important factor for diabetic osteoporosis.^[18] A study by Qu et al.^[19] examined the effect of miR-449 on osteogenic differentiation and its underlying mechanism in human bone marrow-derived mesenchymal stem cells (hBMSC) using high glucose and free fatty acids treatment (FAT) and revealed that after culturing for 14 days, the treatment dramatically decreased mineralization of hBMSC and resulted in impaired bone islets. The study also showed that the miR-449 mimics decreased the protein expression levels of runt-related transcription factor 2 (Runx2), ALP, collagen I, osteocalcin (OCN), and bone sialoprotein (BSP), which were significantly increased by miR-449 inhibitors. Another study that investigated potential abnormalities of bone marrow-derived MSC (BMMSC) in a rat menopause model established by ovariectomy revealed that proliferation, migration, and differentiation of osteoclasts was decreased, and increased by Wharton's jelly-derived MSC.^[20] In an experimental study, ADMSC were cultured to mimic diabetic osteoporosis and the results indicated that the osteopontin (OPN) and Runx2 expressions of ADMSC were decreased and there was also a noticeable reduction in mineralization, which were associated with DNA methylation and Wenti signal.^[21] Likewise, some other studies induced a rat diabetic osteoporosis model with STZ and high-fat diet and reported that the administration of the model with plant extracts improved diabetic osteopenia and also prevented oxidative stress and apoptosis in the fracture induced in the femur.^[22,23]

Chen et al.^[24] investigated the effect of Runx2 on osteoblast differentiation in high-glucose condition and reported that the expression of Runx2, ALP, OC, and OPN, as well as ALP activity and Alizarin Red S staining decreased significantly, whereas administration of 10 mM PI3K/AKT inhibitor LY294002 eliminated this favorable effect. The authors also noted that Runx2 reversed high glucose-induced inhibition of osteoblast differentiation *via* modulation of PI3K/AKT/GSK3b/b-catenin pathway. Some other studies indicated that estrogens had beneficial effects on osteoblasts during differentiation and also increased their survival and mineralization capacity.^[25-28] Additionally, it has been reported that estrogen deficiency has a repressive role on MSC *via* miR-133 and that the expression of Runx2 and Osterix decreases ALP activity as well as the formation of mineralization nodules, which could be significant factors for MSC in patients with postmenopausal osteoporosis.^[29]

In the present study, an experimental diabetic osteoporosis model was induced in a high-glucose culture medium with no estrogen supplement, which allowed osteoblastic differentiation of MSC and the formation of

bone matrix. By using this model, we aimed to investigate the effect of MSC and their niche (*i.e.* factors secreted into 24-h medium) on osteoblastic differentiation, formation of bone islets, and wound healing model induced by scratch assay.

Materials and Methods

Mesenchymal Stem Cell Culture

Adipose-derived MSC (ADMSC) that were cryopreserved in the second passage at -80°C were retrieved in vials and warmed to room temperature in a 37°C water bath. Subsequently, the cells were placed in an α -MEM culture medium including 15% fetal bovine serum (FBS), 50 $\mu\text{g}/\text{ml}$ gentamycin, 100 UI/ml penicillin, 100 UI/ml streptomycin, and 100 UI/ml amphotericin to promote cell proliferation and confluence and then were incubated at 37°C with 5% CO_2 . The samples were morphologically evaluated and photographed under an inverted phase-contrast microscope.^[30-32] The cells were then embedded in a frozen ADMSC culture and inoculated onto 12-well culture plates at 2.5×10^4 cells/ cm^2 .

MTT Assay

Cell viability and proliferation was assessed using MTT (3-[4,5-dimethylthiazol-2-yl]-2,5-diphenyltetrazolium bromide) assay which is a widely used enzymatic test based on the cleavage of the tetrazolium ring of MTT by dehydrogenases. MTT is actively absorbed into living cells and the reaction is reduced to non-water-soluble blue-purple formazan crystals after being catalyzed by succinate dehydrogenases in the mitochondria. The amount of these crystals, which can be determined spectrophotometrically, serves as an estimate for the number of living cells in the sample. An MTT stock solution (5 mg of MTT/ml of distilled water) was prepared in sterile phosphate buffered saline (PBS) and was inoculated onto 96-well culture plates. After remaining in an incubator for 3 h, optical density was determined using an ELISA kit (Bio-Rad, ABD) at the 540 nm wavelength. The mean of absorbance values from control wells was accepted as the control absorbance value indicating 100% cell viability. The mean of absorbance values from the wells treated with solvents and agents was expressed as the percentage of the control value.^[33]

Osteoblastic Differentiation and Characterization of ADMSC

The ADMSCs frozen at -196°C were recovered from fluid nitrogen and warmed to room temperature and then placed in culture medium for proliferation. The osteogenic factors were added with 50 $\mu\text{g}/\text{mL}$ ascorbic acid, 10–8 M dexam-

ethasone, 10 mM β -glycerol phosphate, and 10 nmol/L 17β -estradiol (E2) for osteoblastic differentiation. The cells in the second passage were used for the experiment were characterized as CD90-positive and CD45-negative by immunohistochemical staining. Confluent cultures were examined immunohistochemically using antibodies against OC (Biomedical Technologies, Stoughton, MA, USA), or ON (AON-1; Developmental Studies Hybridoma Bank, Stoughton, MA, USA) as follows. Samples were fixed with 4% paraformaldehyde in PBS, pH 7.4. Endogenous peroxidase was inactivated by incubation with 3% H_2O_2 for 30 min. After incubation with primary antibodies, the sections were incubated with biotinylated secondary antibodies and reacted with peroxidase-conjugated streptavidin using the protocol of a Histostain kit (Zymed, San Francisco, CA). The primary antibody was omitted for negative control. Samples were then incubated with diaminobenzidine/hydrogen peroxide (00-2020, Invitrogen, Camarillo, CA, USA). Cells were counterstained with Mayer's hematoxylin (02274390059, J.T. Barker, Deventer, Holland). After washing in distilled water, cover glasses were removed from the plate, then they were reversed and mounted on to the slides with mounting medium (AML060, Scytek, UT, USA), then evaluated under a light microscope (Olympus BX40, Olympus Corp., Tokyo, Japan).

The osteoblastic differentiated from MSC at confluent level were observed as island of cells in mineralized matrix and stained by Alizarin Red S and Von Kossa. At the end of the incubation of canine BMSC, the cell layers were washed three times with ice-cold PBS, pH: 7.4, scraped off the plates into 300–500 ml ice-cold 0.1% Triton-X 100 and subjected to mild sonication to lyse the cells completely. ALP activity was measured using 2 mM p-nitrophenylphosphate (p-NPP) in assay buffer (0.1 M diethanolamine, 1 mM MgCl_2 , pH 10.5) at 37°C for 10–60 min. ALP activity is expressed as nmol of p-nitrophenol/mg protein/h. Calcium phosphate deposit in the ECM can be detected by the Von Kossa (VK) method in which calcium phosphate deposits are stained brown to black. The media of confluent cultures were removed and the cells were washed once in cold PBS without Ca/Mg. Fixation was carried out for 15 min in 2.5% glutaraldehyde at room temperature and cultures were washed in distilled H_2O for 10 min. Distilled H_2O was removed and cells were covered with 5% AgNO_3 solution for 45 min. BMSC also were processed for AR staining of mineralized matrix. The cells were washed three times in distilled H_2O and allowed to air dry overnight. AR S (sodium 1, 2-dihydroxyanthraquinone-3-sulfonate) was used as a colorimetric reagent for detection of calcium salts. Slides prepared from the tissue culture (Nunc® Lab-Tek® Chamber

Slide™ system; Sigma, Roskilde, Denmark) were fixed in 10% formalin for 24 h and exposed to 1% ARS solution (pH=4.2) for 5 min at room temperature. The cells were washed in distilled water for 30 min to remove unreacted reagent, then air dried and photographed.^[34]

Inducing a Mimicked Model of Diabetic Osteoporosis and Fracture in Culture

Normal glucose with estrogen supplementation in medium was used as the control value for the bone matrix formation in culture. A high-glucose medium without estrogen supplementation was used to mimic osteoporosis in women with diabetic menopause. The bone matrix in culture was scratched with a sterile pipette tip and the effect of glucose and estrogen supplementation was evaluated by comparing with the control values. Healing was accepted as complete close of the wound area by the cells.^[35,36]

Transferring Microscopic Images to Digital Media

Morphological observations were performed using an inverted phase-contrast microscope and the images were transferred to computer environment and evaluated.^[33]

Transforming Histological Images to Digital Data

Closure of wound healing was evaluated as digital data by morphometric measurement of the interval. Immunohistochemical staining and intensity was obtained by H-score. $H\text{-Score} = S \cdot P_i (i+1)$, where i is the intensity of staining with a value of (1), (2) or (3) (minimal, mild, moderate, or strong, respectively) and P_i the percentage of cells stained with each intensity, varying between 0–100%. Results were expressed as mean±SE. Differences among groups were statistically analyzed with one-way ANOVA where appropriate. A p value of 0.05 was considered as statistically significant. All the statistical analyses were performed using Graphpad (GraphPad Software Inc., La Jolla, CA, USA) software.^[33]

Results

The MSC markers elicited *via* mechanical isolation of approximately 1 cm² of adipose tissue harvested from rat abdomen were characterized by immunostaining (Figure 1) as CD90-positive and CD45-negative (Table 1). These cells were added with ascorbic acid, b-glycerol phosphate, dexamethasone, and estrogen factors to allow osteoblastic differentiation and the cells were characterized together with their markers. In culture medium, islet-shaped bone matrix and calcium mineralization were identified *via* Alizarin Red S and Von Kossa staining (Figure 2). It was also noted that cells in the osteogenic medium supplemented with estrogen

Table 1

H-score of MSC characterized as CD90-positive and CD45-negative.

H-score	
CD90	CD45
234.45±22.68	35.22±16.48

expressed the osteogenic markers starting from center to periphery of the islets.

Islet formation and the expression of MSC markers decreased significantly in the mimicked model of diabetic osteoporosis that was formed in culture medium by adding high glucose and removing estrogen (Table 2). The effects of MSC and niche were examined in the wound model formed by the scratch induced with a sterile pipette tip (Figure 3) and it was revealed that MSC and niche which was factors secreted by MSC into their 24-h medium, promoted wound healing. It was also observed that the healing was initiated through cell proliferation beginning on one side of the wound, followed by the reformation of the bony tissue. Additionally, it was also noted the administration of cell-based therapy accelerated wound closure and also achieved more favorable outcomes in terms of wound healing and expression of MSC markers when compared to untreated culture (Table 3).

Discussion

Diabetes is a chronic health problem leading to significant losses due to its complications. Diabetes-associated changes in bone microstructure and osteopenia can pose serious challenges for dentists and orthopedists.^[37,38] Osteoporosis is a bone disease characterized by reduced bone mass and resistance and increased fragility and is known to affect most menopausal women. Osteoporosis becomes more significant when accompanied by diabetes.

Table 2

H-score of differentiated MSC to osteoblast which characterized by ON and OC staining.

	ON	OCN
Control (OM + E2 + NG)	228.36±28.44	244.86±26.08
Mimicked model (OM – E2 + HG)	124.22±24.88	142.18±23.96
Treatment (OM – E2 + HG + MSC + Niche)	174.16±22.24	195.14±26.34

E2: 17β-estradiol; HG: high glucose; NG: normal glucose; Niche: secretion of factors from MSC for 24 hours into medium; OCN: osteocalcin; OM: osteogenic medium; ON: osteonectin.

On the other hand, estrogen deficiency is a condition that leads to decreased osteoblastic function and regeneration capacity and delayed fracture healing. Accordingly, MSC therapies can be effective options for such conditions since MSC can be easily obtained and proliferated for therapeutic purposes and due to their immune tolerance

property.^[39] In the present study, a mimicked model of diabetic osteoporosis and fracture was formed in culture medium which allowed osteoblastic differentiation and bone islet formation. Moreover, the administration of MSC and niche (*i.e.* secreted factors) were found to have a therapeutic effect. The osteoblastic differentiation of

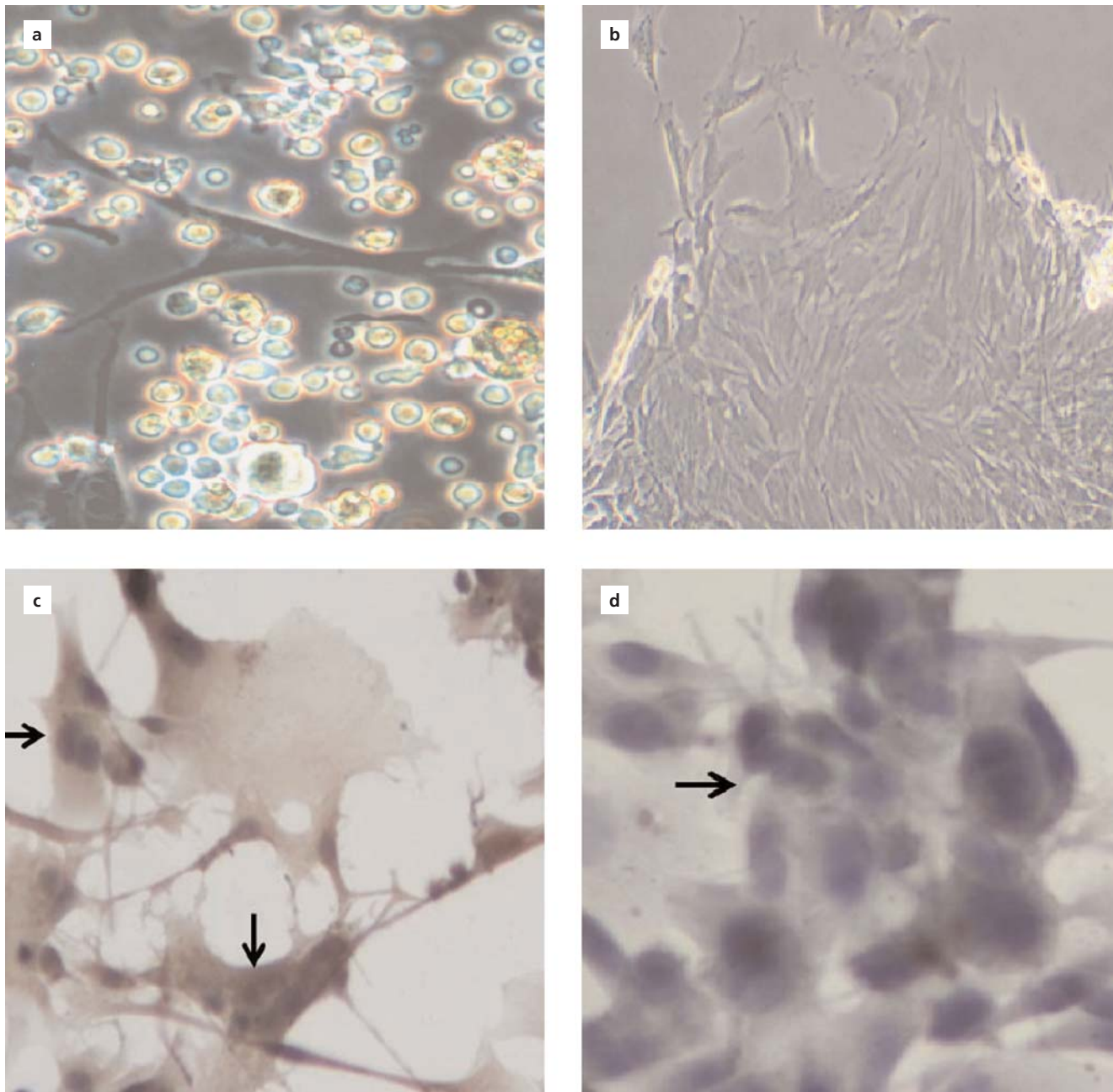


Figure 1. Morphological observation of MSC under phase contrast microscope and immunoperoxidase reactivity of CD90 for MSC which most of the cells stained and CD45 for hematopoietic cells which did not stain positive with antibody against CD45. (a) MSC and adipose tissue cells (x400); (b) Proliferation of MSC (x200); (c) CD90-positive (x400); (d) CD45-negative (x400). [Color figure can be viewed in the online issue, which is available at www.anatomy.org.tr]

MSC in osteogenic culture with 17β -estradiol led to the formation of osteoblasts and bone islets, which was decreased significantly by the administration of a high-glucose medium and removal of estrogen. In a related manner, MSC and their niche significantly improved wound healing in the wound model induced by scratch assay.

The cells seeded in culture medium were confirmed as MSC that were characterized as CD90-positive and CD45-negative. Similarly, this mesenchymal characterization has been reported in previous studies and has also been confirmed by flow cytometry.^[9-11] It was also revealed

that the addition of estrogen into the osteogenic culture medium led to greater bone islet formation and osteoblastic differentiation. Moreover, studies have shown that inhibition of bone islet formation and osteoblastic differentiation in a high-glucose medium can be reversed by the addition of 17β -estradiol (E2).^[37] In our study, a mimicked model of diabetic osteoporosis was formed in a high-glucose culture medium with E2 supplement and without estrogen and was used as control.^[35] In this medium, a wound model was induced by the scratch assay, which is commonly used in fibroblast culture, and the model promoted significant wound healing. Additionally, as consis-

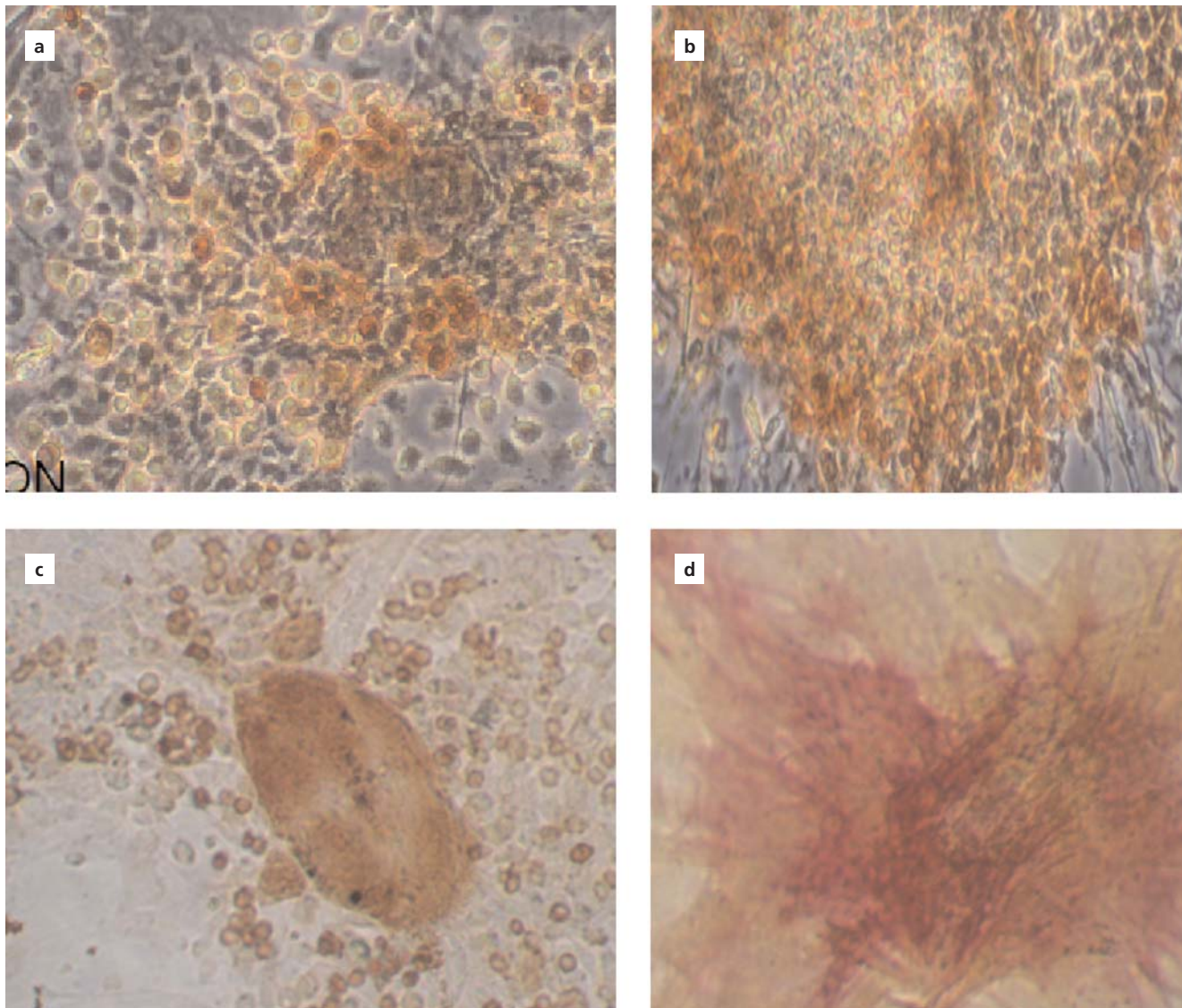


Figure 2. Osteoblast differentiation detected by osteonectin and osteocalcine staining. (a) Osteonectin; (b) Osteocalcin; (c) Von Kossa stain; (d) Alizarin Red S stain. [Color figure can be viewed in the online issue, which is available at www.anatomy.org.tr]

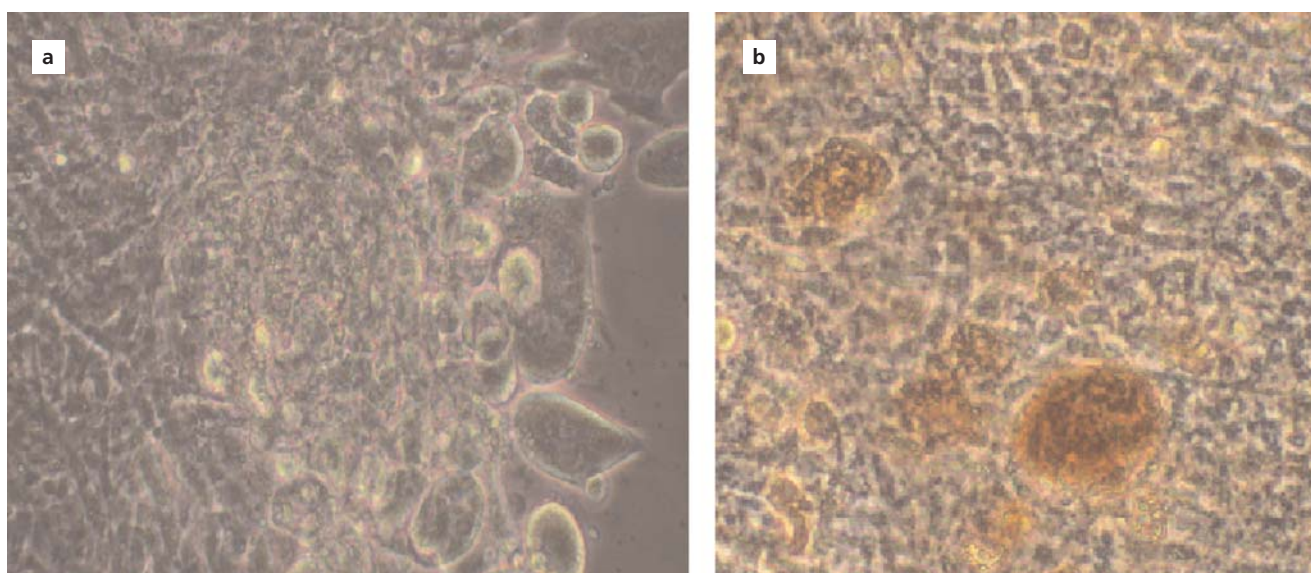


Figure 3. The wound model induced by scratch with pipette tip, where cell growth, differentiation and reformation occurred. The mimicked model of diabetic menopausal osteoporosis with high glucose and no estrogen supplement led to less healing compared to the control group. Wound healing in culture was followed by phase contrast microscope. (a) Wound area; (b) Reformation of bone matrix. [Color figure can be viewed in the online issue, which is available at www.anatomy.org.tr]

tent with the literature, the addition of MSC and niche was found to have a contributory effect on the treatment.

The osteoblastic differentiation from MSC were found to induce mineralized bone matrix shown with Alizarin Red S and von Kossa staining. Similarly, this differentiation and the formation of mineralized bone matrix have also been shown by histochemical staining in previous studies.^[37,39-41] All these results were consistent with the previous literature.

Osteogenesis is a complex process involving three phases: proliferation, matrix formation, and mineralization. RunX2 is a key marker of this process and is associated with the signaling pathways including Wnt/ β -Catenin and PI3K/ AKT. Other markers include collagen I, osteonectin (ON), osteopontin (OPN) and RANKL has also been shown to be an immuno-histochemical marker of osteoblastic and osteoclastic differentiation.^[42-44] In our

study, the differentiation of MSC to osteoblasts in culture medium was detected by the immunohistochemical staining of ON and OCN. Similarly, this differentiation was also shown by staining of these two markers, as well as some other markers including OPN and bone morphogenetic proteins (BMPs).^[14,45]

Scratch assay is commonly used in fibroblast culture for inducing wound models. However, to our knowledge, the use of scratch assay following the formation of bone matrix in culture has never been reported in the literature. Additionally, although this assay has been administered in skin wound healing with fibroblasts.^[35,46-49] it has not been administered for osteoblasts. Accordingly, the present study is the first in the literature to show that the scratch assay as a repeatable experimental model and that MSC and their niche can be used for therapeutic purposes. In the present study, we investigated the effect of high-glu-

Table 3

Scratched area was measured between both edge of the wound at the end of the experiment. The administration of MSC and niche led to osteoblastic differentiation and bone matrix formation at a similar level to that of control group.

	Wound closure	Bone matrix formation	Osteoblast count
Control (OM + E2 + NG)	0.75±0.15 μ m	65.45±25.15	25.12±8.24
Mimicked model (OM – E2 + HG)	0.33±0.12 μ m	21.22±10.88	8.44±2.16
Treatment (OM – E2 + HG + MSC + Niche)	0.58±0.14 μ m	45.37±18.56	15.62±5.72

cose culture medium with no estrogen supplement on wound healing and found that the osteoblasts differentiated from MSC did not induce bone matrix formation and had no significant effect on wound healing. Some previous studies also investigated the effect of high-glucose medium on experimental diabetes in culture.^[20,50] In a similar way to our study, these studies also examined the effect of estrogen supplementation in culture on menopause condition and revealed that it had a favorable effect on osteoblasts.^[29,45,51] Accordingly, our findings are consistent with the literature.

In our study, as shown by previous literature, the osteoblastic differentiation from MSC in an osteogenic medium with E2 supplement was found to express more ON and OC. Using high glucose decreased osteoblastic differentiation shown with ON and OC staining and reduced bone like island formation. Additionally, the removal of the E2 supplement that was used for mimicking osteoporosis further clarified the diabetes-induced damage and significantly decreased the expression of markers, which were also consistent with the literature. In contrast, the use of therapeutic MSC and niche increased the decreasing expression of markers. A previous study indicated that diabetic patients typically damaged osteoblasts and osteoclasts and also had an increased risk of oxidative stress, inflammation, delayed fracture healing associated with drug use, and decreased healing rates.^[8]

A previous study reported that the osteoblastogenesis mineralization of rat bone marrow stromal cells is inhibited in hyperglycemic culture by activation of the Notch2 signaling pathway.^[52] Another study evaluated diabetic rats induced by STZ and revealed that the transplantation of CXCL13-stimulated BMSC in culture increased cell proliferation rate and *in vivo* enhanced the corresponding ALP expression in bone healing.^[16] Some other studies indicated that the administration of human diabetic serum into MSC culture medium lead to reduced osteogenic differentiation in association with high glucose levels and could also be an important factor for diabetic osteoporosis.^[18] A study by Qu et al. examined the effect of miR-449 on osteogenic differentiation and its underlying mechanism in hBMSC using high glucose and free fatty acids treatment and revealed that the 14-day treatment dramatically decreased mineralization of hBMSC and resulted in impaired bone islets. The authors also noted that the miR-449 mimics decreased the protein expression levels of Runx2, ALP, collagen I, OCN, and BSP which were significantly increased by miR-449 inhibitors.^[19] Another study investigated potential abnormalities of BMMSC in a

rat menopause model established by ovariectomy and revealed that proliferation, migration, and differentiation of osteoclasts decreased, but increased by Wharton's jelly derived MSC.^[20] In an experimental study, ADMSC were cultured to mimic diabetic osteoporosis and the results indicated that OPN and Runx2 expressions of ADMSC decreased and there was a noticeable reduction in mineralization, which was associated with DNA methylation and Wenti signal.^[21] Likewise, some other studies established a rat diabetic osteoporosis model with STZ and high-fat diet and reported that administration of the model with plant extracts improved diabetic osteopenia and also prevented oxidative stress and apoptosis in the fracture induced in the femur.^[22,23]

In the present study, a culture model was formed to investigate the effect of MSC and niche therapy on fractures that could result in death by embolies in patients with diabetic osteoporosis. This model could be a cost-effective method for the new treatment products to be applied in dental and orthopedic practice prior to animal experiments and clinical trials and also provides useful information for the drugs to be developed in future. To our knowledge, there are no studies conducted on MSC in the literature other than those investigating the effect of drugs and stem cell therapy on osteoblast differentiation.^[9-11] Accordingly, the present study is the first of its kind to show that MSC and niche therapy leads to a significant improvement in impaired osteoblast function and in the reformation of bone matrix, particularly by increasing the number of osteoblasts, promoting bone matrix formation, and activating mineralization in culture. We consider that these findings can be used to produce a new treatment protocol in clinical practice.

References

1. Squillaro T, Peluso G, Galderisi U. Clinical trials with mesenchymal stem cells: an update. *Cell Transplant* 2016;25:829-48.
2. Garg P, Mazur MM, Buck AC, Wandtke ME, Liu J, Ebraheim NA. Prospective review of mesenchymal stem cells differentiation into osteoblasts. *Orthop Surg* 2017;9:13-9.
3. Wu ZY, Sun Q, Liu M, Grottkau BE, He ZX, Zou Q, Ye C. Correlation between the efficacy of stem cell therapy for osteonecrosis of the femoral head and cell viability. *BMC Musculoskelet Disord* 2020;21:55.
4. Ciuffreda MC, Malpasso G, Musarò P, Turco V, Gnecci M. Protocols for *in vitro* differentiation of human mesenchymal stem cells into osteogenic, chondrogenic and adipogenic lineages. *Methods Mol Biol* 2016;1416:149-58.
5. Hauzeur JP, De Maertelaer V, Baudoux E, Malaise M, Beguin Y, Gangji V. Inefficacy of autologous bone marrow concentrate in stage three osteonecrosis: a randomized controlled double-blind trial. *Int Orthop* 2018;42:1429-35.

6. Cheng C, Wentworth K, Shoback DM. New frontiers in osteoporosis therapy. *Annu Rev Med* 2020;71:277–88.
7. Murray CE, Coleman CM. Impact of diabetes mellitus on bone health. *Int J Mol Sci* 2019;20:19.
8. Rathinavelu S, Guidry-Elizondo C, Banu J. Molecular modulation of osteoblasts and osteoclasts in type 2 diabetes. *J Diabetes Res* 2018;2018:6354787.
9. Karaöz E, Aksoy A, Ayhan S, Sariboyaci AE, Kaymaz F, Kasap M. Characterization of mesenchymal stem cells from rat bone marrow: ultrastructural properties, differentiation potential and immunophenotypic markers. *Histochem Cell Biol* 2009;132:533–46.
10. Karaöz E, Doğan BN, Aksoy A, Gacar G, Akyüz S, Ayhan S, Genç ZS, Yürüker S, Duruksu G, Demircan PC, Sariboyaci AE. Isolation and *in vitro* characterisation of dental pulp stem cells from natal teeth. *Histochem Cell Biol* 2010;133:95–112.
11. Karaöz E, Okçu A, Gacar G, Sağlam O, Yürüker S, Kenar H. A comprehensive characterization study of human bone marrow mscs with an emphasis on molecular and ultrastructural properties. *J Cell Physiol* 2011;226:1367–82.
12. Çelebi B, Elçin YM. Proteome analysis of rat bone marrow mesenchymal stem cell subcultures. *J Proteome Res* 2009;8:2164–72.
13. Michael S, Achilleos C, Panayiotou T, Strati K. Inflammation shapes stem cells and stemness during infection and beyond. *Front Cell Dev Biol* 2016;4:118.
14. Ağacayak S, Gülsün B, Karaöz E, Nergiz Y, Uçan MC. Effects of mesenchymal stem cells in critical size bone defect. *Eur Rev Med Pharmacol Sci* 2012;16:679–86.
15. Huang KC, Chuang PY, Yang TY, Huang TW, Chang SF. Hyperglycemia inhibits osteoblastogenesis of rat bone marrow stromal cells via activation of the Notch2 signaling pathway. *Int J Med Sci* 2019;16:696–703.
16. Jiang H, Wang Y, Meng J, Chen S, Wang J, Qiu Y, Zhao J, Guo T. Effects of transplanting bone marrow stromal cells transfected with CXCL13 on fracture healing of diabetic rats. *Cell Physiol Biochem* 2018;49:123–33.
17. Maycas M, Portolés MT, Matesanz MC, Buendía I, Linares J, Feito MJ, Arcos D, Vallet-Regí M, Plotkin LI, Esbrit P, Gortázar AR. High glucose alters the secretome of mechanically stimulated osteocyte-like cells affecting osteoclast precursor recruitment and differentiation. *J Cell Physiol* 2017;232:3611–21.
18. Deng X, Xu M, Shen M, Cheng J. Effects of type 2 diabetic serum on proliferation and osteogenic differentiation of mesenchymal stem cells. *J Diabetes Res* 2018;5765478.
19. Qu B, Gong K, Yang HS, Li YG, Jiang T, Zeng ZM, Cao ZR, Pan XM. MiR-449 overexpression inhibits osteogenic differentiation of bone marrow mesenchymal stem cells via suppressing Sirt1/Fra-1 pathway in high glucose and free fatty acids microenvironment. *Biochem Biophys Res Commun* 2018;496:120–6.
20. Saito A, Nagaishi K, Iba K, Mizue Y, Chikenji T, Otani M, Nakano M, Oyama K, Yamashita T, Fujimiya M. Umbilical cord extracts improve osteoporotic abnormalities of bone marrow-derived mesenchymal stem cells and promote their therapeutic effects on ovariectomized rats. *Sci Rep* 2018;8:1161.
21. Zhang M, Li Y, Rao P, Huang K, Luo D, Cai X, Xiao J. Blockade of receptors of advanced glycation end products ameliorates diabetic osteogenesis of adipose-derived stem cells through DNA methylation and Wnt signalling pathway. *Cell Prolif* 2018;51:e12471.
22. Xie H, Wang Q, Zhang X, Wang T, Hu W, Manicum T, Chen H, Sun L. Possible therapeutic potential of berberine in the treatment of STZ plus HFD-induced diabetic osteoporosis. *Biomed Pharmacother* 2018;108:280–7.
23. Ding X, Yang L, Hu Y, Yu J, Tang Y, Luo D, Zheng L. Effect of local application of bisphosphonates on improving peri-implant osseointegration in type-2 diabetic osteoporosis. *Am J Transl Res* 2019;11:5417–37.
24. Chen Y, Hu Y, Yang L, Zhou J, Tang Y, Zheng L, Qin P. Runx2 alleviates high glucose-suppressed osteogenic differentiation via PI3K/AKT/GSK3 β / μ -catenin pathway. *Cell Biol Int* 2017;41:822–32.
25. Zavatti M, Guida M, Maraldi T, Beretti F, Bertoni L, La Sala GB, De Pol A. Estrogen receptor signaling in the ferutinin-induced osteoblastic differentiation of human amniotic fluid stem cells. *Life Sci* 2016;164:15–22.
26. Crescitelli MC, Rauschemberger MB, Cepeda S, Sandoval M, Massheimer VL. Role of estrone on the regulation of osteoblastogenesis. *Mol Cell Endocrinol* 2019;498:110582.
27. Gavali S, Gupta MK, Daswani B, Wani MR, Sirdeshmukh R, Khatkhatay MI. Estrogen enhances human osteoblast survival and function via promotion of autophagy. *Biochim Biophys Acta Mol Cell Res* 2019;1866:1498–507.
28. Sun LJ, Li C, Wen XH, Guo L, Guo ZF, Liao LQ, Guo Y. Icarin stimulates hFOB 1.19 osteoblast proliferation and differentiation via OPG/RANKL mediated by the estrogen receptor. *Curr Pharm Biotechnol* 2020. doi: 10.2174/1389201021666200123102550. [Epub ahead of print].
29. Lv H, Sun Y, Zhang Y. MiR-133 is involved in estrogen deficiency-induced osteoporosis through modulating osteogenic differentiation of mesenchymal stem cells. *Med Sci Monit* 2015;27:1527–34.
30. Deliloglu-Gurhan I, Tuğlu I, Vatansever HS, Özdal-Kurt F, Ekren H, Taylan M, Sen BH. The effect of osteogenic medium on the adhesion of rat bone marrow stromal cell to the hydroxyapatite. *Saudi Med J* 2006;27:305–11.
31. Deliloglu-Gurhan SI, Vatansever HS, Özdal-Kurt F, Tuğlu I. Characterization of osteoblasts derived from bone marrow stromal cells in a modified cell culture system. *Acta Histochem* 2006;108:49–57.
32. Yuksel S, Guleç MA, Gultekin MZ, Adanır O, Çağlar A, Beytemur O, Onur Küçükıldırım B, Avcı A, Subaşı C, İnci Ç, Karaöz E. Comparison of the early period effects of bone marrow-derived mesenchymal stem cells and platelet-rich plasma on the Achilles tendon ruptures in rats. *Connect Tissue Res* 2016;57:360–73.
33. Özdal-Kurt F, Tuğlu I, Vatansever HS, Tong S, Şen BH, Deliloglu-Gurhan SI. The effect of different implant biomaterials on the behavior of canine bone marrow stromal cells during their differentiation into osteoblasts. *Biotech Histochem* 2016;91:412–22.
34. Özdal-Kurt F, Tuğlu I, Vatansever HS, Tong S, Deliloglu-Gurhan SI. The effect of autologous bone marrow stromal cells differentiated on scaffolds for canine tibial bone reconstruction. *Biotech Histochem* 2015;90:516–28.
35. Jin E, Kim TH, Han S, Kim SW. Amniotic epithelial cells promote wound healing in mice through high epithelialization and engraftment. *J Tissue Eng Regen Med* 2016;10:613–22.
36. Sharma M, Sahu K, Singh SP, Jain B. Wound healing activity of curcumin conjugated to hyaluronic acid: *in vitro* and *in vivo* evaluation. *Artif Cells Nanomed Biotechnol* 2018;46:1009–17.

37. Paschou SA, Dede AD, Anagnostis PG, Vryonidou A, Morganstein D, Goulis DG. Type 2 diabetes and osteoporosis: a guide to optimal management. *J Clin Endocrinol Metab* 2017;102:3621–34.
38. Gadelkarim M, Abushouk AI, Ghanem E, Hamaad AM, Saad AM, Abdel-Daim MM. Adipose-derived stem cells: effectiveness and advances in delivery in diabetic wound healing. *Biomed Pharmacother* 2018;107:625–33.
39. Li LY, Wang XL, Wang GS, Zhao HY. MiR-373 promotes the osteogenic differentiation of BMSCs from the estrogen deficiency induced osteoporosis. *Eur Rev Med Pharmacol Sci* 2019;23:7247–55.
40. Ceylan H, Balçık OS, Güler MO, Kocabay S, Tekinay AB, Ünal Gülsüner H. Bone-like mineral nucleating peptide nanofibers induce differentiation of human mesenchymal stem cells into mature osteoblasts. *Biomacromolecules* 2014;15:2407–18.
41. Yang C, Wang Y, Xu H. Correction: Fluoride regulate osteoblastic transforming growth factor- β 1 signaling by mediating recycling of the Type I receptor ALK5. *PLoS One* 2017;12:e0170674.
42. Chen S, Yi B, Su LB, Zhang YR, Chen CL. *In vitro* evaluation of a novel osteo-inductive scaffold for osteogenic differentiation of bone-marrow mesenchymal stem cells. *J Craniofac Surg* 2020;31:577–82.
43. Ching HS, Luddin N, Rahman IA, Ponnuraj KT. Expression of odontogenic and osteogenic markers in DPSCs and SHED: a review. *Curr Stem Cell Res Ther* 2017;12:71–9.
44. Kuyucu U, Alpağat Ş, Bender OM, İlkerli E, Köstem Şİ, Güler NT. Kemik yapısı ve kemik metabolizmasında osteoprotegerin, RANKL ve RANK ilişkisi. Ankara: Türkiye Endokrinoloji ve Metabolizma Derneği ve Başkent Üniversitesi Tıp Fakültesi; 2010.
45. Lee SH, Oh KN, Han Y, Choi YH, Lee KY. Estrogen receptor regulates Dlx3-mediated osteoblast differentiation. *Mol Cells* 2016;39:156–62.
46. Nielsen FM, Riis SE, Andersen JI, Lesage R, Fink, T, Pennisi, CP, Zachar V. Discrete adipose-derived stem cell subpopulations may display differential functionality after *in vitro* expansion despite convergence to a common phenotype distribution. *Stem Cell Res Ther* 2016;7:177.
47. Menéndez-Menéndez Y, Otero-Hernández J, Vega JA, Pérez-Basterrechea M, Pérez-López S, Álvarez-Viejo M, Ferrero-Gutiérrez A. The role of bone marrow mononuclear cell-conditioned medium in the proliferation and migration of human dermal fibroblasts. *Cell Mol Biol Lett* 2017;22:29.
48. Kruse CR, Singh M, Sørensen JA, Eriksson E, Nuutila K. The effect of local hyperglycemia on skin cells *in vitro* and on wound healing in euglycemic rats. *J Surg Res* 2016;206:418–26.
49. di Martino O, Tito A, De Lucia A, Cimmino A, Cicotti F, Apone F, Colucci G, Calabrò V. *Hibiscus syriacus* extract from an established cell culture stimulates skin wound healing. *Biomed Res Int* 2017;2017:7932019.
50. Kato H, Taguchi Y, Tominaga K, Kimura D, Yamawaki I, Noguchi M, Yamauchi N, Tamura I, Tanaka A, Umeda M. High glucose concentrations suppress the proliferation of human periodontal ligament stem cells and their differentiation into osteoblasts. *J Periodontol* 2016;87:e44–51.
51. Zong S, Zeng G, Fang Y, Peng J, Zou B, Gao T, Zhao J. The effects of α -zearalanol on the proliferation of bone-marrow-derived mesenchymal stem cells and their differentiation into osteoblasts. *J Bone Miner Metab* 2016;34:151–60.
52. Huang KC, Chuang PY, Yang TY, Huang TW, Chang SF. Hyperglycemia inhibits osteoblastogenesis of rat bone marrow stromal cells via activation of the Notch2 signaling pathway. *Int J Med Sci* 2019;16:696–703.

ORCID ID:

M. Karakayalı 0000-0001-5779-4102;
T. Önal 0000-0002-3650-4046;
I. Tuğlu 0000-0002-0569-8415

**Correspondence to:** Müge Karakayalı, MD

Department of Medical Microbiology, School of Medicine,
Izmir Democracy University, Izmir, Turkey
Phone: +90 232 260 10 01
e-mail: muge.karakayali@idu.edu.tr

Conflict of interest statement: No conflicts declared.

This is an open access article distributed under the terms of the Creative Commons Attribution-NonCommercial-NoDerivs 3.0 Unported (CC BY-NC-ND3.0) Licence (<http://creativecommons.org/licenses/by-nc-nd/3.0/>) which permits unrestricted noncommercial use, distribution, and reproduction in any medium, provided the original work is properly cited. *Please cite this article as:* Karakayalı M, Önal T, Tuğlu İ. Effect of mesenchymal stem cells and their niche on diabetic and osteoporotic wound healing following osteogenic differentiation and bone matrix formation *in vitro*. *Anatomy* 2019;13(3):183–192.

A quantitative evaluation of the academicians in anatomy departments of medical schools in Turkey

Saliha Seda Adanır , İlhan Bahşi , Mustafa Orhan , Piraye Kervancıoğlu , Ömer Faruk Cihan 

Department of Anatomy, School of Medicine, Gaziantep University, Gaziantep, Turkey

Abstract

Objectives: This study aimed to make a quantitative evaluation of the academicians working in anatomy education, investigate the relationship between the number of academicians and the anatomy course hours, and examine the relationship between the ages of the schools and the number of academicians in medical schools in Turkey.

Methods: The number of academicians (professor, associate professor, assistant professor, research assistant and lecturer) working at the department of anatomy were recorded by examining the official websites of 90 medical schools in Turkey between June 22–27, 2019. The number of anatomy course hours was examined in 58 medical schools accessed from their websites. The years of establishment of the medical schools were recorded.

Results: A total of 90 research assistants, 18 lecturers and 291 faculty members were determined to work in the anatomy departments of the 90 medical schools in Turkey. The mean numbers of research assistants, lecturers, faculty members and academicians per faculty were found as 1 ± 1.56 (range: 0–9), 0.20 ± 0.45 (range: 0–2), 3.23 ± 2.41 (range: 0–11) and 4.43 ± 3.45 (range: 0–17), respectively. The mean numbers of theoretical, practical and total hours of anatomy course were 170.14 ± 32.25 (range: 100–245), 104.47 ± 34.78 (range: 32–196), and 274.6 ± 51.92 (range: 132–405), respectively.

Conclusion: There were differences between universities in terms of academicians and anatomy course hours. The course load of anatomy academicians was found rather high. It is concluded that this situation may have disadvantages for anatomy education and academic studies of academicians.

Keywords: academician; anatomy course hours; anatomy education; faculty member

Anatomy 2019;13(3):193–199 ©2019 Turkish Society of Anatomy and Clinical Anatomy (TSACA)

Introduction

Anatomy, one of the oldest known medical sciences, is a branch of science that students start to learn at the beginning of their medical education. Anatomy education provides a background for medical terminology and clinical sciences and also is essential for being a qualified physician.^[1] Anatomy not only constitutes the basis of medical education, but also it is one of the basic sciences with the most course hours.^[2–4] Therefore, the number of academicians who work in the anatomy departments of medical schools is important. According to the Higher

Education Law no 2547, academicians are classified as faculty member, lecturer, and research assistant working at institutions of higher education. Faculty members are professors, associate professors and assistant professors working at higher education institutions. Lecturers are academicians who are responsible for teaching, applying or supervising the application of the course hours taught at higher education institutions. Research assistants are defined as the academicians who assist in research, investigation, and experiments conducted at higher education institutions and perform other related duties assigned by

This study was an oral presentation at 20th National Anatomy Congress, 27th–31st August 2019, Istanbul, Turkey.

the competent bodies.^[5] It is considered that there is a plethora of factors that affect the anatomy education such as the educational infrastructure of the schools, educational strategies as well as the quality and quantity of the academicians.

This study aimed to evaluate the academicians working in anatomy education quantitatively, investigate the relationship between the number of academicians and education hours and the relationship between the age of the faculty and the number of academicians in medical schools in Turkey.

Materials and Methods

The number of faculty members, lecturers, and research assistants working at the anatomy departments were identified by examining the official websites of the 90 medical schools providing education in Turkey between June 22–27, 2019. The number of anatomy course hours of 58 medical schools, which can be accessed through the websites, was examined. The years of establishment of the medical schools were recorded. The relationship between the age of 90 medical schools and the number of academicians as well as the relationship between the number of anatomy course hours and the number of academicians of 58 medical schools were examined. The average number of course hours per academician in 58 medical schools was calculated. In the medical schools with both English and Turkish programs, the course hours per academician were calculated by taking the total course hours of both programs into consideration. Pearson correlation coefficient was used to test the relationship between numerical variables. Descriptive statistics are given as mean±standard deviation for numerical variables and number and percentage values for categorical variables. SPSS for Windows (version 22.0, Chicago, IL, USA) software was used for statistical analysis and $p < 0.05$ was considered statistically significant.

Results

The anatomy departments of the 90 medical schools were examined and the number of research assistants, lecturers, faculty members and the total number of academicians working at the anatomy departments were determined (Table 1). The average number of research assistants, lecturers, faculty members and academicians were identified as 1 ± 1.56 (range: 0–9), 0.20 ± 0.45 (range: 0–2), 3.23 ± 2.41 (range: 0–11), and 4.43 ± 3.45 (range: 0–17), respectively.

The highest numbers of faculty members in anatomy departments were in Ege and Istanbul Universities. The highest numbers of lecturers in the anatomy depart-

ment were in Istanbul Medipol and Necmettin Erbakan Universities, and the highest number of research assistants and academicians were in Çukurova University. There was no academician in three (3.3%), no faculty members in three (3.3%), no lecturer in seventy-four (82.2%), and no research assistants in fifty (55.6%) the anatomy departments.

The mean±standard deviation, minimum and maximum values of the number of professors, associate professors and assistant professors in the anatomy departments are shown in Table 2. It was observed that the Anatomy Departments of Ege University, and İstanbul Cerrahpaşa University had the highest number of professors. The anatomy departments of medical schools of Hacettepe University, Necmettin Erbakan University, Bursa Uludağ University, Sivas Cumhuriyet University, Pamukkale University, and Afyonkarahisar University of Health Sciences had the highest number of associate professors, and İnönü University, Kafkas University, and Yeditepe University had the highest number of assistant professors.

Table 3 shows the number of anatomy course hours including theoretical, practical and total, taught at 58 of 90 medical schools, the syllabuses of which could be accessed from their official web sites. According to this data, the average numbers of theoretical, practical and total course hours were 170.14 ± 32.25 (range: 100–245), 104.47 ± 34.78 (range: 32–196) and 274.60 ± 51.92 (range: 132–405), respectively.

The highest number of theoretical, practical and total course hours were at Balıkesir University, Tekirdağ Namık Kemal University and Necmettin Erbakan University, respectively. Van Yüzüncü Yıl University had the lowest number of theoretical, practical and total course hours. The average number of total course hours per academician in the 58 medical schools was 109.10 ± 80.76 (range: 16.05–434).

No statistically significant relationship was detected between the number of academicians working at the universities and the average number of anatomy course hours ($p > 0.05$). A strong positive correlation was observed between the age of the medical schools and the number of the academicians in the anatomy departments ($p = 0.001$ and $r = 0.667$).

Discussion

Anatomy is a branch of science that examines the structure and functions of the body and is regarded as one of the oldest of basic sciences.^[6] It has a very important place in the practice of medicine as it forms part of the foundations of the basic and clinical sciences.^[1] In order to understand

Table 1
Number of academic staff working in anatomy departments.

University	Foundation date	Research assistants	Lecturers	Faculty members	Academicians
Acıbadem Mehmet Ali Aydınlar University	2009	0	1	1	2
Adıyaman University	2007	2	1	3	6
Afyonkarahisar University of Health Sciences	1998	2	1	3	6
Ahi Evran University	2007	0	0	1	1
Akdeniz University	1973	2	1	7	10
Aksaray University	2015	0	0	1	1
Alanya Alaaddin Keykubat University	2014	1	0	2	3
Amasya University	2011	0	0	0	0
Ankara University	1945	5	0	10	15
Ankara Yıldırım Beyazıt University	2010	0	1	3	4
Atatürk University	1962	0	0	3	3
Aydın Adnan Menderes University	1992	3	0	3	6
Bahçeşehir University	2013	0	0	3	3
Balıkesir University	2006	2	0	3	5
Başkent University	1994	3	1	4	8
Beykent University	2017	0	0	2	2
Bezm-i Alem Vakıf University	2011	0	0	3	3
Biruni University	2015	0	0	2	2
Bolu Abant İzzet Baysal University	1997	0	0	3	3
Bursa Uludağ University	1972	0	0	6	6
Çanakkale 18 Mart University	2000	0	1	1	2
Çukurova University	1970	9	1	7	17
Demiroğlu Bilim University	2006	0	0	2	2
Dicle University	1966	0	0	6	6
Dokuz Eylül University	1978	0	0	10	10
Düzce University	1992	1	0	1	2
Ege University	1955	0	0	11	11
Erciyes University	1964	0	0	6	6
Erzincan Binali Yıldırım University	2008	0	0	2	2
Eskişehir Osmangazi University	1975	6	0	6	12
Fırat University	1985	2	0	4	6
Gazi University	1979	0	0	6	6
Gaziantep University	1987	1	0	4	5
Giresun University	2007	0	0	1	1
Hacettepe University	1967	3	0	10	13
Haliç University	2017	0	0	4	4
Harran University	1995	1	0	2	3
Hatay Mustafa Kemal University	2002	0	1	1	2
Hitit University	2009	0	0	2	2
İnönü University	1988	0	0	5	5
İstanbul Aydın University	2016	0	1	2	3
İstanbul Medeniyet University	2013	2	0	2	4
İstanbul Medipol University	2010	5	2	3	10
İstanbul Okan University	2014	0	0	1	1
İstanbul University	1933	3	0	3	6

Table 1 [Continued]
Number of academic staff working in anatomy departments.

University	Foundation date	Research assistants	Lecturers	Faculty members	Academics
Istanbul University-Cerrahpaşa	1933	2	0	11	13
Istanbul Yeni Yüzyıl University	2012	1	0	1	2
Istinye University	2016	2	0	4	6
Izmir Demokrasi University	2018	0	0	0	0
Izmir Ekonomi University	2017	0	0	2	2
Izmir Kâtip Çelebi University	2011	3	0	3	6
Kafkas University	2003	1	1	3	5
Kahramanmaraş Sütçü İmam University	1996	0	0	2	2
Karabük University	2010	2	0	2	4
Karadeniz Technical University	1976	2	0	4	6
Kastamonu University	2007	0	0	0	0
Kırıkkale University	1997	0	0	1	1
Kocaeli University	1995	0	0	3	3
Koç University	2010	0	0	2	2
KTO Karatay University	2015	1	0	2	3
Kütahya Health Science University	2009	0	0	1	1
Lokman Hekim University	2018	2	0	2	4
Maltepe University	1997	1	0	2	3
Manisa Celal Bayar University	1995	0	0	2	2
Marmara University	1933	3	1	3	7
Mersin University	1998	2	1	6	9
Muğla Sıtkı Koçman University	2009	0	0	3	3
Necmettin Erbakan University	1982	1	2	6	9
Niğde Ömer Halis Demir University	2017	0	0	1	1
Ondokuz Mayıs University	1975	0	0	7	7
Ordu University	2006	0	0	1	1
Pamukkale University	1987	0	0	5	5
Recep Tayyip Erdoğan University	2008	1	0	2	3
University of Health Science	2016	0	0	3	3
Sakarya University	2008	1	0	3	4
SANKO University	2014	0	0	2	2
Selçuk University	2002	1	0	3	4
Sivas Cumhuriyet University	1973	2	0	5	7
Süleyman Demirel University	1993	2	0	3	5
Tekirdağ Namık Kemal University	2008	1	0	1	2
TOBB Ekonomi ve Teknoloji University	2012	0	0	2	2
Tokat Gaziosmanpaşa University	2002	0	0	2	2
Trakya University	1974	4	0	6	10
Ufuk University	2003	0	0	2	2
Uşak University	2006	0	0	2	2
Van Yüzüncü Yıl University	1995	0	0	2	2
Yeditepe University	1996	0	0	3	3
Yüksek İhtisas University	2015	1	1	2	4
Yozgat Bozok University	2006	1	0	2	3
Zonguldak Bülent Ecevit University	2000	0	0	2	2

how diseases affect the structure and function of organs, it is essential to understand the human body from the visible structures to the cellular level.^[7] This is possible with a good anatomy education. In Turkey, anatomy education is taught to students as theoretical and practical courses mostly in the first two years of medical schools.^[2-4]

Özer^[8] reported an increase in the quotas and the number of universities in Turkey in order to meet the demand for higher education and increase the schooling rate in higher education. In line with this finding, the rapidly increasing number of medical schools and quotas in Turkey has led to an increase in the number of medical students.^[9-11] However, the number of academicians in anatomy departments has not increased proportionately with those numbers, and that some schools are lacking in academician in the anatomy departments (Table 1). Özoğlu^[12] stated that the ratio of students per faculty member in medical schools was 4.2 in the 2009–2010 academic year. Although the number of students per faculty member is important, the ratio of course hours per academician in

Table 2

Number of professors, associate professors and assistant professors working in anatomy departments.

Academicians	Mean±SD	Min-Max
Professor	1.86±2.27	0–10
Associate professor	0.4±0.61	0–2
Assistant professor	0.98±0.86	0–3

the anatomy departments of medical schools should also be not neglected. Accordingly, it was noticed that the course load of the academicians in anatomy departments is quite high, especially in the medical schools that provide both English and Turkish programs with a low number of academicians. It is considered that this situation may adversely affect anatomy education.

In anatomy education, practical courses are crucial for long lasting knowledge and the reinforcement of theoretical knowledge. As a matter of fact, in a survey study that

Table 3

Number of anatomy course hours.

University	Theoretical	Practical	Total
Afyonkarahisar University of Health Sciences	192	120	312
Ahi Evran University	201	94	295
Akdeniz University	182	174	356
Ankara University*	170	114	284
Ankara Yıldırım Beyazıt University*	128	100	228
Atatürk University*	166	80	246
Aydın Adnan Menderes University	173	111	284
Balıkesir University	245	118	363
Beykent University	161	94	255
Bezm-i Alem Vakıf University	168	111	279
Biruni University*	136	115	251
Bolu Abant İzzet Baysal University	146	108	254
Bozok University	157	68	225
Bülent Ecevit University	190	66	256
Çanakkale 18 Mart University	184	76	260
Çukurova University	147	120	267
Demiroğlu Bilim University	129	68	197
Dicle University	177	80	257
Düzce University	190	112	302
Ege University	176	50	226
Erciyes University	170	92	262
Erzincan Binali Yıldırım University	193	141	334
Eskişehir Osmangazi University	151	123	274
Fırat University	150	122	272

Table 3 [Continued]
Number of anatomy course hours.

University	Theoretical	Practical	Total
Gazi University*	173	76	249
Gaziantep University*	180	133	313
Giresun University	146	95	241
Harran University	204	144	348
Hatay Mustafa Kemal University	220	62	282
Hitit University	120	72	192
İnönü University*	160	172	332
Istanbul Medeniyet University	171	112	283
Istanbul Okan University*	129	88	217
Istanbul Yeni Yüzyıl University	149	107	256
Izmir Kâtip Çelebi University	172	100	272
Kafkas University	230	82	312
Kahramanmaraş Sütçü İmam University	157	136	293
Karabük University	116	160	276
Karadeniz Technical University	232	112	344
Kocaeli University	186	106	292
KTO Karatay University	224	110	334
Kütahya Health Science University	163	102	265
Manisa Celal Bayar University	155	52	207
Marmara University	142	62	204
Mersin University	143	94	237
Muğla Sıtkı Koçman University*	187	182	369
Necmettin Erbakan University	241	164	405
Niğde Ömer Halis Demir University	171	110	281
Recep Tayyip Erdoğan University	202	124	326
Sakarya University	179	71	250
SANKO University	107	90	197
Selçuk University	202	134	336
Sivas Cumhuriyet University	175	68	243
Süleyman Demirel University	176	114	290
Tekirdağ Namık Kemal University	164	196	360
Ufuk University	121	100	221
Van Yüzüncü Yıl University	100	32	132
Yüksek İhtisas University	189	41	230

*Medicals schools with both Turkish and English programs.

evaluated students' opinions on anatomy education, it was found that the students liked to study practical courses more than theoretical lectures.^[13] In a previous study, Başı et al.^[14] reported that the students paid more attention to practical courses rather than theoretical lectures in terms of attendance. Similarly, Uygur et al.^[15] also reported that the students paid more attention to practical courses than theoretical lectures in terms of attendance and they demanded that the number of practical courses to be increased, similar with the findings of Öğütürk et al.^[15]

According to 2004–2005 data, Gözil et al.^[16] reported that the average number of theoretical and practical anatomy course hours were 181 (range: 110–282) and 111 (range: 74–224). In the present study, the average numbers of theoretical and practical anatomy course hours were found 170.14 (range: 132–245) and 104.47 (range: 32–196), respectively. Gözil et al.^[16] reported that total anatomy course hours ranged from 184 to 408. On the other hand, Benli et al.^[17] found the average number of anatomy course hours as 87 (range: 47–183) in the forty-one medical

schools they investigated in 2018. However, based on the examination of the syllabuses of the 2018–2019 academic year,^[2–4] it is considered that this data may be incorrect. In the present study conducted according to 2018–2019 data, the total number of anatomy course hours was found 274.6 (range: 132–405).

One of the limitations of this study is that some of the websites were not updated. Also, the academicians who were originally affiliated with vocational schools or institutes, but were assigned to the anatomy departments of medical schools, were not evaluated. The course loads of academicians who were included in the medical faculty staff, but teaching at vocational schools, were not also evaluated. Additionally, the curriculum of 58 of 90 medical schools could be reached online, so the number of anatomy course hours of the 32 schools could not be surveyed.

Conclusion

Differences were identified between universities in terms of number of academicians and course hours. The number of academicians was higher in the medical schools that were established at an earlier date. In addition, no relationship was found between the number of academicians and course hours. When the course hours in institutes, vocational schools and schools other than medical schools were taken into account, the course load of the academicians in the anatomy department was found quite high. It is concluded that this situation may adversely affect anatomy education and academic studies of academicians working in anatomy departments.

References

1. Çetkin M, Turhan B, Bahşi İ, Kervancıoğlu P. The opinions of medicine faculty students about anatomy education. *Gaziantep Med J* 2016;22:82–8.
2. Ankara Üniversitesi Tıp Fakültesi dönem I ve dönem II ders programı. [Internet]. [Retrieved on September 12, 2019]. Available from: <http://www.medicine.ankara.edu.tr/donem-i/>, <http://www.medicine.ankara.edu.tr/donem-ii/>.
3. Ege Üniversitesi Tıp Fakültesi ders programı. [Internet]. [Retrieved on September 12, 2019]. Available from: https://med.ege.edu.tr/tr-2102/ders_programi_ve_klavuzlar_notlar.html.
4. Gaziantep Üniversitesi Tıp Fakültesi Ders Programı. [Internet]. [Retrieved on September 12, 2019]. Available from: <http://tipdekanlik.gantep.edu.tr/downloads/2018-2019.pdf>.
5. Resmi Gazete 2547 sayılı yükseköğretim kanunu. [Internet]. [Retrieved on September 11, 2019]. Available from: <http://www.mevzuat.gov.tr/MevzuatMetin/1.5.2547.pdf>.
6. Moore KL, Dalley AF, Agur AMR. Clinically oriented anatomy. 8th ed. Philadelphia: Lippincott, Williams and Wilkins; 2017. p. 15.
7. McCuskey RS, Carmichael SW, Kirch DG. The importance of anatomy in health professions education and the shortage of qualified educators. *Acad Med* 2005;80:349–51.
8. Özer M. Türkiye’de yükseköğretimde büyüme ve öğretim üyesi arzı. *Yükseköğretim ve Bilim Dergisi* 2011;1:23–6.
9. 2019 Yükseköğretim programları ve kontenjanları kılavuzu. [Internet]. [Retrieved on September 13, 2019]. Available from: <https://www.osym.gov.tr/TR,16858/2019-yuksekogretim-programlari-ve-kontenjanlari-kilavuzu.html>.
10. 2018 Yükseköğretim programları ve kontenjanları kılavuzu. [Internet]. [Retrieved on September 13, 2019]. Available from: <https://www.osym.gov.tr/TR,15240/2018-yuksekogretim-programlari-ve-kontenjanlari-kilavuzu.html>.
11. 2017 ÖSYS yüksek öğretim programları ve kontenjanları kılavuzu. [Internet]. [Retrieved on September 13, 2019]. Available from: <https://www.osym.gov.tr/TR,13263/2017-osys-yuksekogretim-programlari-ve-kontenjanlari-kilavuzu.html>.
12. Özoglu, M. Statükodan değişime: 21. yüzyılın başında yükseköğretim. In: B. S. Gür, editor. 2000’li yıllar: Türkiye’de eğitim. İstanbul: Meydan Yayıncılık; 2011. p. 125–161.
13. Uygur R, Çağlar V, Topçu B, Aktaş S, Özen OA. The assessment of the students’ opinions about anatomy education. *Int J Basic Clin Med* 2013;1:94–106.
14. Bahşi İ, Çetkin M, Kervancıoğlu P, Orhan M, Ayan H, Sayın S. Tıp fakültesi derslerinin verimliliği, işleniş şekli ve öğrencilerin devam kontrolünün değerlendirilmesi. *Genel Tıp Dergisi* 2018;28:89–95.
15. Ögetürk M, Kavaklı A, Kuş İ, Songur A, Zararsız İ, Sarsılmaz M. Tıp öğrencileri nasıl bir anatomi eğitimi istiyor? *Tıp Eğitimi Dünyası* 2003;10:7–14.
16. Gözil R, Özkan S, Bahçelioğlu M, Kadioğlu D, Çalgüner E, Öktem H, Şenol E, Mutlu MS, Kürkçüoğlu A, Yücel D, Babus T. Gazi Üniversitesi Tıp Fakültesi 2. sınıf öğrencilerinin anatomi eğitimini değerlendirmeleri. *Tıp Eğitimi Dünyası* 2006;23:27–32.
17. Benli AR, İnci H, Cebecik A, Sunay D. Türkiye’de tıp fakülteleri temel tıp bilimlerinin ders saatleri ve akademisyen sayılarının karşılaştırılması. *Tıp Eğitimi Dünyası* 2018;17:13–20.

ORCID ID:

S. S. Adanır 0000-0002-9098-5194; İ. Bahşi 0000-0001-8078-7074; M. Orhan 0000-0003-4403-5718; P. Kervancıoğlu 0000-0003-3231-3637; Ö. F. Cihan 0000-0001-5290-4384



Correspondence to:

Ilhan Bahşi, MD, PhD
Department of Anatomy, School of Medicine, Gaziantep University,
27310, Gaziantep, Turkey
Phone: +90 342 360 60 60 / 4655
e-mail: dr.ilhanbahsi@gmail.com

Conflict of interest statement: No conflicts declared.

This is an open access article distributed under the terms of the Creative Commons Attribution-NonCommercial-NoDerivs 3.0 Unported (CC BY-NC-ND3.0) Licence (<http://creativecommons.org/licenses/by-nc-nd/3.0/>) which permits unrestricted noncommercial use, distribution, and reproduction in any medium, provided the original work is properly cited. Please cite this article as: Adanır SS, Bahşi İ, Orhan M, Kervancıoğlu P, Cihan ÖF. A quantitative evaluation of the academicians in anatomy departments of medical schools in Turkey. *Anatomy* 2019;13(3):193–199.

Improving the efficacy of cadaveric demonstrations for undergraduate anatomy education

İlker Selçuk¹ , Mehmet Ülkir² , Caner Köse¹ , Burak Ersak¹ , Yağmur Zengin³ ,
İlkan Tatar² , Deniz Demiryürek² 

¹Department of Gynecologic Oncology, Ankara City Hospital Maternity Hospital, University of Health Sciences, Ankara, Turkey

²Department of Anatomy, School of Medicine, Hacettepe University, Ankara, Turkey

³Department of Biostatistics, School of Medicine, Hacettepe University, Ankara, Turkey

Abstract

Objectives: The aim of this study was to investigate if student number is a factor for the efficacy of cadaveric demonstrations in undergraduate anatomy education.

Methods: For a female pelvic anatomy cadaveric demonstration lecture of second-year medical students at the anatomy laboratory of Hacettepe University School of Medicine, students were divided into 3 groups of 45, 30 and 15 participants. Each group was further divided into 3 subgroups. Thus, there were 3 groups with 15 participants, 3 subgroups with 10 participants and 3 subgroups with 5 participants (3×15, 3×10, 3×5). After the cadaveric demonstration, the participants were asked if they had seen the structure previously listed in the checklist or not.

Results: The number of medical students who missed small anatomical structures such as the umbilical artery, ureter or uterine artery during the cadaveric demonstration significantly decreased as the number of students per cadaver table decreased ($p < 0.05$). Best results were obtained when the number of students per cadaver table was 5. On the other hand, no significant difference was found between the groups for missing gross anatomical structures such as the uterus, ovary or uterine tube, irrespective of the number of participants per cadaver table ($p > 0.05$).

Conclusion: As the number of students per cadaver table decreases, the number of overlooked or missed structures will decrease.

Keywords: anatomy teaching; cadaver dissection; education; pelvic anatomy; undergraduate

Anatomy 2019;13(3):200–204 ©2019 Turkish Society of Anatomy and Clinical Anatomy (TSACA)

Introduction

Anatomy forms the basis of medical education and provides a general perspective of the full body for medical students. Additionally, a clinically integrated anatomy education also improves the skills gathered during clinical rotations. Cadaver dissection has an important role in teaching anatomy since centuries, not only for medical students, but also for post-graduate surgery residents.^[1] Theoretical lectures, practical lectures on models and cadaver dissections are classical teaching anatomy methods. However, recently, many novel options are used in teaching anatomy such as computer-based programs,

three-dimensional (3D) printed materials, augmented or virtual reality and radiology assisted techniques.^[2] This multimodal education with traditional and novel techniques maintains an integrated and problem-based educational activity.

Cadaver dissection in the education of medical students provides a three-dimensional understanding which facilitates a better understanding of the relationship of anatomic structures in a real tissue architecture.^[3] The medical curriculum of faculties follows a dissection-based education in many countries, though it is not usually feasible to allow all medical students perform a self-

dissection. The students usually examine and try to identify the structures on previously dissected specimens.

Nevertheless, the number of medical students per cadaver table will affect the quality of anatomy education. The aim of this study therefore was to evaluate the relation between the number of students per cadaver and the efficacy of cadaveric demonstrations.

Materials and Methods

This study was conducted during the female pelvic anatomy cadaveric demonstration lecture of second-year medical students at the anatomy laboratory of Hacettepe University School of Medicine in April 2019. A full pelvic dissection was applied to a formalin-embalmed cadaver by the authors of this study (DD, IT, IS) two days prior to the cadaveric demonstration lecture. A checklist for the anatomical landmarks was prepared (Table 1). The medical students were divided into 3 groups of 45, 30 and 15 participants. Each group was further divided into 3 subgroups. Thus, there were 3 groups with 15 participants, 3 groups with 10 participants and 3 groups with 5 participants (3×15, 3×10, 3×5). After the cadaveric demonstration lecture, the checklists were distributed to the students

and they were asked whether they had observed the structure in the checklist or not.

IBM SPSS Statistics for Windows (Version 21, Armonk, NY, USA) was used for statistical analysis. Percentages and frequencies were calculated and chi-square (χ^2) test was used to analyze the significance between the groups. $p < 0.05$ was determined as statistically significant.

Results

During the cadaveric demonstration lecture, anatomical structures - umbilical artery, common iliac artery, external iliac artery, internal iliac artery, uterine artery, ureter, genitofemoral nerve, psoas major muscle, paravesical space, pararectal space, round ligament, broad ligament, infundibulopelvic ligament, proper ovarian ligament, uterine tube, ovary, uterus, rectosigmoid colon and bladder - were shown. The number of the medical students who missed the anatomical structures was determined after the cadaver lecture by a verbal quiz (Table 1). The results showed that the number of medical students who missed the anatomical structures during the cadaver lecture significantly decreased for small and isolated anatomical structures such as the umbilical

Table 1

Anatomical structures and number of medical students who missed the anatomical structures per group during the cadaveric demonstration lecture.

Anatomical structure	Group 1 (n=15)			Group 2 (n=10)			Group 3 (n=5)		
Umbilical artery	11	9	8	5	6	3	1	1	2
Common iliac artery	10	9	10	4	7	5	2	0	1
External iliac artery	8	9	8	3	7	5	0	0	1
Internal iliac artery	8	9	9	3	4	2	0	0	1
Uterine artery	10	8	8	5	2	3	2	2	0
Ureter	9	9	7	4	5	5	0	0	1
Genitofemoral nerve	8	9	7	4	4	3	1	0	1
Psoas major muscle	7	7	8	3	5	3	0	1	1
Paravesical space	8	5	9	4	7	4	1	1	1
Pararectal space	7	5	7	4	5	4	1	1	1
Round ligament	6	4	5	3	3	4	1	0	0
Broad ligament	4	4	4	2	4	3	0	0	0
Infundibulopelvic ligament	4	4	3	2	2	3	0	0	1
Proper ovarian ligament	6	4	5	2	3	1	0	1	0
Uterine tube	5	2	4	2	4	1	0	0	0
Ovary	4	4	3	2	2	1	0	0	0
Uterus	3	4	3	2	2	1	0	0	0
Rectosigmoid colon	4	4	3	1	2	1	0	0	0
Bladder	3	4	2	1	2	1	0	0	0

artery, ureter and uterine artery when the number of participants per cadaver table decreased ($p < 0.05$) (Table 2). Best results were obtained when 5 participants attended the cadaver table. On the other hand, no significant difference was found between the groups for overlooked/missed gross anatomical structures such as uterus, ovary and uterine tubes irrespective of the number of participants per cadaver table; 15, 10 or 5 ($p > 0.05$) (Table 2).

Discussion

The practical cadaver dissection-based lectures focus on demonstrative education in medical curriculum and attendance to the anatomy laboratory lectures is mandatory for medical students. However, there is not a clear rule for defining the best practice methods in teaching anatomy. This study evaluates how medical students will gain the best knowledge during cadaveric demonstration lectures. During this study, the medical students were divided into three groups consisting of 45 (3×15), 30 (3×10) and 15 (3×5) participants totally. In each group, three subgroups with 15, 10 and 5 students per dissection

table were evaluated to investigate if the students would miss less objects if the number of participants per cadaver decreased.

There is not a standardized approach in teaching anatomy among the universities and countries. Widespread use of user-friendly and repeatable methodologies brought a new insight to anatomy teaching. Anatomical Society of Great Britain and Ireland recommended a national guide on teaching anatomy that included the steps of dissection/prosection, interactive multimedia, practical procedures, surface and clinical anatomy, and radiological imaging.^[4] Cadaver dissections present a hands-on approach for studying the anatomical subject and maintain a deeper understanding than textbooks and models. The key objective of cadaveric demonstration is its role on exploring the relevant anatomical structures in the field of dissection and identification of the relations between the planes and tissues.^[5] Despite these facts, the best way to teach anatomy is still controversial and the novel approaches with the implementation of software technologies are drawing interest. With this point of view, the argument is on improving the effectiveness and quality of anatomy education.

Table 2

The percentage and comparison of missed anatomical structures per group during the cadaveric demonstration lecture.

Anatomical structure	Group 1 45 p (n/%)		Group 2 30 p (n/%)		Group 3 15 p (n/%)		p (χ^2)
Umbilical artery	28/45	62.2%	14/30	46.7%	4/15	26.7%	0.015*
Common iliac artery	29/45	64.4%	16/30	53.3%	3/15	20.0%	0.012*
External iliac artery	25/45	55.5%	15/30	50.0%	1/15	6.6%	0.004*
Internal iliac artery	26/45	57.7%	9/30	30.0%	1/15	6.6%	0.001*
Uterine artery	26/45	57.7%	10/30	33.3%	4/15	26.7%	0.036*
Ureter	25/45	55.5%	14/30	46.7%	1/15	6.6%	0.004*
Genitofemoral nerve	24/45	53.3%	11/30	36.6%	2/15	13.3%	0.048*
Psoas major muscle	22/45	48.8%	11/30	36.6%	2/15	13.3%	0.052
Paravesical space	22/45	48.8%	15/30	50.0%	3/15	20.0%	0.096
Pararectal space	19/45	42.2%	13/30	43.3%	3/15	20.0%	0.251
Round ligament	15/45	33.3%	10/30	33.3%	1/15	6.6%	0.068
Broad ligament	12/45	26.6%	9/30	30.0%	0/15	0	0.061
Infundibulopelvic ligament	11/45	24.4%	7/30	23.3%	1/15	6.6%	0.322
Proper ovarian ligament	15/45	33.3%	6/30	20.0%	1/15	6.6%	0.090
Uterine tube	11/45	24.4%	7/30	23.3%	0/15	0	0.106
Ovary	11/45	24.4%	5/30	16.6%	0/15	0	0.098
Uterus	10/45	22.2%	5/30	16.6%	0/15	0	0.139
Rectosigmoid colon	11/45	24.4%	4/30	13.3%	0/15	0	0.074
Bladder	9/45	20.0%	4/30	13.3%	0/15	0	0.154

p: participant; χ^2 : Chi square. * $p < 0.05$.

Besides the new advances in medical education, the current perspective on teaching anatomy is the combination of mixed-modalities. However, there is no particular way of objective comparison for effectiveness between the teaching modalities. Cadaver dissection lectures are important as they provide a three-dimensional anatomy and a deeper understanding. However, Azer and Eizenberg^[6] showed that perception of students for the importance of dissection-based learning decreased gradually and suggested that dissection-based learning should be replaced by recent novel methodologies. The research by Cottam et al.^[7] revealed that less than one-third of new residents had adequate anatomy knowledge, since anatomy knowledge is essential in surgical practice. Selcuk et al.^[8] described the importance of cadaver dissection courses in improving surgical anatomy knowledge and learning the basic steps of a surgical procedure. Consequently, the type of anatomy teaching should be determined according to the needs and demands of the target population and the primary methodology will change among medical students and residents. In this study, we designed a structured educational plan to demonstrate all the anatomical landmarks of female pelvic anatomy. All pelvic anatomical landmarks were determined before the cadaver lecture as a core syllabus. We showed the anatomical structures to the medical students with a checklist, so no objects were missed or forgotten during the lecture.^[9] In this perspective, the major issue was to test whether the increased number of attendees per cadaver table negatively affected the efficacy of education or not.

The cognitive processes related to three-dimensional understanding of cadaver are tactile handling, visual scanning, appreciation of the form and storage in the memory. This educational strategy will structure a clinical competence.^[10] High costs of cadavers and time spent to perform dissections with the smell, environmental and emotional conditions constitute the disadvantages of cadaver dissection lectures.^[11] However, making cadaver dissection lectures more effective is more important. Students may observe and learn anatomical structures around the master table, so we deal with the question of optimally maintaining each student to get all the anatomical knowledge in the dissection area. This study proved that when the number of attendees per cadaver decreased, the medical students would miss fewer objects with the structured educational program, and the efficacy of cadaver educational lecture improved. In this study, the best results were obtained when students worked in groups of 5 per cadaver; however, when in groups of 10,

there was a dramatic increase in the number of missed objects during the education. Additionally, students missed especially small structures such as the uterine artery rather than gross structures such as the broad ligament when the number of students per cadaver table increased.

Moreover, an optional anatomy course additional to the standard program, devoted to specific tasks with supplementation of active cadaver dissection, will break the deficiency in anatomy education in the undergraduate medical curriculum.^[12] Many anatomy seniors still highly support the importance of cadaver dissections in education of medical students. On the other hand, many suggest dissection-based learning as a more suitable educational tool for post-graduate surgical training.^[1,13] Despite the debate on this issue, cadaver dissection lectures are still highly important in undergraduate medical education, and improve learning anatomical structures with probable variations in a real tissue level.

Conclusion

Cadaver dissection is a fundamental issue in anatomy education and the number of students per cadaver table plays a major role in the efficacy of teaching and learning. Less number of students per cadaver table will decrease the number of missed objects in a structured educational plan and improve the efficacy.

References

1. Selcuk I, Tatar I, Huri E. Cadaveric anatomy and dissection in surgical training. *Turk J Obstet Gynecol* 2019;16:72–5.
2. Dissabandara LO, Nirthanan SN, Khoo TK, Tedman R. Role of cadaveric dissections in modern medical curricula: a study on student perceptions. *Anat Cell Biol* 2015;48:205–12.
3. Estai M, Bunt S. Best teaching practices in anatomy education: a critical review. *Ann Anat* 2016;208:151–7.
4. Sugand K, Abrahams P, Khurana A. The anatomy of anatomy: a review for its modernization. *Anat Sci Educ* 2010;3:83–93.
5. Winkelmann A. Anatomical dissection as a teaching method in medical school: a review of the evidence. *Med Educ* 2007;41:15–22.
6. Azer SA, Eizenberg N. Do we need dissection in an integrated problem-based learning medical course? Perceptions of first- and second-year students. *Surg Radiol Anat* 2007;29:173–80.
7. Cottam WW. Adequacy of medical school gross anatomy education as perceived by certain postgraduate residency programs and anatomy course directors. *Clin Anat* 1999;12:55–65.
8. Selçuk İ, Barut Ç, Çalışkan E. Impact of a gynecologic oncology cadaveric dissection course for surgical training. *Anatomy* 2019;13:56–60.
9. Smith CF, Finn GM, Stewart J, Atkinson MA, Davies DC, Dyball R, Morris J, Ockleford C, Parkin I, Standring S, Whiten S, Wilton J, McHanwell S. The Anatomical Society core regional anatomy syllabus for undergraduate medicine. *J Anat* 2016;228:15–23.

10. Jeyakumar A, Dissanayake B, Dissabandara L. Dissection in the modern medical curriculum: an exploration into student perception and adaptations for the future. *Anat Sci Educ* 2019; doi: 10.1002/ase.1905 [Epub ahead of print]
11. Aziz MA, McKenzie JC, Wilson JS, Cowie RJ, Ayeni SA, Dunn BK. The human cadaver in the age of biomedical informatics. *Anat Rec* 2002;269:20–32.
12. Pais D, Casal D, Mascarenhas-Lemos L, Barata P, Moxham BJ, Goyri-O'Neill J. Outcomes and satisfaction of two optional cadaveric dissection courses: a 3-year prospective study. *Anat Sci Educ* 2017; 10:127–36.
13. Stringer MD, Nicholson HD. Modern approaches to teaching and learning anatomy: modern models are already being applied. *BMJ* 2008;337:a1966.

ORCID ID:

I. Selçuk 0000-0003-0499-5722; M. Ülker 0000-0001-5615-8913;
C. Köse 0000-0002-3044-4804; B. Ersak 0000-0003-3301-062X;
Y. Zengin 0000-0002-9855-2449; I. Tatar 0000-0003-2532-8582;
D. Demiryürek 0000-0001-8781-1719

deomed®

Correspondence to: Ilker Selçuk, MD

Department of Gynecologic Oncology, Ankara City Hospital Maternity
Hospital, University of Health Sciences, Çankaya, Ankara, Turkey
Phone: +90 530 201 05 46
e-mail: ilkerselcukmd@hotmail.com

Conflict of interest statement: No conflicts declared.

This is an open access article distributed under the terms of the Creative Commons Attribution-NonCommercial-NoDerivs 3.0 Unported (CC BY-NC-ND3.0) Licence (<http://creativecommons.org/licenses/by-nc-nd/3.0/>) which permits unrestricted noncommercial use, distribution, and reproduction in any medium, provided the original work is properly cited. *Please cite this article as:* Selçuk İ, Ülker M, Köse C, Ersak B, Zengin Y, Tatar İ, Demiryürek D. Improving the efficacy of cadaveric demonstrations for undergraduate anatomy education. *Anatomy* 2019;13(3):200–204.

The impact of a clinical anatomy training and research unit in graduate and postgraduate medical education

Muzaffer Sindel¹ , Umut Özsoy¹ , Ege Alkan¹ , Serra Öztürk¹ , Ramazan Yavuz Arıcan² ,
Bahadır Murat Demirel³ , Nurettin Oğuz¹ , Yeşim Şenol⁴ 

¹Department of Anatomy, School of Medicine, Akdeniz University, Antalya, Turkey

²Department of Anatomy, Graduate School of Health Sciences, Near East University, Nicosia, Turkish Republic of Northern Cyprus

³Department of Anatomy, School of Medicine, Yozgat Bozok University, Yozgat, Turkey

⁴Department of Medical Education, School of Medicine, Akdeniz University, Antalya, Turkey

Abstract

Objectives: Continuing medical education practices are activities that ensure the continuity of medical education. The aim of these activities is to improve the knowledge and skills of medical doctors for better health care for patients and community. The purpose of this study was to present the feedback received from the participants in the first clinical education and research unit in Turkey in workshops held between 2008–2020.

Methods: Medical students, and specialist physicians in continuing medical education attended the workshops. Knee, shoulder and hip arthroscopical procedures, surgeries related with temporomandibular joint, peripheral nerve dissection, ear surgery, nail surgery and cadaver aesthetic application techniques were some of the organized courses. Feedbacks regarding the anatomy unit were received from the participants and instructors at the end of the courses, regarding the education period of 2008–2020. A total of 443 participants and 97 instructors filled the questionnaire.

Results: 79.2% of the participants who filled out the questionnaire had very positive expectations prior to the course; the rate of expectations met was 97.4% at the end of the course. The ratio of satisfied participants was 88.3%. Among the instructors, the level of positive expectations prior to the training was 83.5%, and the rate of expectations met was 97.5% following the end of the course. The rate of satisfaction from the quality of the training was 91.8%.

Conclusion: The Clinical Anatomy Training and Research Unit in Akdeniz University School of Medicine was assessed as of highly beneficial for both undergraduate medical students and specialist physicians in continuing medical education. The majority of the participants were satisfied with the applications, quality of training, and available resources.

Keywords: clinical anatomy; questionnaire study; training

Anatomy 2019;13(3):205–210 ©2019 Turkish Society of Anatomy and Clinical Anatomy (TSACA)

Introduction

Continuing medical education applications are activities that ensure the continuity of medical education. The purpose of these activities is to enhance knowledge and skills of medical doctors for the better health of patients and society.^[1,2] There are numerous courses and workshops in Turkey and all around the world, with the purpose of enhancing knowledge and skills within the scope of continuing medical education. One of the important

elements of these courses/workshops, particularly in the surgical field, is training on cadavers and plastic models in clinical anatomy laboratories.^[3–8]

Anatomy, which teaches the normal morphology of the human body, is one of the core courses in medical education, and an essential field for good medical practice. The concept of clinical anatomy became widespread in the late 1970s. Integrated courses have especially taken part in continuing education activities.

Clinical anatomy is the study of human anatomy with regard to clinical applications and focuses on special tissues and structures. Medical doctors make use of the field of clinical anatomy in the process of gaining new experiences in their own fields. Many surgeons and scientists enhance their knowledge and skills necessary for their fields through applied cadaver dissections. Through these courses, required efforts of clinicians decrease while efficacy increases. These courses also ensure safe surgical procedures and patient safety, contribute to determining surgical strategies, and help surgeons identify anatomical variations and be prepared for unexpected situations. Despite the vast number of techniques, the human cadaver is widely accepted as the gold standard for surgical training prior to performing surgical procedures on patients.^[3,9] It is also important for the training courses in clinical anatomy units to allow the transfer of knowledge to skill and support meaningful learning. Meaningful learning supports the connection of current knowledge with newly learned materials and ensures its permanence. Feedback received from the participants of the trainings at the clinical anatomy laboratories revealed a high rate of gladness and satisfaction regarding the efficacy of the courses.^[3,6,9]

The studies on clinical anatomy in Akdeniz University School of Medicine started in 2000. In the year 2006, the Akdeniz University School of Medicine Clinical Anatomy Education and Training Unit was founded to ensure the continuity of national and international symposiums and courses, workshops and contribute to the scientific studies. The purpose of this study was to present the feedback received from the participants in the first clinical education and research unit in Turkey. Thus, we aimed to conclude on the level of satisfaction of the participants.

Materials and Methods

In the Akdeniz University School of Medicine Clinical Anatomy Education and Training Unit, three courses were performed in 2007, followed by 9 in 2008, 11 in 2009, 6 in 2010, and 13 in 2011, 14 in 2012, 10 in 2013, 7 in 2014, 9 in 2015, 10 in 2016, 9 in 2017, 7 in 2018, 11 in 2019, and 2 in 2020. Participants consisted of medical students pursuing their medical residencies, as well as specialist physicians. Courses included wrist, ankle, knee, shoulder and hip arthroscopic surgeries, peripheral nerve dissection, ear surgery, therapeutic injections, ultrasound guided injections, microsurgical course, laparoscopic anatomical dissection course, interventional ultrasound course, temporomandibular joint course, advanced airway support course, neurostimulation course, endoscopic skull

base surgery course, algology pain course, transoral medical robotic surgery courses, nail surgery, cadaver aesthetic application techniques.

Feedbacks regarding the anatomy unit were received from the participants and instructors at the end of the courses. A total of 443 participants and 97 instructors have filled the questionnaire. All feedbacks were recorded regarding the education period of 2008–2020. There were seven items in the questionnaire: the specialty fields of the participants, years of experience as a specialist, previous participation in a similar course, expectations from the anatomy laboratory, expectations met at the anatomy laboratory, available resources, satisfaction from the training, and whether the participants would recommend this training to others or not. A 10-point Likert scale was used to evaluate the three items regarding the participants' expectations from the anatomy laboratory, expectations met at the anatomy laboratory, and their satisfaction from the training (0 = no expectations prior to the training, no expectations met, and unsatisfactory; 10 = very positive expectations prior to the training, all expectations met, and very satisfactory, respectively), while a five-point Likert scale was used to evaluate the item regarding available resources. For the analyses of the responses, responses to the 10-point Likert scale was used to evaluate expectations prior to the training, expectations met, and satisfaction from the training were grouped as "Bad: 0, 1, 2, 3", "Undecided: 5, 6, 7", and "Very good: 8, 9, 10". The participants' responses to the five-point Likert scale regarding available resources were groups as "Bad: 1, 2, 3" and "Good: 4, 5". The participants' years of experience were evaluated as "<10 years" and "≥11 years".

Feedbacks regarding the facility were received *via* interviews with the participants and instructors at the end of the course. Descriptive tables, chi-square test, and correlation analysis were performed and SPSS for Windows (version 22.0, Chicago, IL, USA) software was used for statistical analysis.

Results

98.6% of the participants were Turkish citizens. Of these, 38.8% (n=172) were specialists of orthopedics, 8.8% (n=39) internal medicine, 12.6% (n=56) anesthesiology, 7.7% (n=34) otorhinolaryngology, 6.5% (n=29) urology, 10.6% (n=47) dermatology, 8.6% (n=38) emergency medicine, and 6.3% (n=28) were dentists. Approximately half of the participants (54.4%; n=241) stated that they participated in a similar course before.

92.7% of the instructors were Turkish citizens (n=90). 53.6% (n=52) were specialists of orthopedics, 11.3% (n=11)

internal medicine, 7.2% (n=7) anesthesiology, 4.1% (n=4) otorhinolaryngology, 6.2% (n=6) urology, 5.2% (n=5) dermatology, 6.2% (n=6) emergency medicine, and 6.2% (n=6) were dentists. 85.6% (n=83) had prior instructing experience.

While 79.2% of the participants who filled out the questionnaire had very positive expectations prior to the training, the rate of expectations met was 97.4% at the end of the course. The ratio of satisfied participants was 88.3%.

Among the instructors, the level of positive expectations prior to the training was 83.5%, and the rate of expectations met was 97.5% following the end of the course. The rate of satisfaction from the quality of the training was 91.8% (Figure 1).

Evaluation of the distribution of the responses regarding the training resources revealed that 98% of the participants were satisfied with the available resources, 98.4% were satisfied with the plastic model, 97.5% were satisfied with the cadavers, 97.7% were satisfied with the instruments and materials, and 100% were satisfied with the location.

Evaluation of the responses of the instructors regarding the training resources showed that 97.9% of the instructors were satisfied with the available resources, 99% were satisfied with the plastic models, 98% were satisfied with the cadavers 97% were satisfied with the instruments and materials, and 100% were satisfied with the location (Figure 2).

“Would you recommend this course to others?” question was responded as “Absolutely.” by 98.7% of the participants and 96.9% of the instructors. The average

work experience of the instructors was 16.5 years, while it was 8.6 years for the participants. There was a statistically significant correlation between years of experience and expectations met ($p=0.007$). It was also determined that participants and instructors with an experience of more than 10 years had higher levels of expectations met. While the rate of expectations met was 64% in participants and instructors with an experience of 10 years or below, it was 91.7% in participants and instructors with an experience of 11 years and over.

Even though there was no statistically significant relationship between the expectation levels of the participants prior to the course, and years of experience and prior training, there was a statistically significant relationship between the levels of expectation and satisfaction ($p=0.025$). The group with higher expectations also had higher satisfaction at the end of the course. There were also statistically significant relationships between the level of satisfaction, and being satisfied with the resources ($p=0$) and cadavers ($p=0.004$), though there was no statistically significant relationship between being satisfied with the plastic model and years of experience.

Evaluation of the correlation between the expectations of the participants prior to the training, expectations met at the end of the training, and overall satisfaction with the training revealed that there were statistically significant relationships between each of the three variables. Accordingly, the higher the expectations of the participants prior to the training, the significantly higher were the levels of expectations met ($p=0.02$) and overall satisfaction ($p=0.011$). In parallel, meeting the expectations of the participants resulted in a significant and

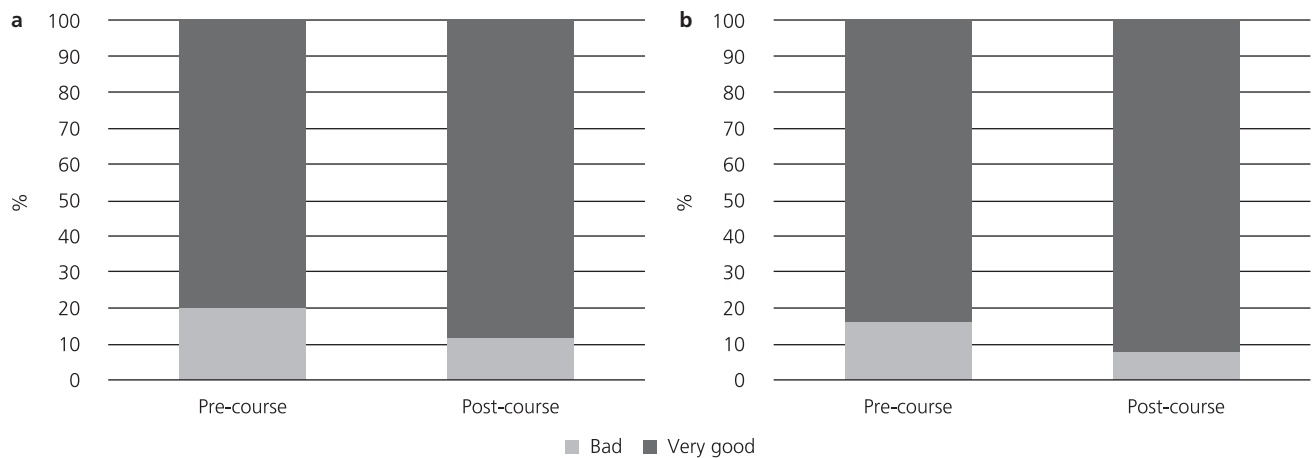


Figure 1. Expectations of the participants (a) and instructors (b) prior to the training, expectations met at the end of the course, and satisfaction rates.

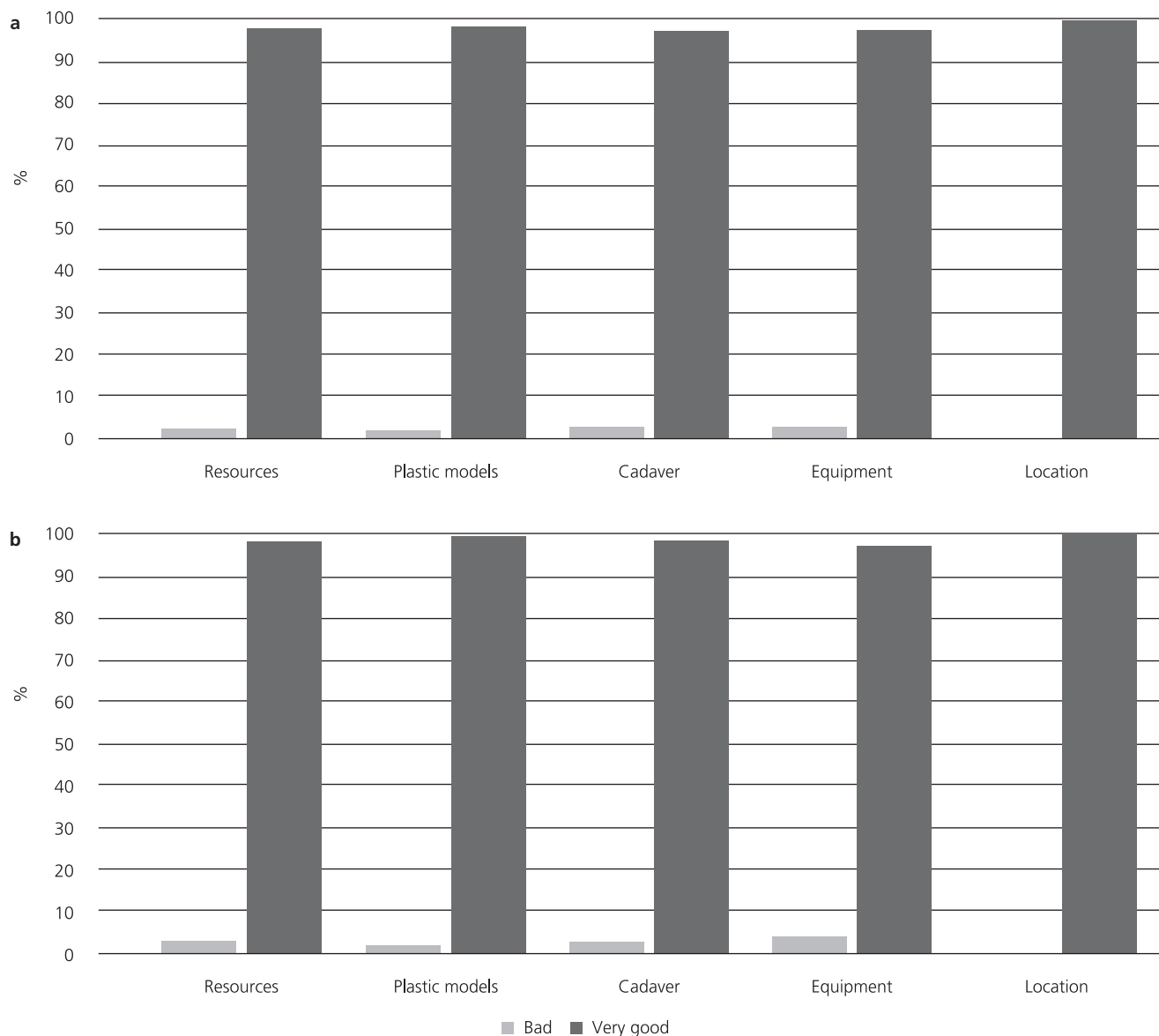


Figure 2. Distribution of responses of the participants (a) and instructors (b) regarding training resources.

drastic increase in overall satisfaction from the training ($p=0$; $r=0.652$).

A medium level of significant relationship was determined between the instructors' levels of expectations met and satisfaction from the training ($r=0.577$; $p=0.001$).

Below are some of the feedbacks received following the courses at the clinical anatomy education and research unit: "The skill training quality has increased with the unit"; "We only had the opportunity to work with plastic models before these applications. The clinical anatomy education and research unit gave us the

opportunity to maximize the practical training quality with the fresh cadaver trainings"; "Your center presents the opportunity for basic and clinical science studies"; "The laparoscopic anatomic dissection training using a fresh cadaver was the best training I have ever participated in"; "I felt like as if this center unifies the basic and clinical sciences".

Discussion

The majority of the participants and instructors stated that their expectations from the courses were met. More than

half of the participants mentioned that their expectations prior to the training were positive. The vast majority of the instructors stated that their expectations prior to the training were very positive. We believe that offering courses and improving them over the years at the clinical anatomy unit might have significantly contributed to the satisfaction rates. Satisfaction rate was higher at the end of the course. The increased values were due to the undecided participants. Also, trainings with cadavers still being accepted as the gold standard, despite all the 3-dimensional techniques and improvements, might be leading to increased satisfaction rates.^[3,9] Almost all of the participants and instructors were satisfied with the available resources. Plastic models, available resources in each course, and the experience levels of the instructors have all played an important role in the rate of overall satisfaction.

The relationship between the expectations of the participants prior to the training and levels of satisfaction at the end of the course is line with the outcomes of adult learning techniques. The need-oriented behaviors of adults, their eagerness to learn, and high expectations from the training might have been effective.^[10] Studies have shown that, in general, expectations of participants are met when courses are designed using the adult learning techniques. The satisfaction rates are high in all courses designed in accordance with the adult learning techniques. In a study by Unalan et al.,^[6] the satisfaction score on a 5-point scale was 4.36 for the arthroscopy course. In another study, feedback received following a minimally invasive surgical training with a cadaver revealed a satisfaction rate of 72.7%. Similarly, nearly all the participants from surgical fields yielded a very good/perfect satisfaction rate in a training in which a cadaver was used.^[3] Some feedback from the participants mentioned that training with human cadavers in these courses boosted confidence, particularly in surgical application that require skill, and that the participants mastered certain skills throughout these courses.^[11,12]

Anatomy is a science that is based on the dissection of the human body, and it is well-known that the use of cadavers is essential in surgical trainings.^[13] However, very few people donate their bodies for this purpose.^[14] Certain actions are being taken to increase the use of cadavers in surgical studies in order to increase cadaver donations and their use for these purposes. Although the Department of Anatomy in Akdeniz University School of Medicine is one of the leading institutions in terms of cadaver number, the lack of cadaver donations remains one of the biggest obstacles for anatomy training at our unit, as well. Training with cadavers at our unit allows surgeons to

learn new techniques and improve their skills without endangering human lives. By using protocols that provide more genuine colors and elasticity compared to traditional formaldehyde fixation in the upcoming years, we aim to minimize to a certain extent the difficulties in storage and short-term usage of frozen cadavers, and use available cadavers more efficiently. As researchers, we believe that clinical anatomy units possess very positive attributes, such as creating a safe frame for improving skills in applications, enhancing skills in applications, reducing costs, and preventing applications on real patients without mastering certain skills. There is a crucial mission for clinical and basic sciences in this regard. It is clear that increasing the number of similar units will allow surgeons to acquire new skills and improve them, as well as increase collaboration and communication between basic, surgical, and clinical sciences.

Conclusion

The Clinical Anatomy Education and Research Unit of Akdeniz University School of Medicine, the first of its kind in Turkey, was assessed as highly beneficial in continuing medical education at pregraduate and postgraduate levels that also enabled multidisciplinary studies. The majority of the participants were satisfied with the applications, quality of training, and available resources.

References

1. Davis N, Davis D, Bloch R. Continuing medical education: AMEE Education Guide No 35. *Med Teach* 2008;30:652–66.
2. Tian J, Atkinson NL, Portnoy B, Gold RS. A systematic review of evaluation in formal continuing medical education. *J Contin Educ Health Prof* 2007;27:16–27.
3. Holland JP, Waugh L, Horgan A, Paleri V, Deehan DJ. Cadaveric hands-on training for surgical specialties: is this back to the future for surgical skills development? *J Surg Educ* 2011;68:110–6.
4. Rainsbury RM. Supporting modern postgraduate surgical training programmes in the UK through greater use of cadaveric material. *European Journal of Anatomy* 2007;11(S1):105–9.
5. Standing S. New focus on anatomy for surgical trainees. *ANZ J Surg* 2009;79:114–7.
6. Unalan PC, Akan K, Orhun HD, Akgun U, Poyanli O, Baykan A, Yavuz Y, Beyzadeoglu T, Nuran R, Kocaoglu B, Topsakal N, Akman M, Karahan M. A basic arthroscopy course based on motor skill training. *Knee Surg Sports Traumatol Arthrosc* 2010;18:1395–9.
7. Ruiz-Tovar J, Prieto-Nieto I, Garcia-Olmo D, Clasca F, Enriquez P, Villalonga R, Zubiaga L. Training courses in laparoscopic bariatric surgery on cadaver thiel: results of a satisfaction survey on students and professors. *Obes Surg* 2019;29:3465–70.
8. Sañudo J, Vazquez T, Marañillo E, Mirapeix R, Rodriguez-Niedenführ M, Mompeo B, Marco F, Arráez-Aybar LA. The participation of anatomy departments in the continuing professional development of surgeons. *European Journal of Anatomy* 2007;11(S1): 111–9.

9. Blaschko SD, Brooks HMS, Dhuy M, Charest-Shell C, Clayman RV, McDougall EM. Coordinated multiple cadaver use for minimally invasive surgical training. *JLS* 2007;11:403–7.
10. Abela J. Adult learning theories and medical education: a review. *Malta Medical Journal* 2009;21:11–8.
11. Cundiff GW, Weidner AC, Visco AG. Effectiveness of laparoscopic cadaveric dissection in enhancing resident comprehension of pelvic anatomy. *J Am Coll Surg* 2001;192:492–7.
12. Katz R, Hoznek A, Antiphon P, Van Velthoven R, Delmas V, Abbou CC. Cadaveric versus porcine models in urological laparoscopic training. *Urol Int* 2003;71:310–5.
13. McLachlan JC. New path for teaching anatomy: living anatomy and medical imaging vs. dissection. *Anat Rec B New Anat* 2004;281:4–5.
14. Greene JR. Effects of detailed information about dissection on intentions to bequeath bodies for use in teaching and research. *J Anat* 2003;202:475–7.

ORCID ID:

M. Sindel 0000-0002-6594-1325; U. Özsoy 0000-0003-3708-7077;
E. Alkan 0000-0002-7805-5808; S. Öztürk 0000-0003-1002-0059;
R. Y. Arıcan 0000-0001-7668-1103; B. M. Demirel 0000-0002-5869-9753;
N. Oğuz 0000-0001-6864-8872; Y. Şenol 0000-0002-7842-3041



Correspondence to: Muzaffer Sindel, PhD

Department of Anatomy, School of Medicine,
Akdeniz University, Antalya, Turkey

Phone: +90 242 227 44 85

e-mail: sindelm@akdeniz.edu.tr

Conflict of interest statement: No conflicts declared.

This is an open access article distributed under the terms of the Creative Commons Attribution-NonCommercial-NoDerivs 3.0 Unported (CC BY-NC-ND3.0) Licence (<http://creativecommons.org/licenses/by-nc-nd/3.0/>) which permits unrestricted noncommercial use, distribution, and reproduction in any medium, provided the original work is properly cited. *Please cite this article as:* Sindel M, Özsoy U, Alkan E, Öztürk S, Arıcan RY, Demirel BM, Oğuz N, Şenol Y. The impact of a clinical anatomy training and research unit in graduate and postgraduate medical education. *Anatomy* 2019;13(3):205–210.

Kamus-ı teşrih: the possible first anatomy dictionary in Latin-Turkish

Ayşegül Fırat , M. Mustafa Aldur 

Department of Anatomy, School of Medicine, Hacettepe University, Ankara, Turkey

Abstract

'Kamus-ı teşrih' (Anatomical Dictionary) was examined in order to introduce it as a rare, probably the first and important work for Turkish Medical History in its category. This is an exceptional book published in Germany in 1923. It can be accepted as the first Latin-Turkish dictionary of anatomy when considered separately from the medical dictionary called 'Lugat-ı tıb' (medical dictionary). 'Kamus-ı teşrih' was published in Latin-Ottoman Turkish. The heading of the dictionary in Latin is 'Vocabularium anatomiae'. The original copy of this book is found in the National Library in Ankara, Turkey. 'Kamus-ı teşrih' was written by Zeki Haşmat Kırım, MD. First six pages of the book are composed of the title, dedication, abbreviation, legends and preface. Anatomical terms are listed in Latin in alphabetical order between pages 7–84 and their meanings are written in Ottoman Turkish. Pages 85–86 include the last word of the author. Page 87 comprises the list of other books published by the author. Last pages include some medical advertisements. This manuscript aimed to bring the importance of introducing and providing access to such rare works for the history of anatomy and medicine.

Keywords: anatomy; dictionary; Latin; Ottoman language; Turkish

Anatomy 2019;13(3):211–214 ©2019 Turkish Society of Anatomy and Clinical Anatomy (TSACA)

Introduction

Medicine is one of the oldest professions in human history. The profession of medicine, which has been shaped by the interaction and accumulation of different practices in different geographies for thousands of years, has pioneered many issues besides healing the people. The word 'hekim' (physician) in Turkish comes from an Arabic word 'hakim', which means wise person, philosopher.^[1] In terms of medical training and practices, anatomy is one of the cornerstones of medicine dating back to ancient times, with a history as long as the profession itself. The first written texts containing anatomy practices date back to the drawings of Herophilus (born in Chalcedon) who lived in Alexandria between 335–280 BC. Galen (129–216) has quoted many of Herophilus' drawings. About 1600 years after the first dissection drawings, dissection became

important again with Vesalius (1514–1564), when dissection drawings and written texts formed the basis of anatomy education.^[2] 'Gray's Anatomy', which contains 363 drawings, written by the British anatomist and surgeon Henry Gray (1827–1861), the 'Sobotta, atlas of descriptive human anatomy' written by German anatomist Robert Heinrich Johannes Sobotta (1869–1945), and 'The Netter collection' written by Frank H. Netter (1906–1991), an American medical doctor and painter, are among the books that are still being published and used as reliable sources for medical students, today.

During the Renaissance, there were significant developments in Western medicine and especially in the field of anatomy as information and resources increased and Ottoman medicine was also influenced by these developments. Several Western sources were translated into Ottoman Turkish during this period and the first medical

This study was an oral presentation at the 19th National Anatomy Congress and International Mediterranean Anatomy Congress (IMAC 2018), September 6–9, 2018, Konya, Turkey.

school was opened in the first half of the 19th century. 'Risale-i Teşrih-i Ebdan (Illustrated Human Anatomy)' by Şemsettin-i İtaki from Şirvan (1572–1632) is one of the first remarkable works written in this field.^[3] This work is a good example not only in terms of anatomical information and images, but also in language features and anatomical terminology. In addition to the Arabic equivalent of the medical terms mentioned in this work, Turkish, and sometimes Persian and Greek equivalents are included.

Learning new knowledge as well as teaching and transferring it to the new generation is important to ensure the continuity of knowledge. During this transition period, there were problems in understanding, teaching, and the use of medical terminology. The probably first Latin-Ottoman Turkish dictionary, 'Kamus-ı teşrih', is an example of efforts to overcome these problems.^[4] This work, which laid the basis of understanding anatomy as one of the fundamental fields in medical sciences, is the first anatomy dictionary prepared in accordance with the internationally accepted anatomical terminology. In our opinion, 'Kamus-ı teşrih' is the source of the first steps towards the translation of anatomical terms into Turkish, and therefore has been examined in order to introduce it as a rare, important and probably the first work for Turkish Medical History.

"Vocabularium Anatomiae"

'Kamus-ı teşrih' is a rare Latin-Turkish anatomical dictionary published in 1923 at the Kaviani Printing House (Leibnizstr. 43, Berlin) in Germany. The author of the dictionary is Dr. Zeki Haşmet Kiram (1886–1946), owner of the Morgen und Abendland-Verlag (Berlin, Karlstr. 10, Berlin) bookstore. The term 'Kamus-ı teşrih', written in Ottoman Turkish, can be translated into English as 'anatomical dictionary' (Figure 1). The Latin name of the book is 'Vocabularium anatomiae'. We have evaluated the original copy of this book that is found in the National Library, Ankara, Turkey (Code: 06 Mil EHT A 36083).

Content of 'Kamus-ı Teşrih'

'Kamus-ı teşrih' can be accepted as the first Latin-Turkish anatomical dictionary besides 'Lugat-ı tıp' (medical dictionary), the French-Ottoman dictionary of general medicine first published in 1873.^[5] It was prepared in three years and referred to the 'Nysten's medical dictionary' that was written in French and published in 1855. This dictionary was the only Ottoman-Turkish medical dictionary for nearly 25 years. In 1900, the sec-

ond edition was published by the 'Cemiyet-i Tıbbiye-i Osmaniye' (Ottoman Medical Society). This was the result of the first attempts to change the language of medical education from French to Ottoman Turkish.

The first six pages of the dictionary are reserved for the colophon, dedication, abbreviations and signs, and the author's foreword. The first page of the dictionary contains its name in Latin and Ottoman languages, information on the year of publication and the bookstore, and the author's name. In the dedication part, the author has dedicated this book to his father Mirza Ali Kiram Bey and to his relative Mirza Muhammed Zeman Khan, a medical doctor and vizier. This is followed by signs and abbreviations. In the foreword, the author states that the dictionary aims to provide support to overcome the difficulties in understanding medical terminology and his own medical experiences. On pages 7–84, anatomical terms are listed in alphabetical order according to the Latin alphabet and their equivalents are

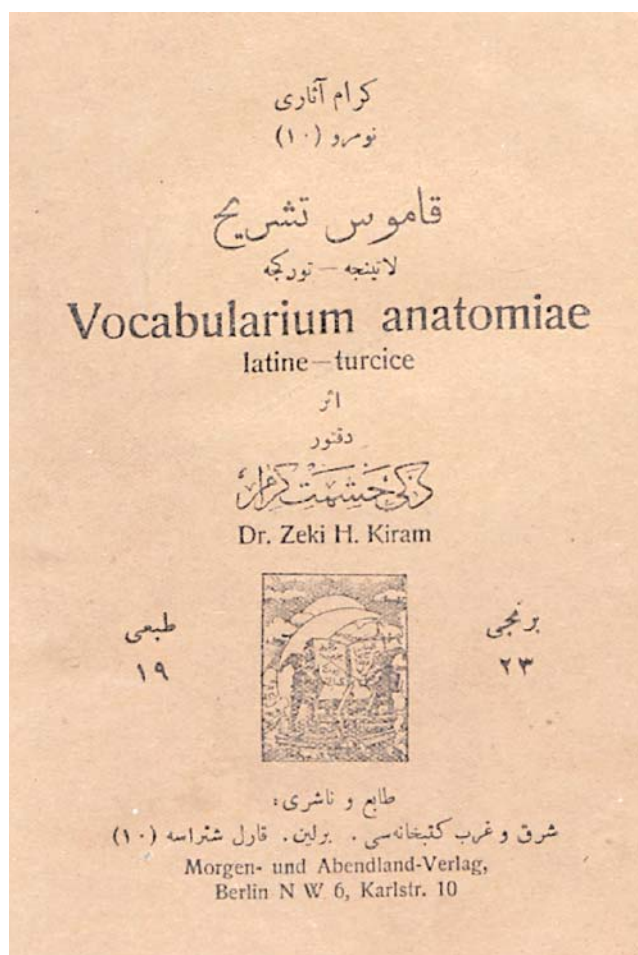


Figure 1. Title page of the dictionary.^[4]



Figure 4. Kiram in front of a bookstore.^[6]

(Figure 4). ‘Kamus-ı teşrih: Latin-Ottoman anatomy dictionary’ is the first work published in 1923 in the printing house of this bookstore.

Umar Ryad was stated Zeki Hışmet Kiram’s fields of work as military, journalism, armament representation and was focused on his life as a Muslim activist in Berlin.^[4] During this period, Kiram published many articles about the Arab and Muslim world. It is stated that he has works in Arabic, Ottoman, and German languages, but they were not allowed to be published in Germany at that time. In the article, almost no mention was made of his medical studies, except for a pedagogical article he wrote in 1927, reports of new research on the causes of cancer, and information about the printing of labels of drugs he produced in his private laboratory in the printing press. In his writings, he described himself as an Islamic missionary and, from 1928 onwards, began to

mediate German-Arab arms treaties as a military expert. He was arrested by the United States for his role in the arms trade, as a translator for the German Foreign Office, and for some of his visits to Spain, and died of cancer while being held at an American hospital.^[4,7]

Conclusion

Kiram was unable to pursue an academic career in medicine. His limited works in this field, like his other political works, were limited to translations. However, his work named ‘Kamus-ı teşrih: Latin-Ottoman anatomy dictionary’, which he prepared based on his own experiences during his medical education, is a rare work published in 1923. In Turkey, it is important to introduce and provide access to these rare works in terms of the history of anatomy and medicine which may have a contribution to determine appropriate Turkish equivalents of anatomical terms in Latin.

References

1. Gökçe N. Tarih öncesinden günümüze hekim ve hekimlik. Balkan Medical Journal 2000;17:117–21.
2. Bay NS, Bay BH. Greek anatomist Herophilus: the father of anatomy. Anat Cell Biol 2010;43:280–3.
3. Kahya E. Şemseddin-i İtâkî’nin resimli anatomi kitabı. Ankara: Atatürk Kültür, Dil ve Tarih Yüksek Kurumu, Atatürk Kültür Merkezi Yayını; 1996. p. 56–164, 199–204, 255–358.
4. Dr. Zeki Hışmet Kiram. Kamus-ı teşrih. Vocabularium anatomiae. Berlin: Kaviani Press; 1923. p. 94.
5. Pierre H. Nysten. Lugat-ı tıp İstanbul: Cemiyet-i Tıbbiye-i Osmaniye; 1900. p. 1255.
6. Ryad U. From an officer in the Ottoman army to a Muslim publicist and armament agent in Berlin, Zeki Hışmat-Bey Kiram (1886–1946). Bibliotheca Orientalis 2006;63:235–268.
7. Şeker M, Fırat A, Aldur M. Kamus-ı teşrih. Vocabularium anatomiae. Konya: Necmettin Erbakan Üniversitesi Kültür Yayınları; 2018. p. 134.

ORCID ID:

A. Fırat 0000-0001-5105-0057;
M. M. Aldur 0000-0002-5530-4234

deomed®

Correspondence to:

Ayşegül Fırat, MD
Department of Anatomy, School of Medicine,
Hacettepe University, Sıhhiye, Ankara, Turkey
Phone: +90 312 305 21 32
e-mail: aysfirat@hacettepe.edu.tr

Conflict of interest statement: No conflicts declared.

This is an open access article distributed under the terms of the Creative Commons Attribution-NonCommercial-NoDerivs 3.0 Unported (CC BY-NC-ND3.0) Licence (<http://creativecommons.org/licenses/by-nc-nd/3.0/>) which permits unrestricted noncommercial use, distribution, and reproduction in any medium, provided the original work is properly cited. Please cite this article as: Fırat A, Aldur MM. Kamus-ı teşrih: The possible first anatomy dictionary in Latin-Turkish. Anatomy 2019;13(3):211–214.

Author Index to Volume 13, 2019

(The bold typed references are the ones in which the person is the first author.)

A		E	
Abd El-kader M	137	Ekici C	98
Abegaz BA	122	Elvan Ö	13
Adamu YW	122	Erer Kafa S	49
Adamır SS	193	Ersak B	200
Adegoke AA	1		
Adekomi DA	1	F	
Adıgüzel E	66	Fırat A	211
Agudelo M	149		
Aigbogun Jr EO	107	G	
Akçiçek E	116	Gül Ş	126
Akkaşoğlu S	87	Gülekon İN	80
Akkaya M	168	Güngör Aydın A	66
Aldur MM	211	Gürsoy S	168
Alim E	80	Gwala FO	92
Alkan E	205		
Apaydın N	168	H	
Arıcan RY	205	Hashish HA	137
Arráez-Aybar LA	61		
Atalar K	80	I-İ	
Aydın MD	155	Ibeachu CP	107
Aydın OÖ	27	Ijomone OK	1
		İzci M	71
B			
Babacan S	49	K	
Bahşi İ	193	Kafa İM	49
Barut Ç	56	Karaca Saygılı Ö	33
Beger O	102	Karakayalı M	183
Bekel AA	122	Kaya Ö	168
Bobuş A	13	Keet K	40
Botero-González D	149	Kervancıoğlu P	193
Bozkurt M	168, 174	Keskinbora M	13
		Keyik B	33
C-Ç		Kılınç S	98
Cihan ÖF	193	Kiros MD	122
Çalışkan E	56	Koçak MN	155
Çalışkan S	87	Koçyiğit AS	116
Çelebioğlu EC	87	Kömür M	13
Çelikcan HD	13	Köse C	200
Çorumlu U	27	Kurtoğlu Olgunus Z	13
		Kuş İ	33
D		Kürkçüoğlu A	71
Demirci T	155		
Demirel BM	205	L	
Demiryürek D	33, 200	Lemuel AM	107
Diyarbakır S	21	Louw G	40

M			
Malkoç İ	155	Shakya R	163
Mansoor DI	163	Shrestha Sh	163
Mehta DK	163	Shrestha Su	163
		Sibuor WO	92
O-Ö		Sindel M	205
Ogeng'o JA	92	Sungur S	116
Ogunrinda AE	1	Şahinoğlu S	126
Oğuz N	205	Şençelikel T	71, 116
Olabu BO	92	Şenol Y	205
Olaniyan OO	1	Şimşek ME	168, 174
Orhan M	193		
Öktem H	71, 116	T	
Önal T	183	Tanrıyakul B	116
Özcan E	33	Tatar İ	200
Özdikici M	21	Truneh ST	122
Özgür A	13	Tuğlu İ	183
Özsoy U	205	Tuncel Çini N	49
Öztürk C	21, 155		
Öztürk H	98	U-Ü	
Öztürk S	205	Ulupınar E	27
		Ulusoy BN	116
P		Ülkir M	200
Pazarcı Ö	98		
Pelin C	71	V	
Penekli US	116	Vatansever A	33
Pulei AN	92		
		W	
R		Woldeyes DH	122
Romero-Reverón R	61		
		Y	
S-Ş		Yazıcı K	98
Sancak İT	87		
Selçuk İ	56, 200	Z	
		Zengin Y	200

Acknowledgment

www.anatomy.org.tr

Anatomy 2019;13(3):216 ©2019 Turkish Society of Anatomy and Clinical Anatomy (TSACA)

Acknowledgment of Reviewers for Volume 13, 2019

The Editorial Staff of Anatomy expresses their appreciation to the following reviewers who have evaluated the manuscripts for Volume 13, 2019.

Mustafa Aldur	Ömür Dereci	Tuna Karahan	İlkan Tatar
Aslıhan Avcı	Mirela Eric	Necdet Kocabıyık	İbrahim Tekdemir
Çağatay Barut	Tolga Ertekin	Zeliha Kürkçüoğlu Olgunus	Trifon Totlis
Okan Bilge	Ali Fırat Esmer	Ayla Kürkçüoğlu	Selçuk Tunali
Deniz Billur	Zeliha Fazlıoğulları	Eren Öğüt	Emel Ulupınar
Belgin Can	Figen Gövsa	Mustafa Fevzi Sargon	İlknur Uysal
Safiye Çavdar	Nadir Gülekon	Isabel Stabile	Aysun Uz
Servet Çelik	Ceren Güneç Beşer	Selçuk Sürücü	Bülent Yalçın
Deniz Demiryürek	Mehmet Ali Güner	Tülin Şen Esmer	Fatoş Yıldırım
	David Kachlick	Gülgün Şengül	

Table of Contents

Volume 13 / Issue 3 / December 2019

(Continued from back cover)

Teaching Anatomy

A quantitative evaluation of the academicians in anatomy departments of medical schools in Turkey 193

Saliha Seda Adanır, İlhan Bahşi, Mustafa Orhan, Piraye Kervancıoğlu, Ömer Faruk Cihan

Improving the efficacy of cadaveric demonstrations for undergraduate anatomy education 200

İlker Selçuk, Mehmet Ülker, Caner Köse, Burak Ersak, Yağmur Zengin, İlkan Tatar, Deniz Demiryürek

The impact of a clinical anatomy training and research unit in graduate and postgraduate medical education 205

Muzaffer Sindel, Umut Özsoy, Ege Alkan, Serra Öztürk, Ramazan Yavuz Arıcan, Bahadır Murat Demirel, Nurettin Oğuz, Yeşim Şenol

Historical View

Kamus-ı teşrih: the possible first anatomy dictionary in Latin-Turkish 211

Ayşegül Fırat, M. Mustafa Aldur

Index

Author Index to Volume 13, 2019 215

Acknowledgment

Acknowledgment of Reviewers for Volume 13, 2019 216

On the Front Cover:

Photomicrographs of ultrathin section of the glomerulus. (a) The control group shows normal fenestrated endothelial cell (**arrowhead**); (b, c) Regular basement membrane, podocytes, foot processes of podocytes. The diabetic group shows areas of fusion of the foot processes (**arrowheads**) with thickened basement membrane (**arrows**) and degenerated podocytes. (d) The treated group shows regular basement membrane, foot processes of normal podocytes, intact endothelial lining (**arrow**). **BM**: basement membrane; **F**: foot processes of podocytes; **P**: podocytes. From Abd El-kader M, Hashish HA. Potential role of empagliflozin in prevention of nephropathy in streptozotocin-nicotinamide-induced type 2 diabetes: an ultrastructural study. *Anatomy* 2019;13(3):137–148.

Colored images of the published articles can be found in the online version of the journal which is available at www.anatomy.org.tr

Table of Contents

Volume 13 / Issue 3 / December 2019

Original Articles

- Potential role of empagliflozin in prevention of nephropathy in streptozotocin-nicotinamide-induced type 2 diabetes: an ultrastructural study** 137
Marwa Abd El-Kader, Hagar A. Hashish
- Comparison of macerations with dermestid larvae, potassium hydroxide and sodium hypochlorite in Wistar rat crania** 149
Daniela Botero-González, Marcela Agudelo
- The underestimated role of a somatosensory neural network on thyroid gland morphology: an experimental subarachnoid hemorrhage model study** 155
Cengiz Öztürk, Mehmet Nuri Koçak, Tuba Demirci, İsmail Malkoç, Mehmet Dumlu Aydın
- Estimation of sex using mandibular canine index in a young Nepalese population** 163
Sunil Shrestha, Rojina Shakya, Dil Islam Mansoor, Dilip Kumar Mehta, Shamsher Shrestha
- Macroscopic footprint of the glenoid labrum** 168
Mehmet Emin Şimşek, Mustafa Akkaya, Safa Gürsoy, Özgür Kaya, Nihal Apaydın, Murat Bozkurt
- Clinical significance of the relationship between 3D analysis of the distal femur and femoral shaft anatomy in total knee arthroplasty** 174
Mehmet Emin Şimşek, Murat Bozkurt
- Effect of mesenchymal stem cells and their niche on diabetic and osteoporotic wound healing following osteogenic differentiation and bone matrix formation *in vitro*** 183
Müge Karakayalı, Tuna Önal, İbrahim Tuğlu

(Contents continued on inside back cover)